1980

Analysis and sensitivity of electromagnetic fields on high voltage transmission lines

Charles DeHart Cowan
Iowa State University

COWAN, CHARLES DEHART

ANALYSIS AND SENSITIVITY OF ELECTROMAGNETIC FIELDS ON HIGH VOLTAGE TRANSMISSION LINES

Iowa State University PH.D. 1980

Analysis and sensitivity of electromagnetic fields on high voltage transmission lines

by

Charles DeHart Cowan

A Dissertation Submitted to the
Graduate Faculty in Partial Fulfillment of the
Requirements for the Degree of
DOCTOR OF PHILOSOPHY

Department: Electrical Engineering
Major: Electrical Engineering (Electric Power)

Approved:

Signature was redacted for privacy.

Signature was redacted for privacy.

In Charge of Major Work

Signature was redacted for privacy.

For the Major Department

Signature was redacted for privacy.

For the Graduate College

Iowa State University
Ames, Iowa

1980

TABLE OF CONTENTS

I. INTRODUCTION

A. Study Objectives

This investigation has been undertaken to determine the effects of changes in certain of the transmission line parameters on the electrostatic fields generated by an excited three-phase EHV transmission line, particularly at the nominal line-to-line voltage of 345 kV. Changes in conductor diameters, bundle configurations, and relative placement of the phase bundles have been considered with a view to optimizing electric field distributions. This optimization will be with respect to minimization of corona discharge suspectability and the reduction of electric field magnitudes within the right-of-way which might effect either animal or plant life beneath the lines.

B. Background

The phenomenal growth in electric energy consumption in the United States and in the rest of the world community during the twentieth century has created a number of challenging problems for the electrical engineer as well as others closely associated with this key industry. Although the population of the United States has increased by a factor of three in the eighty years since the beginning of the century, the energy demands have increased by a factor of four hundred (1). To meet these demands, thousands of generation plants have been built throughout the

nation. Many of these have been fossil-fuel burning plants and are located in the vicinity of the principal consumers. The dramatic growth of metropolitan areas has made it impractical, in many cases, to locate new fossil fuel plants, or, more recently, nuclear generation stations close to these population centers. These restrictions have made it necessary to transport large quantities of electrical energy over distances which may range up to several hundreds of miles. The development of hydroelectric plants, such as those on our major rivers, has also required efficient transmission systems to deliver energy to areas far removed from the generation sites.

To provide for reasonably efficient transmission of energy over distances ranging from a few miles to hundreds of miles, the maximum transmission line voltages have been increased from approximately 35 kV in 1900 to a nominal 765 kV in 1980, with active proposals to increase this maximum to 1500 kV (1; 2). The mileage of high voltage transmission line circuits has also grown rapidly, particularly in the last 25 to 30 years. In 1950, there were only 75,000 circuit miles of transmission lines operating at voltages in excess of 100 kV and the maximum line-to-line voltage being used was around 245 kV. Twenty years later, in 1970, the circuit miles of EHV[1] and UHV lines had increased nearly three times to approximately 220,000 miles and the maximum line-to-line voltages had increased to a nominal 765 kV. Nearly 65% of the power handling capa-

[1]The division between EHV and UHV is somewhat arbitrary, but for the purposes of this study, we will define EHV as lying between 100 kV and 500 kV, and UHV will include all voltages in excess of 500 kV.

bility was at voltages in excess of 300 kV. By 1980, this portion of the power-handling capability was nearly 85% with 60% being handled at voltages of 500 kV or higher (2).

C. Criteria Impacting EHV Lines

The uncertainty of certain fuel sources and the increasing costs of fuel transportation, coupled with the ecological pressures to move large generator sites away from heavily populated areas, have added impetus to plans for centralizing the power generation resources in remote areas and transporting the energy over high voltage lines to the industrial and population centers where it is needed. The efficient transmission of these large blocks of energy from such central generation sites to the ultimate consumers will inevitably require the utilization of line voltages in the EHV and UHV ranges. In certain areas, EHV networks are already being overlaid with UHV systems. The EHV systems are being kept intact to supply peaking power and to provide emergency back-up power in cases of an outage on the UHV lines. In these EHV and UHV systems, efficiencies which were reasonable at lower voltages are no longer acceptable due to the magnitudes of the energy involved. For a 100 kV, 25 MVA system, a transmission line efficiency of 96% represents a loss of 1 MW. On the other hand, a 500 kV, 625 MVA system with the same efficiency would involve the loss of 25 MW in a single circuit, which is intolerable.

At the lower voltages, controlling transmission line efficiency has been largely a matter of reducing I^2R losses by maintaining high power factors and increasing conductor diameters to reduce the effective resistance in the circuit. Losses due to corona phenomena are generally limited to periods of very unusual atmospheric conditions and tend to diminish with time as the sharp protrusions are worn away by weathering, or burned away by the discharges themselves.

A discussion of all of the criteria involved in the design of EHV and UHV transmission line systems is beyond the scope of this present work. Any list of the more important design criteria should include (2; 3):

1. The power levels at which the system is to operate under full load conditions and the minimum acceptable efficiency of the transmission line.
2. The maximum allowable voltage gradients, both at the surface of the conductors where corona phenomena will be prevalent, and in the vicinity of the ground where people, livestock or mobile equipment might be effected.
3. The effects of the transmission system on overall system stability. A transmission system of any appreciable size will store very large amounts of energy when excited. Under transient conditions, this energy can effect the flow of energy in interconnected external systems.

4. The ecological, economical, physiological, psychological and sociological impact of the system on its environment.

These general criteria will be important in the determination of such transmission line parameters as those shown below:

1. Conductor size and current carrying capacity.
2. Bundling configurations per phase.
3. Multiple circuit configurations.
4. Insulator design for electrical and mechanical strength.
5. Minimum clearances between the lines and adjacent structures, lines, or the ground.
6. Switching gear and overvoltage protection.
7. Tower dimensions and configurations.
8. Right-of-Way requirements.

D. Power Transmission Efficiency

The actual load carrying capability of a particular transmission line involves a number of factors, but for a standard of comparison, the Surge Impedance Load factor (SIL) is commonly used (3; 4). This power transmission capability factor assumes that the transmission line is terminated at its load end by a characteristic impedance, such that the impedance seen by the generator is equal to the impedance at the load end. This surge impedance, or characteristic impedance, is usually based on

the assumption that the losses in the transmission line are negligible (see Appendix A).

Defining the characteristic impedance Z_o in terms of a lossless transmission line, we have

$$Z_o = \sqrt{L/C}$$

where

L = inductance per unit length

C = capacitance per unit length

For comparing power carrying capability of different transmission lines, the SIL is defined as

$$SIL = \frac{V^2}{Z_o} \text{ watts}$$

where V is line-to-neutral on a per phase basis, or line-to-line for total three-phase capabilities.

Typical surge impedance values vary from about 377 ohms for single conductor lines, to about 240 ohms for lines with four subconductors per phase.

From the definitions of Surge Impedance Loading, and characteristic impedance, it appears that the smaller the series inductance per unit length, the greater will be the power handling capability of a particular transmission line. In a.c. circuit analysis, this inductance is generally represented as a reactance. To illustrate the importance of this series reactance to the allowable power transfer, let us use the "pi" equivalent

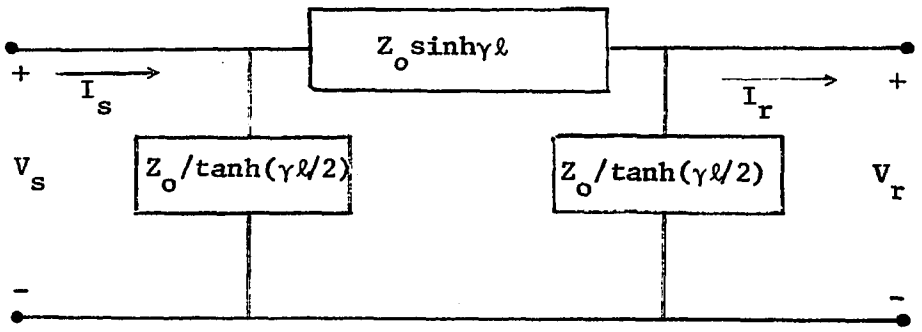

Figure 1. π-equivalent of ℓ meter section of transmission line

developed in Appendix B. If the transmission line is electrically short, the shunt elements and the series resistance can be neglected and the transmission line between the generator V_g and the infinite bus V_b can be represented by a single series inductive reactance jX_L. Since a power system generally involves a very large number of subsystems, the analysis

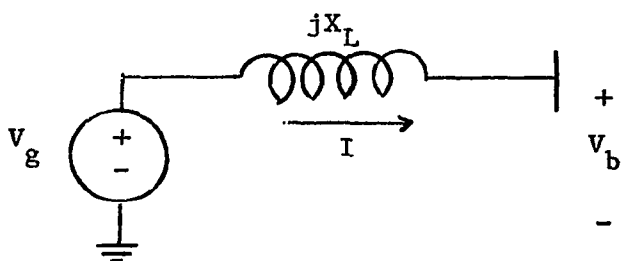

Figure 2. Simplified model of transmission line circuit

of a particular subsystem assumes that the remainder of the system may be represented by a constant frequency, constant voltage source at the end of an infinite transmission line from which there can be no reflected voltages or currents. This has been termed an "infinite bus" (4; 5). We shall assume that the generator is supplying power to the bus, so that

current I flows through the reactance from the generator to the bus, as shown. We can then write the equation

$$V_g = V_b + jX_L I$$

which can be rearranged to give the current as

$$I = \frac{V_g - V_b}{jX_L}$$

and its complex conjugate

$$I^* = \frac{V_g^* - V_b^*}{-jX_L}$$

To obtain the power delivered to the bus from the generator, we can write

$$P = \text{Re } V_b I_b^* = \text{Re } \frac{V_b V_g^* - V_b V_b^*}{-jX_L}$$

$$= \text{Re } j \frac{|V_b||V_g|\cos\delta - |V_b|^2 - j|V_b||V_g|\sin\delta}{X_L}$$

$$= \frac{|V_g||V_b|\sin\delta}{X_L}$$

where δ is the phase angle between the generator voltage V_g/δ and the bus voltage V_b/o. Maximum power transfer then depends upon minimizing X_L and increasing the angle as much as possible. For transient stability, δ is usually limited to about 30°. Where economically feasible, series compensation is often inserted in the lines to reduce the effective value of X_L and to increase the power transfer (3).

E. Bundled Conductors

If the current in one phase conductor is divided between two subconductors which are then separated by some reasonable distance, the mutual coupling between these two halves of the current will be reduced and the effective inductance of the combination will be lowered accordingly. This distribution of currents in a particular phase between several separate subconductors is known as "bundling." Bundling can be used to reduce the effective inductance per phase in a transmission line. This reduction of the series inductance and the resultant inductive reactance is very important because it is this reactance which effectively limits the power which can be transmitted over a given line.

Although bundling does, in general, improve the electrical characteristics of a transmission line, it introduces additional mechanical problems, such as increased strain on insulator strings due to increased wind and ice loading, as well as the inherent increase in the weight of the conductors themselves. It will also effect the fields in the vicinity of the ground.

F. Electric Field Limitations

One of the most important effects of bundled conductors, as far as EHV and UHV transmission line circuits are concerned, is the ability to reduce the maximum value of the surface voltage gradients at the conductors themselves. Dividing the charge required to produce a given

line potential between several subconductors of the same size reduces the maximum electric field magnitude at the surface of each conductor, even though the net charge per phase has been increased.

As an example of how this is accomplished, a very simplistic example will be used in which the effects of any induced charges due to imaging

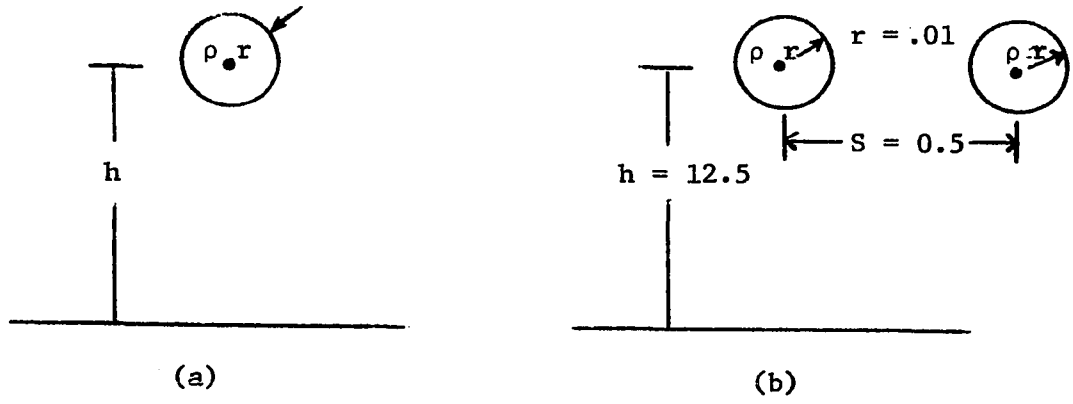

(a) Single conductor above ground

(b) Two subconductors above ground

Figure 3. Two-dimensional models of transmission lines

in the ground plane or the conductors themselves will be neglected. The effects of image charges will be explained later. A point at the ground level directly beneath the center of the conductor configuration will be used as a reference in each case. In each case, r = 1 cm, h = 12.5 m, and the potential with respect to the ground is 200 kV peak. In the two-conductor case, the separation will be 50 cm.

From electromagnetic field theory, the potential voltage at a radius r from a uniformly charged filament ρ (coulombs per meter), with respect to a point at radius h from the same line of charge, can be written as

$$V = \frac{\rho}{2\pi\epsilon} \ln(h/r)$$

Knowing the voltage, the required linear charge density is found to be

$$\rho_1 = \frac{2\pi\epsilon V}{\ln(h/r)} = \frac{4\pi\epsilon \times 10^5}{\ln(2350)} = 1.56 \times 10^{-6} \text{ Coulombs/m}$$

The electric field intensity or voltage gradient at the surface of the conductor will be radially directed from the filament and equal to

$$E_r = \frac{\rho}{2\pi\epsilon r} = \frac{1.56 \times 10^{-6}}{2\pi\epsilon \times .01} = 2.805 \times 10^6 \text{ V/m}$$

This is close to the dielectric breakdown of air, which is usually given as 3×10^6 V/m (6).

For the two-conductor case illustrated in Figure 3b, it is assumed that the diameter of the conductors are negligible with respect to the separation (50 cm), and that the equal charge on each conductor is uniformly distributed over the surface of that conductor. It will be seen later that this is not actually the case, but such an assumption does not effect the conclusions to be made here.

By superposition, the equation for the potential at either conductor can be written as

$$V(r) = \frac{\rho}{2\pi\epsilon} \ln(h/r) + \frac{\rho}{2\pi\epsilon} \ln(h/s)$$

$$= \frac{\rho}{2\pi\epsilon} \ln(h^2/sr)$$

from which the line charge density per conductor is obtained.

$$\rho = 2\pi\varepsilon V/\ln(h^2/sr) = 4\pi\varepsilon \times 10^5/\ln(31250) = 1.075 \times 10^{-6}$$

By superposition, the maximum electric field intensity occurs on the side of the conductor where both fields will add to give

$$|E_{max}| = \frac{\rho}{2\pi\varepsilon}\left(\frac{1}{r} + \frac{1}{s}\right) = 1.971 \times 10^{+6} \text{V/m}$$

This is a reduction of almost 30% in the maximum electric field strength from the single conductor case, even though the total charge and, therefore, the capacitance has increased by 38%.

II. TRANSMISSION LINE CHARACTERISTICS

A. Introduction

Most high voltage transmission lines are still operated above ground with the conductors suspended from large towers by insulator strings and spaced far enough apart to prevent mechanical interference due to swinging cables or the generation of excessive corona discharges due to high intensity electric fields. These lines may be spaced horizontally or vertically either in a planar or staggered configuration. In some cases, two or more three-phase circuits may be mounted on the same towers. Shielding wires are generally mounted above the power lines to provide a grounding path for lightning discharges independent of the power circuits themselves.

The basic electrical parameters of any transmission line are the inductance, capacitance, resistance, and conductance per unit length (5). From these parameters, such characteristics as surge impedance, wave velocity and transmission efficiency can be determined. Since the shunt losses on a high voltage transmission line are primarily due to corona phenomena and insulator deficiencies, we shall consider only inductance, resistance, and capacitance parameters at this point. Corona losses will be considered separately in the context of maximum allowable electric fields at the conductor surfaces.

B. Inductance

From Maxwell's expression of the interrelation between time-varying electric and magnetic fields, the concept of inductance has been deduced and is commonly used in the formulation of circuit equations (6; 7; 8). The changing magnetic fields are related to the currents producing them by the current voltage relationships

$$v_i = \sum_i L_{ij} \frac{di_j}{dt}$$

or

$$v_i = L_{ii} \frac{di_i}{dt} + \sum_{j \neq i} M_{ij} \frac{di_j}{dt}$$

where v_i is the total voltage induced into circuit i by all of the changing magnetic fluxes enclosed by that circuit. L_{ii} is commonly termed "self-inductance" and represents the action of the field due to current flow in circuit i upon itself. The mutual inductance M_{ij}, which is reciprocal in most practical cases, is then a measure of the effect of currents in circuit j upon the flow of current in circuit i.

The basic, or "d.c.," inductance of a circuit is easily obtained by determining the total flux linkages to a given circuit and dividing by the magnitude of the current producing that flux. The flux linkages within a conductor will depend upon the current distribution within the conductor. The inductance of a transmission line conductor can be defined as two parts: the internal inductance L_i, due to varying linkages within

the conductor itself, and external inductance L_e, due to the linkages between the conductor and the return current conductors.

For a uniform current density over the cross section of a cylindrical conductor, the internal inductance can easily be shown to be

$$L_i = \frac{\mu}{8\pi} \text{ H/m}$$

and is independent of the size of the conductor. This is sometimes referred to as the internal d.c. inductance per unit length. The effect of nonuniform current distribution on this value is discussed in the section on resistance.

1. Single conductor lines

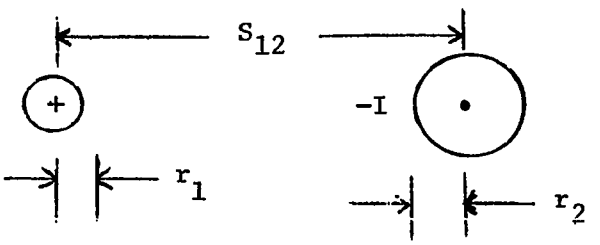

Figure 4. Typical parallel conductor configuration

If the current density is not uniform due to skin effect or some other cause, the value of the internal inductance is no longer independent of the conductor radius and must be modified accordingly.

If all currents in the circuit are confined to two conductors as shown in Figure 4, any flux lines due to I at a radius greater than $S_{12} + r_2$ will enclose no net current, and the linkages beyond this radius will

be zero. This limits the external linkages for the current in conductor 1 to a radius no larger than $S_{12} + r_2$. Although the net current linked by the flux changes between $S_{12} - r_2$ and $S_{12} + r_2$, the mean value S_{12} will give exact results for uniform current density in conductor 2. The total external flux linkages to conductor 1 can therefore be obtained by integrating the flux linkages from r_1 to S_{12}

$$\lambda_e = \frac{\mu I d\ell}{2\pi} \int_{r_1}^{S_{12}} \frac{dr}{r} = \frac{\mu I d\ell}{2\pi} \ln \frac{S_{12}}{r_1}$$

from which the external inductance per unit length can be obtained.

$$L_e = \frac{\lambda_e}{I d\ell} = \frac{\mu}{2\pi} \ln \frac{S_{12}}{r_1}$$

The contribution of the internal linkages of conductor 1 to the total can be added to give a total inductance per unit length of

$$L_1 = L_i + L_e = \frac{\mu_o}{2\pi} \left[\frac{\mu_r}{4} + \ln \frac{S_{12}}{r_1} \right]$$

If the conductors are nonmagnetic, ($\mu_r = 1$), and $r_1' = r_1 e^{-\frac{1}{4}}$ is the equivalent radius of conductor 1 for inductance calculations,

$$L_1 = \frac{\mu_o}{2\pi} \left[\frac{1}{4} + \ln \frac{S_{12}}{r_1} \right] = \frac{\mu_o}{2\pi} \ln \frac{S_{12}}{r_1'}$$

and similarly,

$$L_2 = \frac{\mu_o}{2\pi} \ln \frac{S_{12}}{r_2'}$$

The total inductance per unit length for this pair of lines would be

$$L_{eq} = L_1 + L_2 = \frac{\mu_o}{\pi} \ln \frac{S_{12}}{\sqrt{r_1' r_2'}}$$

The contribution of each conductor to the overall inductance per unit length for a symmetrical line should then be equal to half of the total inductance, or

$$L = \frac{\mu_o}{2\pi} \ln \frac{S_{12}}{r'} \text{ H/m}$$

2. Effects of multiple conductors

Neglecting for the moment the internal inductance of each conductor, the mutual inductance between conductor 3 and the two subconductors 1 and 2, as shown in Figure 5, may be calculated. If the current is divided

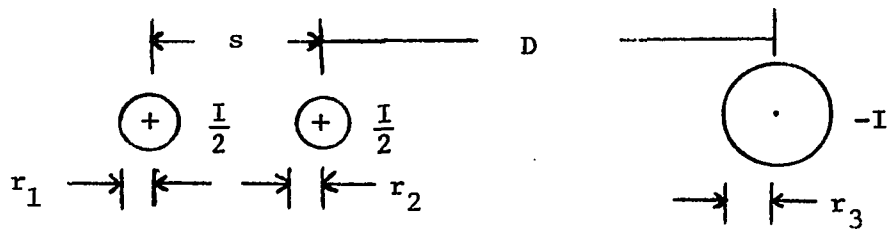

Figure 5. Multiple conductor coupling configuration

equally between conductors 1 and 2 with the total return current flowing in conductor 3, the linkages due to the positive current will be

$$\lambda_1 = \frac{\mu}{2\pi} \left(\frac{I}{2}\right)\left(\frac{1}{2}\right) \ln \frac{s}{r_1} + \frac{\mu}{2\pi} \left(\frac{I}{2}\right) \ln \frac{D+s}{s}$$

$$\lambda_2 = \frac{\mu}{2\pi} \left(\frac{I}{2}\right)\left(\frac{1}{2}\right) \ln \frac{s}{r_2} + \frac{\mu}{2\pi} \left(\frac{I}{2}\right) \ln \frac{D}{s}$$

The linkages due to the negative current will be

$$\lambda_3 = \frac{\mu}{2\pi} (I) \ln \frac{D}{r_3} + \frac{\mu}{2\pi} \left(\frac{I}{2}\right) \ln \frac{D+s}{s}$$

Summing the linkages and dividing by the current I obtains

$$L = \frac{\lambda_1+\lambda_2+\lambda_3}{I} = \frac{\mu}{2\pi} \ln \frac{\sqrt[4]{D^2(D+s)^2}}{\sqrt[4]{s^2 r_1 r_2}} + \frac{\mu}{2\pi} \ln \frac{\sqrt[4]{D^2(D+s)^2}}{r_3}$$

Comparing this to the single conductor case, it can be seen that the distance term in the numerator has become the geometrical mean distance (GMD) between the positive and negative conductors, while the radical in the denominator of the first logarithmic term represents a geometric mean of the radii and the separations in the group of positive conductors. This term is commonly referred to as the geometric mean radius (GMR), or more precisely, the <u>self</u>-geometrical mean distance (D_s), as opposed to the <u>mutual</u>-geometrical mean distance (D_m = GMD) above.

The inductance per unit length can be generalized for multiple conductor single phase systems as

$$L = \frac{\mu_o}{2\pi} \ln \frac{(GMD)^2}{(GMR_1)(GMR_2)} \text{ H/m}$$

The division of current between subconductors can be seen to reduce the effective inductance per unit length by increasing the effective radius of the conductor. For the two and three subconductor cases, this can be shown to be a reduction of $2N \times 10^{-7} \ln(s/r')$, where N is the number of subconductors, s is the subconductor spacing, and r' is the equivalent conductor radius as previously defined.

In general, the GMR of a bundle of N subconductors can be found from

$$GMR = \sqrt[N^2]{e^{-N/4} \left(\prod_i^N r_i\right)\left(\prod_{i,j}^N S_{ij}\right)}$$

which, for a symmetrical bundle with N>1, becomes

$$GMR = \sqrt[N]{N(r') \left(\frac{s}{2\sin\frac{\pi}{N}}\right)^{N-1}}$$

These equations are based on a uniform current density within the conductors. Any distortion of this current density due to skin effects will reduce the internal inductance of the conductors and the resulting total inductance accordingly.

3. Inductance in three-phase system

If no ground return current is assumed in a three-phase system so that $I_a + I_b + I_c = 0$, the inductance per meter per phase can be calculated by assuming that at some distance D_x, very remote from the circuit

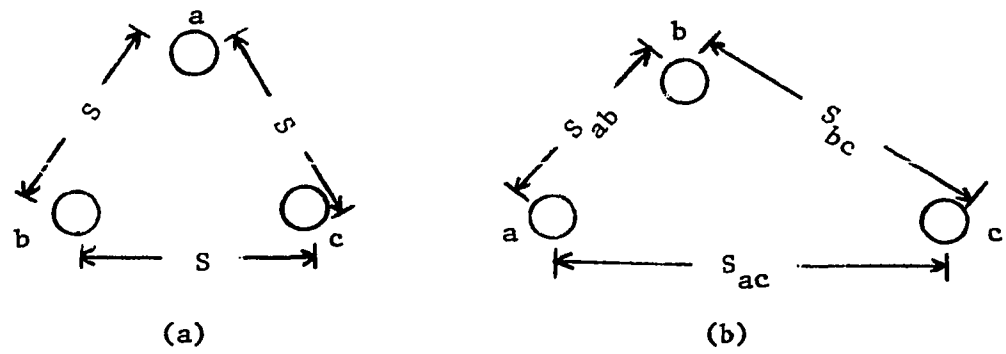

Figure 6. Three-phase transmission line configurations

conductors, the flux density approaches zero. The flux linkages to conductor a will then be

$$\lambda_a = \frac{\mu_o}{2\pi}\left[I_a \ln \frac{D_x}{r_a'} + I_b \frac{D_x}{S_{ab}} + I_c \ln \frac{D_x}{S_{ac}} \right]$$

$$= \frac{\mu_o}{2\pi}\left[I_a \ln \frac{1}{r_a'} + I_b \ln \frac{1}{S_{ab}} + I_c \ln \frac{1}{S_{ac}} + (I_a + I_b + I_c) \ln D_x \right]$$

Since $I_a = -I_b - I_c$, letting $S_{ab} = S_{ac} = S_{bc}$, the flux linkages become

$$\lambda_a = \frac{\mu_o}{2\pi} I_a \ln \frac{S}{r_a'}$$

and the inductances

$$L_a = \frac{\mu_o}{2\pi} \ln \frac{S}{r_a'}$$

$$L_b = \frac{\mu_o}{2\pi} \ln \frac{S}{r_b'}$$

$$L_c = \frac{\mu_o}{2\pi} \ln \frac{S}{r_c'}$$

which are obviously equal if $r_a = r_b = r_c$.

Making the same assumptions concerning D_x and the currents for Figure 6b, it follows that

$$\lambda_a = \frac{\mu_o I_a}{2\pi}\left[\ln \frac{S_{ab}}{r_a'} + \frac{I_c}{I_a} \ln \frac{S_{ab}}{S_{ac}} \right]$$

$$\lambda_b = \frac{\mu_o I_b}{2\pi}\left[\ln \frac{S_{bc}}{r_b'} + \frac{I_c}{I_b} \ln \frac{S_{bc}}{S_{ab}} \right]$$

$$\lambda_c = \frac{\mu_o I_c}{2\pi} \quad \ln \frac{S_{ca}}{r_c'} + \frac{I_b}{I_c} \ln \frac{S_{ca}}{S_{bc}}$$

Assuming an equal division of the return current between the two other lines,

$$L_a = \frac{\mu_o}{2\pi} \ln \frac{\sqrt{S_{ab} S_{ac}}}{r_a'}$$

$$L_b = \frac{\mu_o}{2\pi} \ln \frac{\sqrt{S_{ab} S_{ac}}}{r_b'}$$

$$L_c = \frac{\mu_o}{2\pi} \ln \frac{\sqrt{S_{bc} S_{ac}}}{r_c'}$$

If the three lines are transposed twice to obtain equal lengths at each phase position as shown, the average inductance per phase becomes

$$L_{av} = \frac{\mu_o}{2\pi} \ln \frac{\sqrt{S_{ab} S_{bc} S_{ca}}}{r'}$$

or

$$L_{av} = \frac{\mu_o}{2\pi} \ln \frac{S_{eq}}{GMR}$$

for bundled conductors where

$$S_{eq} = \sqrt[3]{S_{ab} S_{bc} S_{ca}}$$

and r' and GMR the effective conductor radius and bundled radius as defined earlier.

C. Resistance

For d.c. transmission lines, the current distribution over the cross section of a cylindrical conductor is essentially uniform. For a single solid conductor of circular cross section and radius a, the resistance per unit length will be

$$R_{DC} = \frac{1}{\sigma\pi a^2} \ \Omega/m$$

where σ is the conductivity of the conductor material relating the current density $\overline{J}$ to the electric field intensity $\overline{E}$.

$$\overline{J} = \sigma\overline{E}$$

For stranded conductors, the resistance is not exactly 1/N times the resistance of a single strand since the out layers will be slightly longer than the core, due to the twisting necessary to add mechanical stability to the group. If k is the pitch factor which gives this additional length with respect to the core, a 7-strand conductor should have a d.c. resistance of

$$R_{DC} = \frac{1}{2\pi\sigma a^2} \left(\frac{k}{k+6}\right)$$

1. Skin effect

For the smaller conductors with diameters of approximately 1 cm or less, resistance varies approximately as the inverse square of the conductor diameter for both a.c. and d.c. systems. In larger conductors,

however, internal a.c. magnetic fields tend to force the current toward the outer surface of the conductor and produce a nonuniform current density. This concentration of current near the surface of a conductor is known as "skin effect" and is typical of a.c. currents in any conductor. Skin effect is associated with a "depth of penetration" which is inversely proportional to the square root of the conductivity and permeability of the material and the frequency at which the system is operating. At a frequency of 60 Hz, the depth of penetration for copper is 8.5 mm, while for aluminum, it is 11 mm.

One result of this skin effect is a reduction of the effective cross section of a conductor which increases the effective resistance per unit length for a.c. currents. Another result is a reduction of the internal flux linkages within the conductor which reduces its internal inductance. These phenomena are shown in the following development.

Solution of the equations of Maxwell within a cylindrical conductor of finite conductivity leads to a current density function in terms of the zero order bessel function of a complex argument.

$$J_z(r) = A\, J_o\, (\sqrt{-j\omega\mu\sigma}\, r)$$

$$= A[\mathrm{ber}(\sqrt{\omega\mu\sigma}\, r) + j\, \mathrm{bei}(\sqrt{\omega\mu\sigma}\, r)]$$

where ber x and bei x are the real and imaginary parts respectively of the function $J_o(\sqrt{-j}\, x)$ (9; 10). For planar conductors, the depth of penetration of an electromagnetic field into the conductor is measured in terms of a skin depth, δ, at which the field at the surface has been

attenuated to e^{-1} times its surface value. This can be shown to be related to the material conductivity, σ, and permeability, μ, by

$$\delta = \sqrt{\frac{2}{\omega\mu\sigma}}$$

Substituting this quantity into the current density equation changes the variable to a ratio of radius to skin depth, and the current density equation can be written as

$$J_z(r) = A[\text{ber}(\sqrt{2}\ r/\delta) + j\ \text{bei}(\sqrt{2}\ r/\delta)\ ]$$

Tables and graphs of these functions are available (11; 12; 13), but for 60 Hz, r/δ is small enough that series approximations with two or three terms are sufficiently precise for most practical applications.

From the series expansion of the zero order bessel function of the first kind,

$$J_o(r) = \sum_{k=o}^{\infty} \frac{(-1)^k}{(k!)^2} \left(\frac{r}{2}\right)^{2k}$$

the first terms of Kelvin's ber and bei functions in series form can be shown to be (14)

$$\text{ber}(r) \simeq 1 - 64\left(\frac{r}{8}\right)^4 + \frac{1024}{9}\left(\frac{r}{8}\right)^8 \cdots\cdots$$

$$\text{bei}(r) \simeq 16\left(\frac{r}{8}\right)^2 - \frac{1024}{9}\left(\frac{r}{8}\right)^6 \cdots\cdots$$

To find the ratio of the current density at any radius r within a cylindrical conductor of radius a to the current density at the surface,

$$\frac{J_z(r)}{J_z(a)} = \frac{\text{ber}\left(\frac{\sqrt{2}r}{\delta}\right) + i\,\text{bei}\left(\frac{\sqrt{2}r}{\delta}\right)}{\text{ber}\left(\frac{\sqrt{2}a}{\delta}\right) + i\,\text{bei}\left(\frac{\sqrt{2}a}{\delta}\right)}$$

2. A.C. impedance of a solid cylindrical conductor

Defining

$$Z = R + j\omega L_i = \frac{E_z(a)}{I_z} = \frac{J_z(a)}{\sigma I_z}$$

the ratio of the a.c. resistance to the d.c. resistance of a solid cylindrical conductor can be shown to be

$$\frac{R_{ac}}{R_{dc}} = \frac{\sqrt{2}a}{2\delta}\left\{\frac{\text{ber}\left(\frac{\sqrt{2}a}{\delta}\right)\text{bei}'\left(\frac{\sqrt{2}a}{\delta}\right) - \text{ber}'\left(\frac{\sqrt{2}a}{\delta}\right)\text{bei}\left(\frac{\sqrt{2}a}{\delta}\right)}{\left[\text{ber}'\left(\frac{\sqrt{2}a}{\delta}\right)\right]^2 + \left[\text{bei}'\left(\frac{\sqrt{2}a}{\delta}\right)\right]^2}\right\}$$

Since the internal inductance of a conductor also depends upon the current distribution within the conductor, the ratio of the a.c. inductance to the "d.c." inductance for a solid cylindrical conductor can be found in a similar manner to be

$$\frac{L_i}{L_{iDC}} = \frac{4\delta}{\sqrt{2}a}\left\{\frac{\text{ber}\left(\frac{\sqrt{2}a}{\delta}\right)\text{ber}'\left(\frac{\sqrt{2}a}{\delta}\right) + \text{bei}\left(\frac{\sqrt{2}a}{\delta}\right)\text{bei}'\left(\frac{\sqrt{2}a}{\delta}\right)}{\left[\text{ber}'\left(\frac{\sqrt{2}a}{\delta}\right)\right]^2 + \left[\text{bei}'\left(\frac{\sqrt{2}a}{\delta}\right)\right]^2}\right\}$$

As might be expected, the ratio of R_{AC} to R_{DC} increases as a/δ increases while the ratio of $L_i(AC)$ to $L_i(DC)$ decreases. This will place some practical limits on the sizes of conductors which will be efficiently utilized in high voltage transmission line designs.

D. Capacitance

The characteristic of a transmission line most closely associated with the electric field distribution is the capacitance. Capacitance can be defined as the ability of a system or device to store electric charge. Most generally it is defined mathematically as

$$C = \frac{Q}{V}$$

where C is in Farads, Q is charge in Coulombs and V is the electric potential in volts.

Since transmission lines are usually made up of long cylindrical conductors over which the charge can distribute itself, the distributed capacitance per unit length can be defined in terms of a distributed line charge per unit length ρ_ℓ as

$$C = \frac{\rho_\ell}{V} \text{ Farads/unit length}$$

These filaments of distributed line charge lend themselves to the development of cylindrical equipotential surfaces since there is an inherent radial symmetry to their fields.

In almost any textbook on electromagnetic fields, the electrical potential and electric field intensity produced by a uniform line charge of essentially infinite length are shown to be (6-9)

$$V(a) - V(b) = \frac{\rho_\ell}{2\pi\epsilon} \ln(b/a) \quad \text{volts}$$

where b and a are radial distances from the line charge, and

$$E_r(a) = \frac{\rho_\ell}{2\pi\varepsilon a} \qquad \text{volts/meter}$$

Since the electric field intensity from a single line charge will be constant on a cylinder of radius a, the potential on this surface must be constant and will determine an equipotential surface. The electric field intensity is the gradient of the potential field, and therefore is always orthogonal to an equipotential surface.

1. Electrostatic fields

If two line charges of equal magnitude but opposite polarity, ρ_1 and $-\rho_1$, are placed parallel to the z axis on opposite sides of the x,z plane and equidistant from that plane at y = h and y = -h respectively, the y = 0 plane will be an equipotential surface (V=0). It can then be

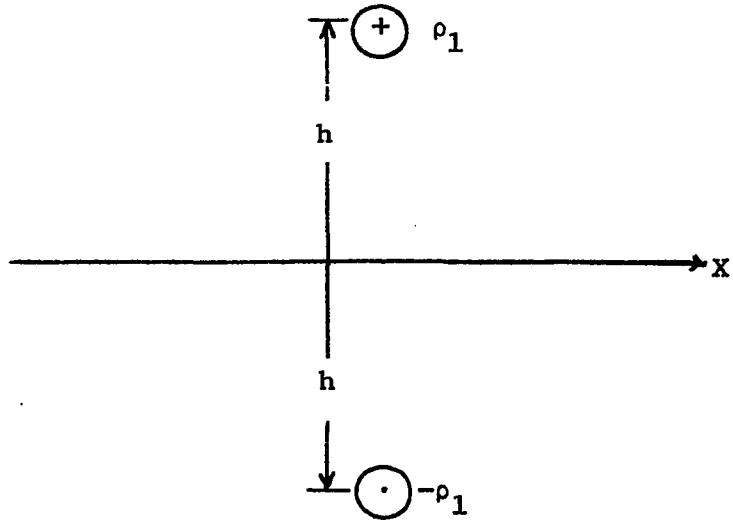

Figure 7. Line-charge pair with odd symmetry

shown that the other equipotential surfaces of such a system are represented by a family of eccentric circular cylinders whose centers converge to the position of line charges. The potentials of these surfaces can be found from the relationship

$$V = \frac{\rho_1}{2\pi\varepsilon} \ln K$$

where K is the ratio of the two radii from the sources to the position where V is measured. The locus of this equipotential surface is defined by

$$x^2 + y^2 + h^2 = 2hy\ (K^2 + 1)/(K^2 - 1)$$

K = 1 represents the y = 0 plane, and V will be greater than zero for K > 1. For K < 1, the potentials will be negative and the surfaces mirror images of the surfaces with a reciprocal K.

This solution for the case of odd symmetry leads to the theory of images (6-8). For parallel cylinders, this theory postulates that the charge distribution induced on a cylindrical conducting surface of radius r by a line charge parallel to its axis, and D meters away will be equivalent to the field produced by a line charge of opposite polarity d meters from the axis and an equal line charge at the center of the cylinder. This radial distance d can be found from

$$d = r^2/D$$

The zero reference for the system potentials can be changed by increasing or decreasing the axial charge.

If two parallel line charges are of the same sign, the equipotential surfaces are no longer circular cylinders, but form a family of curves

known as "the ovals of Cassini." Their locus in the x,y plane can be defined mathematically as

$$(x^2 + y^2 + h^2)^2 - 4h^2y^2 = c^4$$

where the product of the distances from the two foci at ± h to any point on the curve is equal to c^2. Since none of these curves are perfectly circular, it is necessary to use multiple images when matching circular cylindrical boundaries to line charges of the same polarity.

2. Single wire above ground

This study will deal primarily with horizontal configurations with bundled conductors in each phase. However, to understand the effects of bundling, it is first necessary to look at the simplest open-wire line, a single conductor over a conducting ground.

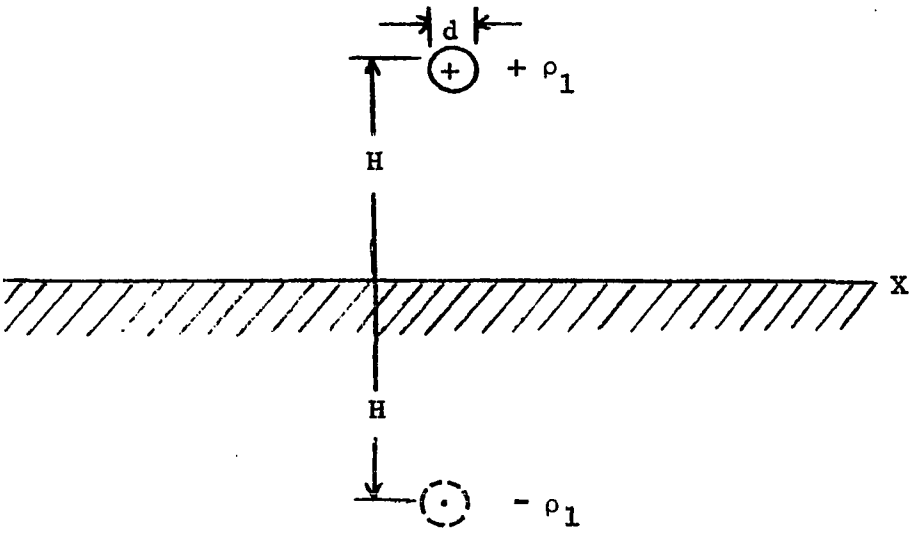

Figure 8. A single-charged conductor over conducting ground

The assumption of a perfectly conducting ground will be justified elsewhere.

Assuming a perfectly conducting ground, any linear charge ρ placed on the cylindrical conductor at $y = H$ will produce an image charge $-\rho$ in the ground plane which will appear to be on a conductor at $y = -H$ directly beneath the actual charge. This is the classical case of odd symmetry and has a very simple analytical solution. The line charges will be slightly eccentric to the cylinder axes at a height determined by the ratio of the radius squared to the separation between conductors

$$h = \sqrt{H^2 - (d/2)^2}$$

The potential of the conductor with respect to the ground will be

$$V_1 = \frac{\rho_1}{2\pi\epsilon} \ln \left[\frac{2H}{d} + \sqrt{\left(\frac{2H}{d}\right)^2 + 1} \right]$$

If V_1 is fixed, the solution for the necessary line charge density will be

$$\rho_1 = \frac{2\pi\epsilon V_1}{\ln \left[\frac{2H}{d} + \sqrt{\left(\frac{2H}{d}\right)^2 + 1} \right]}$$

From the definition of capacitance, the capacitance per unit length between the conductor and the conducting ground plane becomes

$$C = \frac{\rho_1}{V} = \frac{2\pi\epsilon}{\ln \left[\frac{2H}{d} + \sqrt{\left(\frac{2H}{d}\right)^2 + 1} \right]}$$

In most practical cases, the conductor is so far from its image and so small in diameter that the electric fields can be obtained by assuming

that the equivalent charge is concentric with the conductor. This allows the capacitance to be calculated from the simplified equation

$$C = \frac{2\pi\varepsilon}{\ln \frac{4H}{d}}$$

3. Multiple conductor systems

The analytical solution of a multiple conductor system becomes much more complicated than the single conductor system since the theory of images requires each conductor to carry image charges for each of the other conductors, as well as images of the charges induced in the ground plane. For a first order approximation of the simple two wire line over ground such as might be used in a d.c. or single phase a.c. system, a minimum of sixteen line charges would be required. A second order

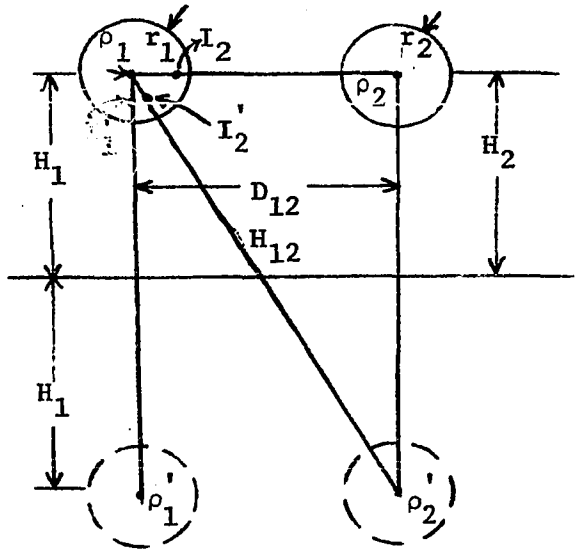

$$H_{12} = \sqrt{(H_1+H_2)^2 + D_{12}^2}$$

$$S_{12} = \sqrt{(H_1-H_2)^2 + D_{12}^2}$$

Figure 9. Two-wire transmission line over ground

approximation would require at least 48 line charges. Some of these line charges in close proximity can be merged into a single line charge.

In those cases where the radii of the conductors is very small with respect to the separations between conductors, the displacement of line charges from the center of the conductor due to imaging is very small and does not appreciably effect the potential or the distant fields, but may appreciably effect the near fields at the conductor surface. This simplification will not appreciably effect the capacitance calculations since the total charge remains essentially the same.

For the two-conductor case shown above, the equations for the potentials V_1 and V_2 at the surface of the conductors 1 and 2 respectively can be written

$$V_1 = \frac{\rho_1}{2\pi\epsilon} \ln \frac{H_1}{r_1} + \frac{\rho_1'}{2\pi\epsilon} \ln \frac{H_1}{2H_1-r_1} + \frac{\rho_2}{2\pi\epsilon} \ln \frac{H_2}{S_{12}-r_1} + \frac{\rho_2'}{2\pi\epsilon} \ln \frac{H_2}{H_{12}-r_1}$$

$$V_2 = \frac{\rho_1}{2\pi\epsilon} \ln \frac{H_1}{S_{12}-r_2} + \frac{\rho_1'}{2\pi\epsilon} \ln \frac{H_1}{H_{12}-r_2} + \frac{\rho_2}{2\pi\epsilon} \ln \frac{H_2}{r_2} + \frac{\rho_2'}{2\pi\epsilon} \ln \frac{H_2}{2H_2-r_2}$$

With the ground plane at zero potential, symmetry requires that

$$\rho_1' = -\rho_1 \text{ and } \rho_2' = -\rho_2$$

so that

$$V_1 = \frac{\rho_1}{2\pi\epsilon} \ln \frac{2H_1-r_1}{r_1} + \frac{\rho_2}{2\pi\epsilon} \ln \frac{H_{12}-r_1}{S_{12}-r_1}$$

$$V_2 = \frac{\rho_1}{2\pi\epsilon} \ln \frac{H_{12}-r_2}{S_{12}-r_2} + \frac{\rho_2}{2\pi\epsilon} \ln \frac{2H_2-r_2}{r_2}$$

This can be written in matrix form using Maxwell's potential coefficients, p_{ij}

$$\begin{bmatrix} V_1 \\ V_2 \end{bmatrix} = \begin{bmatrix} p_{11} & p_{12} \\ p_{21} & p_{22} \end{bmatrix} \begin{bmatrix} \rho_1 \\ \rho_2 \end{bmatrix}$$

or simply

$$[V] = [P]\ [Q]$$

Since the dimensions of r are much less than the dimensions of H, the r in the numerator can be dropped and the matrix elements are then

$$p_{11} \simeq \frac{1}{2\pi\epsilon} \ln \frac{2H_1}{r_1} \qquad p_{12} \simeq \frac{1}{2\pi\epsilon} \ln \frac{H_{12}}{S_{12}}$$

$$p_{21} \simeq \frac{1}{2\pi\epsilon} \ln \frac{H_{12}}{S_{12}} \qquad p_{22} \simeq \frac{1}{2\pi\epsilon} \ln \frac{2H_2}{r_2}$$

Inverting the P matrix to solve for Q shows that the inverse P matrix is the partial capacitance matrix C since

$$[Q] = [P^{-1}]\ [V] = [C]\ [V]$$

This is a general solution for an n conductor system where Q and V are n dimensional column matrices (vectors), and P and C are n x n square matrices.

From the definitions of p_{ij} above, it can be seen that the C matrix for the two-conductor system becomes, by inverting the P matrix,

$$C = \frac{2\pi\epsilon \begin{bmatrix} \ln \frac{2H_2}{r_2} & -\ln \frac{H_{12}}{S_{12}} \\ -\ln \frac{H_{12}}{S_{12}} & \ln \frac{2H_1}{r_1} \end{bmatrix}}{\left\{ \ln \frac{2H_2}{r_2} \ln \frac{2H_1}{r_1} - \left(\ln \frac{H_{12}}{S_{12}} \right)^2 \right\}}$$

For a symmetrical system in which $r_1 = r_2$ and $H_1 = H_2$, $C_{11} = C_{22}$ and the determinant in the denominator reduces to the product

$$\left(\ln \frac{2H_1 \, H_{12}}{r_1 \, S_{12}} \right) \quad \left(\ln \frac{2H_1 \, S_{12}}{r_1 \, H_{12}} \right)$$

The negative sign on the off-axis terms implies that the charge required to establish a particular potential on a conductor in the presence of another similarly charged conductor will be less than that required to obtain the same potential in the absence of the other conductor.

The total capacitance from any conductor to ground, or to another conductor, involves the addition of the capacitance through each separate path between the two conductors.

It may be seen that the computation of individual capacitances for each subconductor of a multiphase circuit with four or more subconductors per phase becomes quite a prodigious task, even with the assumption of a single line charge per conductor. The solutions for a more exact set of

capacitances must be left to high speed digital computers, assuming some simplifying approximations.

4. Capacitance of bundled conductors

Since most HV, EHV and UHV systems use bundled conductors, it is often useful to treat the bundle as an equivalent single conductor. To see the effect of bundling on the capacitance of such an equivalent conductor, let $V_1 = V_2$ in Figure 9. For simplicity, let $r_1 = r_2$ and $H_1 = H_2$. If $r_1 \ll D_{12} \ll H_1$, then $H_{12} \simeq 2H_1$, and

$$\rho_1 = \rho_2 = \frac{2\pi\varepsilon \left[\ln \frac{2H_1}{r_1} - \ln \frac{2H_1}{D_{12}} \right] V_1}{\left(\ln \frac{2H_1}{r_1} \right)^2 - \left(\ln \frac{2H_1}{D_{12}} \right)^2}$$

$$\simeq \frac{2\pi\varepsilon\, V_1}{\ln \left(\frac{4H_1^2}{D_{12} r_1} \right)}$$

$$\rho_1 = \rho_2 = \frac{2\pi\varepsilon\, V_1}{2\ln \frac{2H_1}{\sqrt{D_{12} r_1}}}$$

The total charge density will be $2\rho_1$ to give an effective capacitance for the two conductors together as

$$C_o = \frac{2\rho_1}{V_1} = \frac{2\pi\varepsilon}{\ln \frac{2H_1}{\sqrt{D_{12} r_1}}}$$

which is the capacitance of an equivalent single conductor with a radius of

$$r = \sqrt{D_{12} r_1}$$

This would be identical to the GMR of the equivalent conductor for calculating inductance, except that there is no reduction of r_1 to account for internal inductance.

III. ELECTROSTATIC FIELD CALCULATIONS

A. Introduction

The growing concern of ecologists over the environmental effects of electric fields in the vicinity of EHV and UHV transmission lines, as well as the necessity of reducing corona phenomena for more efficient power transmission, have created a new interest in the field configurations obtained in the neighborhood of such lines. The availability of high speed computers with graphical capabilities has made such studies much more practical with detail which was impossible only a few years ago. The basic principles of such calculations are reviewed here followed by a description of the HIVAC2 computer program, which is used to obtain the numerical solutions and graphic outputs produced in this investigation.

B. Verification of Perfectly Conducting Ground Assumption

Most analytical techniques and numerical methods used for determining the electrostatic fields in the vicinity of open wire transmission lines assume that the ground is essentially a perfect conductor. Since the actual conductivity may range from one mho/meter in saturated clay, down to as little as 10^{-9} mho/meter for dry limestone, the validity of such an assumption is not obvious. Over the same range

of ground materials, the relative dielectric constant ranges from about 4 for dry sand or stone, to 30 for saturated sand, and up to 81 for fresh water (15).

With this wide variation in both conductivity and dielectric constant, it might appear questionable to assume a perfectly conducting earth in the calculation of electric fields, due to charged lines over a planar earth. A careful examination of the boundary conditions does, in fact, show this assumption to be valid in most cases.

1. Continuity of electric fields at a planar boundary

Any good text on electromagnetics develops the continuity of electric fields across a planar boundary between two dissimilar materials in much the same way (6-8). In the absence of any free surface charge at the interface, the normal component of the electric flux density must be continuous across the boundary, and the tangential electric field intensity components must also be continuous across the boundary. If the interface is between a dielectric and a conducting material, the field within a conductive material will be largely a function of the conductivity rather than the dielectric. In the case of a perfectly conducting medium, no fields can exist within the conductor and the external fields induce a surface charge upon which the normal electric flux will terminate. The tangential field in this case must be zero at the surface to satisfy the continuity conditions.

When the fields are to be determined in only one region, it is often possible to postulate an equivalent set of discrete charges which will produce the same field at the interface as the induced surface charge. This method of images for determining the fields in the vicinity of a conducting surface is quite commonly used, and is the basis of the development of electric fields due to high voltage transmission lines over ground.

The assumption of a partial image in a high dielectric constant material has been shown by Smythe and others to provide a fairly simple solution to this type of boundary problem for static fields (7). For the region of lower dielectric constant, the fields can be calculated by assuming that the image charges are reduced by a factor determined from the relative dielectric constants.

$$\rho_i = \frac{1 - \varepsilon_r}{1 + \varepsilon_r} \rho_o$$

For the region of higher dielectric constant, the electric fields can be obtained by assuming a uniform region in which the original charge is replaced by a partial charge

$$\rho_o' = \frac{2\varepsilon_r}{1 + \varepsilon_r} \rho_o$$

where ε_r is the ratio of the higher to the lower dielectric constant, assuming that the true charge is in the lower dielectric constant medium.

A typical field plot of the partial fields and the resultant fields matched at the interface are shown in Figure 10. The true fields are

shown as solid lines, while the apparent fields are shown as dotted lines in the construction.

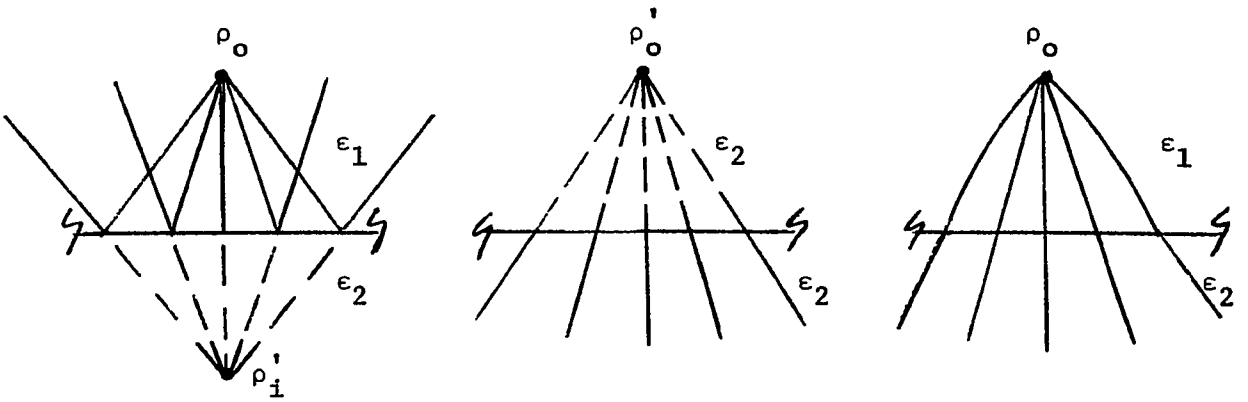

(a) (b) (c)

(a) Construction of field in region 1

(b) Construction of field in region 2

(c) Matched boundary for actual fields

Figure 10. Electric fields in the vicinity of a dielectric boundary

2. Images in partially conducting dielectrics

For quasi static fields, it is necessary to allow for displacement currents across the boundary between the two media. In this case, we can make use of Ampere's Law, as expressed by the field equations to show that the divergence of the total current is zero in the absence of any induced voltages due to a changing magnetic field. This leads to a complex coefficient for the electric fields ($\sigma + j\omega\varepsilon$), which will determine the continuity of the normal components across the boundary. If the current divergence is zero, then the continuity expression must be

$$(\sigma_1 + j\omega\varepsilon_1)E_{n1} = (\sigma_2 + j\omega\varepsilon_2)E_{n2}$$

The partial image expression used for nonconducting media should be replaced by

$$\rho_i = \frac{(\sigma_1+j\omega\varepsilon_1) - (\sigma_2+j\omega\varepsilon_2)}{(\sigma_1+j\omega\varepsilon_1) + (\sigma_2+j\omega\varepsilon_2)} \rho_o$$

and the equivalent source for region 2,

$$\rho_o' = \frac{2(\sigma_2+j\omega\varepsilon_2)}{(\sigma_1+j\omega\varepsilon_1) + (\sigma_2+j\omega\varepsilon_2)} \rho_o$$

Assuming that the source region (1) is air, the image factor will reduce to

$$K_i = \frac{j\omega\varepsilon_o - (\sigma_2+j\omega\varepsilon_2)}{j\omega\varepsilon_o + (\sigma_2+j\omega\varepsilon_2)} = \frac{1 - \varepsilon_r + j\frac{\sigma_2}{\omega\varepsilon_o}}{1 + \varepsilon_r - j\frac{\sigma_2}{\omega\varepsilon_o}}$$

At the power frequency of 60 Hz, $\omega = 377$, so that

$$K_i = \frac{1 - \varepsilon_r + j3\text{x}10^9\sigma}{1 + \varepsilon_r - j3\text{x}10^9\sigma}$$

It can be seen that this expression will be essentially -1 unless the conductivity is so small that

$$\sigma \leq \varepsilon_r/3\text{x}10^9$$

which rarely occurs except in very dry sand. The assumption of perfect conduction at the ground surface appears to be quite appropriate except at extremely high frequencies or over extremely dry sand or rock surfaces.

C. Electric Field Distribution

Since the ground can be assumed a perfect conductor at power frequencies, the electric field can be calculated using the theory of images where the image charge is the negative of the actual line charge. To allow for phasor differences, the charges can be determined as phasor quantities to match the phasor voltages at the conductors with respect to some reference point, usually the ground.

As in the discussion of capacitance, the procedure here shall be to consider one and two conductors above ground, and then generalize the solution for three or more conductors.

1. Single conductor above ground

For a single conductor above gound, an exact analytical solution is easily obtained by applying the familiar image theory which allows for

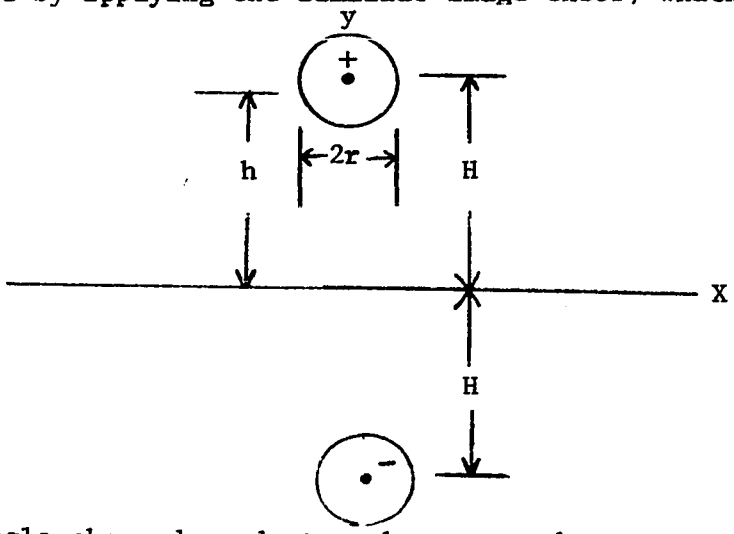

Figure 11. Single charged conductor above ground

exact location of a charge filament with respect to the conductor surface. If the conductor of radius r is centered at a height H above the ground plane, the filament of charge required to produce an equipotential at the conductor surface must be at the height

$$h = \sqrt{H^2 - r^2}$$

with its image an equal distance below the midplane. The electric field in the region of interest is then the sum of the fields from these two line charges and can be obtained from the gradient of the electric potential.

$$\bar{E}(R) = -\nabla \left\{ \frac{\rho}{2\pi\epsilon} \ln \frac{R_2}{R_1} \right\} = \frac{-\rho}{2\pi\epsilon} \nabla (\ln R_2 - R_1)$$

Letting

$$R = \sqrt{x^2 + y^2}$$

$$R_1 = \sqrt{x^2 + (y-h)^2}$$

$$R_2 = \sqrt{x^2 + (y+h)^2}$$

The expression for the electric field becomes

$$\bar{E}(R) = \frac{-\rho}{2\pi\epsilon} \left[\frac{x\hat{a}_x + (y+h)\hat{a}_y}{x^2 + (y+h)^2} - \frac{x\hat{a}_x + (y-h)\hat{a}_y}{x^2 + (y-h)^2} \right]$$

At the plane y = 0, the x component of the field disappears and the normal component of the electric field becomes simply a function of the x coordinate, or the angle which a ray from the conductor to the point x makes with the vertical.

$$\bar{E}(x) = \frac{-2\rho}{2\pi\varepsilon}\left[\frac{h\,\hat{a}_y}{x^2 + h^2}\right] = \frac{-\rho}{2\pi\varepsilon h}\,[2\cos^2\theta]\,\hat{a}y$$

The electric field in the plane can be written in terms of the conductor potential, V_o, as

$$\bar{E}(x) = \frac{2V_o\hat{a}_y}{h\ \ln\ (2H/r)}\left(\frac{h^2}{h^2 + x^2}\right)$$

In most cases, the error involved by replacing h with H is insignificant, and the equation becomes

$$E_y(x) = \frac{2HV_o}{(H^2+x^2)\ \ln\ (2H/r)}$$

For a single conductor, this can be written in terms of the line capacitance as

$$E_y(x) = \frac{2CV_oH}{2\pi\varepsilon(H^2+x^2)}$$

The electric field at ground level is directly proportional to the capacitance if the potential and the dielectric constant remain unchanged.

At the surface of the conductor, the electric field intensity or voltage gradient can be written in its two components as

$$E_x = \frac{\rho}{2\pi\varepsilon}\left[\frac{4hxy}{(x^2+y^2+h^2)^2 - 4h^2y^2}\right]$$

$$E_y = \frac{-\rho}{2\pi\varepsilon}\left[\frac{2h\ (x^2-y^2+h^2)}{(x^2+y^2+h^2)^2 - 4h^2y^2}\right]$$

These can be simplified to

$$E_x = \frac{\rho}{2\pi\epsilon r}\left[\frac{hx}{ry}\right]$$

$$E_y = \frac{-\rho}{2\pi\epsilon r}\left[\frac{h(H-y)}{ry}\right]$$

where

$$x^2 + (y-H)^2 = r^2$$

is the locus of the conductor surface.

2. Multiple conductors above ground

The case of two conductors over a conducting ground does not lend itself very easily to analytical solution since the required multiple

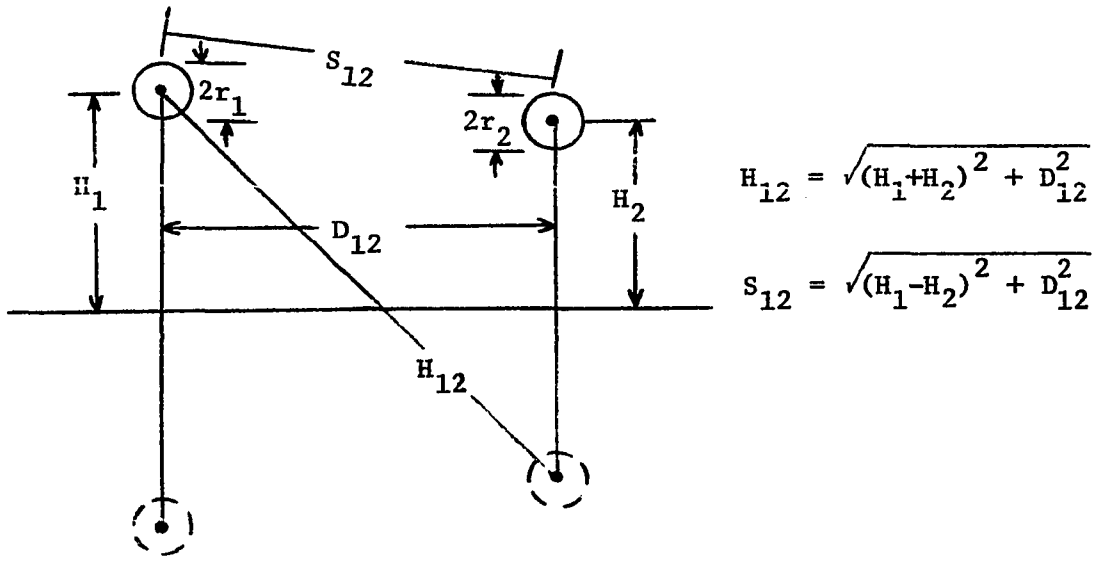

Figures 12. Two conductors and their images in plane

images can be identified only by a very tedious iterative process. The capacitances and charges can be calculated quite closely by assuming the total charge to be located on the axis of the conductor. The error term for such an assumption is on the order of r/2H.

As in Chapter II, the equivalent line charges can be found from the potential equations

$$V_1 = \frac{\rho_1}{2\pi\epsilon} \ln \frac{2H_1}{r_1} + \frac{\rho_2}{2\pi\epsilon} \ln \frac{H_{12}}{S_{12}}$$

$$V_2 = \frac{\rho_1}{2\pi\epsilon} \ln \frac{H_{12}}{S_{12}} + \frac{\rho_2}{2\pi\epsilon} \ln \frac{2H_2}{r_2}$$

which in matrix form can be written

$$[V] = [P]\ [Q]$$

Solving for Q by inverting the potential coefficient matrix P, the equation becomes

$$[Q] = [P^{-1}]\ [V] = [C]\ [V]$$

The electric field intensity can then be found by superposition, or by constructing a row matrix $\overline{A}$ with two-dimensional vector elements which multiplied by the column matrix Q obtains the desired fields. The elements of this $\overline{A}$ matrix for the two-dimensional field associated with line charges would be

$$\overline{A}_i = \frac{\overline{R} - \overline{R}_i}{2\pi\epsilon|\overline{R}-\overline{R}_i|^2} = \frac{\overline{R} - \overline{R}_i}{2\pi\epsilon(R^2+R_i^2 - 2R\ R_i\cos\alpha_i)}$$

where $\overline{R}$ is the two dimensional vector describing the field point of

interest, and $\overline{R}_i$ is the vector position of the ith line charge with respect to some abritrary common origin. α_i is the included angle between $\overline{R}$ and $\overline{R}_i$.

For the two-dimensional system, the electric field vector can be written in terms of these matrices as

$$\overline{E}(\overline{R}) = [\overline{A}]\ [Q] = [\overline{A}]\ [C]\ [V]$$

This method can be extended to any number of conductors. If only one filament of charge is attributed to each conductor, the calculated potential can only be correct at one point on each conductor. A corresponding error in the voltage gradients will also be obtained.

3. Effects of bundling on electric fields

We have already seen that increasing the capacitance of a conductor to ground will increase the magnitude of the electric field at the ground level. In Chapter II, it was shown that bundling caused an increase in the effective capacitance per phase, and therefore would be expected to increase the ground level field intensity. At the conductor surface, the distribution of the necessary charge over several conductors effectively reduces the field intensitities at the conductor surfaces.

As shown in Chapter II, if two conductors with equal radii and separated by a distance D have equal potentials with respect to the ground, a single line charge density approximation can be calculated for each conductor from the matrix equation

$$\begin{bmatrix} \rho_1 \\ \rho_2 \end{bmatrix} = \begin{bmatrix} C_{11} & C_{12} \\ C_{21} & C_{22} \end{bmatrix} \begin{bmatrix} V_1 \\ V_1 \end{bmatrix}$$

where

$$C_{11} = \frac{2\pi\varepsilon \ln 2H/r}{\left(\ln \frac{2H\sqrt{4H^2+D^2}}{Dr}\right)\left(\ln \frac{2HD}{r\sqrt{4H^2+D^2}}\right)}$$

$$C_{12} = \frac{-2\pi\varepsilon \ln(\sqrt{4H^2+D^2}/D}{\left(\ln \frac{2H\sqrt{4H^2+D^2}}{Dr}\right)\left(\ln \frac{2HD}{r\sqrt{4H^2+D^2}}\right)}$$

and if $C_{11} = C_{22}$ and $C_{12} = C_{21}$ as is to be expected in a symmetrical system,

$$\rho_1 = \rho_2 = (C_{11}+C_{12})\ V_1$$

$$= \frac{2\pi\varepsilon\ V_1}{\ln \frac{2H\sqrt{4H^2+D^2}}{Dr}}$$

$$\simeq \frac{2\pi\varepsilon\ V_1}{\ln \frac{2H}{r} + \ln \frac{2H}{D}}$$

The charge on each subconductor will be somewhat larger than half of the charge to maintain a single conductor of the same size at the required potential. The exact change in charge is dependent upon the "partial capacitance" between the two conductors. The average electric field at the conductor surface is proportional to the average charge density on

the conductor. The proximity of other charged conductors will cause some variation of the electric field around the periphery as the field from these nearby conductors aid or oppose the radial field at the conductor surface. The maximum electric field intensity on a bundled conductor will be located radially outward from the center of the bundle if the bundling is symmetrical, as indicated in Figure 13. The effect

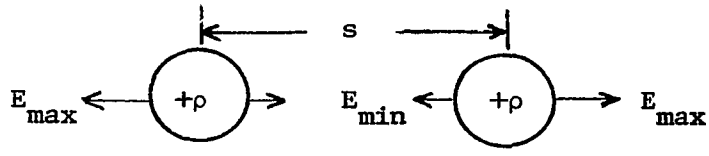

Figure 13. Maximum and minimum fields on two adjacent conductors

of distant images upon these fields is very minor compared to the proximity effects of the other conductors of a bundle.

It is seen that bundling may be used to reduce the maximum electric field intensity, or voltage gradient, at the conductor surfaces, but at the expense of increased field intensity at the ground level. It may be necessary, therefore, to adjust other physical parameters of a transmission line to obtain the most satisfactory field distribution for both surfaces. The sensitivity of these electric fields to certain line parameters is to be discussed in a later chapter.

D. Point Matching

To obtain a more accurate solution for the multiple conductor case, it is possible to approximate the surface charge distribution by a multiplicity of line-charge filaments on each conductor. Rather than attempt to locate these charges in the positions determined by an iterative application of the image principle, an arbitrary pattern may be established to facilitate the computer programming. For each charge filament within a given conductor, there can be a fixed potential established at the conductor surface.

In the HIVAC2 program which was developed for this study, a set of charges is postulated which are evenly spaced on a circular cylinder whose radius is equal to half the radius of the conductor. The potential coefficient matrix is then calculated to match the conductor potential at a line on the surface nearest to each of these charges. As the number of line charges attributed to a conductor is increased, the undulation of the potential around the surface is reduced accordingly. In most cases, six or eight charge filaments are found to be sufficient for very good results. This allows the calculation of the fields around 12 subconductors and two ground wires in a two-circuit, three-phase configuration within a reasonable time. Additional storage space may be used to refine the charge distribution on each conductor, but the increase in computation and plotting time destroys many of the advantages of the program as used on the interactive VAX system.

The electric fields generated in the vicinity of multiple conductor n-phase transmission systems can be calculated using computer programs such as HIVAC2 for point matching. Any specified voltage relationships between the conductors may be chosen. As in HIVAC2, these voltages, with their corresponding phases, are generally specified with respect to a common ground. With such computer programs, it is easy to look at the fields generated by parallel circuits with any combination of phase configurations from a "super-bundle" configuration in which corresponding phases in each circuit are adjacent to each other, to an intersticial configuration in which the parallel three-phase systems form a six-phase system by shifting the phase in one of the circuits by approximately 60 degrees.

The solution of such systems involves large matrices. For a six-phase system with three subconductors per phase and the charge distribution approximated by eight charge filaments per conductor, the partial capacitance matrix and the potential coefficient matrix must be a square 144 x 144 element matrix. The recognition of some symmetries in such a system allows for considerable savings in the necessary storage space to handle such a problem.

IV. CORONA

A. Introduction

The more or less visible discharges created in the converging electric fields near conductors of small cross section have been commonly called "corona." The origin of the term is probably due to the crown-like appearance of such phenomena near pointed conductors, such as a mast or tower (16; 17). Although similar in many respects to the total dielectric breakdown of air in a uniform electric field, the nonuniformity of these converging fields places some limitations on the extent of the observed phenomena.

Corona is basically the result of the excitation of gas molecules (17; 18) by inelastic collisions between charged particles in a nonuniform high-intensity electric field. Although these collisions may be of different types, the most important are between atoms or ions and high-velocity-free electrons liberated from their parent atom by various ionization processes. When these excited molecules return to a stable energy state, they radiate electromagnetic energy which is manifested as corona discharges.

Corona discharges may be manifested in several ways. Besides the more obvious visual and acoustical phenomena, a broad spectrum of electromagnetic radiation may also occur. This broad-band noise often

creates severe interference with broadcast and communications channels (16; 17; 18).

B. Ionization Mechanisms

The loss of electrical neutrality by an atom or molecule is known as ionization. This process is very important in many chemical reactions and generally involves both positively and negatively charged ions. Ionization may occur in solids as well as liquids and gasses (19; 20). The ionization of solids if often enhanced by solution in liquids which aid in the dissociation of the ions. It is ionization which makes electrical conductivity possible.

The ionization of gasses due to the loss or addition of electrons by otherwise neutral molecules may occur in a number of ways (16; 18; 20; 21). In each case, however, there must be an exchange of energy. This energy may be mechanical or electromagnetic, although the differentiation between these becomes clouded when dealing with quanta of energy from high-velocity particles.

1. Photoionization

Although the principal source of ionization in corona generation is from electron-atom collisions, the initial ionization is probably due to cosmic radiation or some other form of high-energy electromagnetic radiation, such as x-rays (17; 18). The α and β "rays" of cosmic origin

are actually charged particles with velocities within an order of two of the velocity of light. γ "rays" are true electromagnetic radiation with wavelengths approaching a few Angstrom units (19). Since, by Einstein's theory, the energy of a photon is inversely proportional to its wavelength,

$$W_p = hf = hc/\lambda$$

where W_p is the photon energy in joules, h is Planck's constant, c is the velocity of light, and λ is the wavelength. It can be seen that these γ ray photons must have tremendously high energy levels.

There is always some cosmic radiation of a gas, and a few atoms will gain sufficient energy from these gamma rays to excite an electron beyond the ionization potential (16; 18; 21). This creates an electron-ion pair by the process known as photoionization. The momentum of the electron will give it a velocity much greater than the heavier positive ion, so that it can ricochet through the gas particles with largely elastic collisions until captured by another atom or positive ion.

The capture of an electron by a positive ion is called recombination. The rate of recombination is a statistical function which depends upon the ion and electron densities. Equilibrium will be reached when the number of ionizations equals the number of recombinations. The energy released during these recombinations will generally be at different wavelengths than the incident energy.

2. Collisions

The great majority of the collisions between particles in a gas will be elastic. That is, there will be no energy transformations so that although kinetic energy may be transferred from one particle to another, the net kinetic energy of the system is unchanged.

On the other hand, it is possible for particles to collide in such a manner that part of the kinetic energy of one particle will be used to excite one of the other particles into a higher potential energy state. These collisions are called inelastic. How long this excited state will exist depends upon the energy states of the atom involved. If excited to an unstable state, the atom will return to a lower, more stable state very quickly (approximately 10^{-6} s). In changing states, the atom will emit a photon of radiant energy with a frequency which depends upon the energy gap to the ground state or some other lower stable state.

$$f = \frac{W_e - W_o}{h}$$

This can be represented by the symbolic equation

$$e + K.E. + A \longrightarrow A^* + e \longrightarrow A + hf + e$$

where e an electron particle, A is a neutral atom, A^* is an excited atom, and A^+ is an ionized atom. h is Planck's constant and f is the frequency of the radiation in Hertz.

If the excited state of the atom is metastable, (i.e., lasting for periods up to the order of 1 s), it is possible for a second collision to occur before the atom has returned to its ground state. This allows

further excitation to occur. If the energy gained in the second collision is sufficient the atom may become ionized, although the kinetic energy of the second electron could not have ionized the atom directly from its ground state. This step ionization is typical of the ionization of mercury vapor, where the ionization energy is approximately 12.3 eV, but ionization can occur with much lower energy particles (on the order of 3.8 eV) (17).

If the incident electron does have sufficient energy, it may impart enough energy to the neutral atom to ionize in a single step, creating a new ion-electron pair without the intermediate excited states being populated. This process, of course, increases the number of free electrons.

Ionization may also occur due to collisions between excited atoms or molecules in which the resultant may be a neutral atom, a positive ion, and a free electron.

$$A^* + A^* \longrightarrow A + A^+ + e$$

Other heavy particle collisions are also possible sources of ionization, but these are generally minor sources of free electrons. Loeb (18) lists at least twelve distinct interaction processes between ions and atoms.

In a continuous electric field, as an electron moves toward the anode, it may liberate a number of other electrons due to collisions with the gas molecules. Each of these liberated electrons accelerated by the electric field may ionize other molecules as they move toward the anode. The electron density will, therefore, be an exponential function

of the distance from the cathode so that a single electron emitted from the cathode may cause thousands of electrons to strike the anode. This multiplication of the number of free electrons along the path to the anode is called an "electron avalanche" (17).

3. Secondary emission

The energy of high-velocity gas particles colliding with the electrode surfaces is generally transformed into heat and absorbed by the electrode through heat conduction processes. It is possible, however, for such collisions to produce ionization if the energy transfer between gas and electrode atoms is sufficient to overcome the work function associated with the particular electrode material. If the gas ion strikes the electrode with a high enough velocity, its energy will be sufficient to ionize several surface atoms and free a number of electrons. These phenomena are called "secondary emission" and are generally considered as the initial mechanism in creating Trichel pulses at negative electrodes.

A similar ionization by high velocity electrons at the anode can produce a space charge near the anode which temporarily reduces the flow of electrons into the anode until the space charge is drawn back into the anode.

C. Free Electron Decay

In the absence of an electric field to separate the electrons and positive ions, the electron will ricochet through the gas in a random manner with largely elastic collisions until absorbed by a positive ion. This absorption involves the emission of a photon of radiant energy. The wavelength of the emission will depend upon the ionization potential of the gas involved and the kinetic energy of the electron. This process of recombination is a statistical function and, as mentioned earlier, depends upon the density of the ions and electrons. The lower the density of atoms, the lower will be the probability of a recombination of charge particles so that higher ionization levels generally persist in rarer gasses. This is due in part to the diffusion of the particles as they are formed.

It is also possible for the electrons to be captured by a neutral atom or molecule to form a negative ion. Because of its greater mass, this negative ion does not have the mobility of the electron and can create a barrier to electron motion if present in sufficient densities. These negative ions are very important in explaining the mechanisms of corona discharges.

D. Corona Discharges

In the presence of a strong electric field, the free electrons and the positive ions will be accelerated in opposite directions. If large

numbers of charged particles are concentrated within a region, the local field may be greatly modified. The column of positive ions moving slowly toward the cathode may increase the local field in such a way as to draw free electrons radially into the ionized region. These free electrons may in turn create additional ionized branches radially outward from the main avalanche column. It is this tree-like structure of the ionized region which gives the characteristic branched appearance to most streamer discharges. As the density of these positive ions increases, the recombination processes increase and radiation from these neutralized ions increases accordingly. Ion-ion discharges also increase, particularly where the electric field is very strong and an accelerated ion may strike a relatively stationary ion which has just been formed.

1. Trichel pulses

At a cathode, free electrons may attach themselves to neutral molecules, particularly O_2 and H_2O, in such numbers as to create a cloud of slowly moving negative ions. These negative ions will inhibit the flow of current until the positive ions which are nearer the cathode are removed by neutralization at the cathode. Without the region of positive ions, the negative ions are more readily diffused toward the anode and restore the normal field configuration. As the field near the cathode returns to normal, the ionization processes begin again and the field is again distorted. This creation and elimination of the ionized regions causes short bursts of current to flow. The frequency of these pulses will increase as the applied field increases (18). The pulses them-

selves appear to be approximately the same shape but their periodicity depends upon the applied field. These sharp pulses will contain a broad spectrum of electromagnetic energy, but will be particularly strong at the frequency represented by the pulse separation.

2. Cathode glow discharges

Above the critical field intensity for a given environmental condition, the Trichel pulses lose their distinct character and appear to merge into a continuous glow discharge in the region near the negative electrode (16-18). As the field magnitude continues to increase, streamers will appear and a complete dielectric breakdown will occur with very evident sparking.

3. Anode glow discharges

The slow drift of negative ions toward the anode can create very high electric fields between this space charge and the anode as the converging ions form a negative cap over the anode. Streamer pulses can be formed between this space charge and the anode as some of the ions are forced to release their electrons. As the external field is increased, these streamer pulses will tend to merge much like the Trichel pulses and produce a self-sustained glow discharge (16-18). These discharges tend to sustain themselves due to an increase in the photoionization which maintains the space charge region.

4. Streamers

If the potential of the electrodes is reduced still further, the space charge region will be swept away and true streamer breakdown will occur. These lightning-like discharges will reach out some distance from the electrode before reaching a region where the diverging field and ion densities are no longer great enough to sustain the process. These streamers may form at either the anode or the cathode, although the onset voltage is different for each polarity (17; 18).

Since the voltage is constantly changing on an a.c. line, all of these phenomena may appear in a cycle as the potential changes from one region to another.

E. Corona Losses

The losses associated with corona phenomena depend upon a number of factors which are difficult to quantize and include in any general formula. Since F. W. Peek's monumental work first published in 1911, a number of investigators have sought to refine his "Law of Corona" to make it fit measured data more accurately (22; 23; 24).

Having established a critical breakdown voltage for a single wire by combining the radial E field and the charge per volt (capacitance) for a cylindrical conductor in a single phase circuit

$$V_c = m_o g_o \, \delta r \, \ln(s/r)$$

Peek proceeded to determine a loss equation

$$p = \frac{k}{\delta}\sqrt{\frac{r}{s}}\, f(V_n - V_c)^2 \qquad \text{kW/km per conductor}$$

The values of g_o and k will depend on whether rms or peak values are used for the voltages. If the voltages are rms g_o = 21.1 kV/cm, $k = 3.44 \times 10^{-5}$, r is the conductor radius in cm, s is the phase separation in the same units, V_n is the rms voltage to neutral, f is the frequency in Hertz.

Substituting the critical voltage into this equation obtains

$$p = \frac{kf}{\delta}\sqrt{\frac{r}{s}}\,\{V_n - m_o g_o\, \delta r\, \ln(s/r)\}^2$$

δ and m_o depend upon air density and conductor surface conditions respectively.

$$\delta = \frac{3.92b}{T}$$

where b is the barometric pressure in cm and T is temperature in Kelvin. m_o may vary anywhere from 1 for a polished dry solid conductor to as low as 0.68 for a wet stranded conductor in high humidity. Dust particles or other protrusions on the conductor surface may lower m_o even further.

Peterson modified these formulas giving the constants in English units and calculating the effects on surface roughness caused by using stranded conductors (24). More recent investigators have added further embellishments to force a closer fit to measured loss data. Much of this more recent work has been summarized in families of curves to show the variations due to several parameters. Comber and Zaffanella have pointed out that fair weather corona losses and insulator losses may be insig-

nificant with respect to I^2R losses in the conductors, but under other conditions the corona losses may be several times the conductor losses (25).

If corona losses are a function of the square of the difference between the operating voltage and a threshold voltage, slight changes in the threshold may make considerable changes in the losses. In the example given by Comber and Zaffanella, a 5.8% difference in gradient at the centerphase conductor with respect to the outer phase conductors makes a 31% difference in the corona losses. Equalizing the maximum fields by reducing the center phase value could produce a net reduction in corona loss of 10%.

V. SENSITIVITY OF ELECTRIC FIELDS TO PARAMETER VARIATION

A. Introduction

To modify the electric field distribution in the vicinity of high voltage transmission lines in some desired manner, it is helpful to determine a sensitivity factor for the electric field functions with respect to the parameters to be considered variable. Such a function is used in circuit theory to determine the sensitivity of system performance to critical component values (26).

The sensitivity function may be normalized in the form

$$S_u^F = \frac{\Delta F/F}{\Delta u/u} = \frac{dF}{du}\frac{u}{F}$$

or unnormalized in the form

$$S_u^F = u\frac{dF}{du} = FS_u^F$$

where F is some function of the independent variable u. For convenience in making comparisons between different transmission line configurations, the normalized form of the sensitivity function is used in this study and termed "sensitivity factor" when specific values are used to evaluate its magnitude and phase angle.

B. Line Charge Sensitivity

For a transmission line system in which the voltages are held essentially constant by the generators in the system, changes in mechanical parameters of the system will cause corresponding changes in the equivalent line charges required to maintain constant voltages at the conductor surfaces.

From the matrix equation which we used to determine these equivalent charges, the solution can be written

$$[Q] = [C]\ [V]$$

so that the derivative of the charge vector can be written

$$\left[\frac{dQ}{du}\right] = \frac{d}{du}\ [C]\ [V] = \left[\frac{dC}{du}\right]\ [V]$$

A direct differentiation of the partial capacitance matrix can be quite complicated, since it involves derivatives of the products of logarithm terms of an order equal to the matrix dimensions. Since, however, the [C] matrix is the inverse of a much simpler potential coefficient matrix, it is possible to make use of the identity (27; 28)

$$[P]\ [C] = [I]$$

Applying the chain rule to this equation gives

$$\left[\frac{dP}{du}\right]\ [C] + [P]\ \left[\frac{dC}{du}\right] = 0$$

or

$$[P]\ \left[\frac{dC}{du}\right] = -\ \left[\frac{dP}{du}\right]\ [C]$$

The derivative of the [C] matrix can then be written

$$\left[\frac{dC}{du}\right] = -[C]\left[\frac{dP}{du}\right][C]$$

and the derivative of the charge as

$$\left[\frac{dQ}{du}\right] = -[C]\left[\frac{dP}{du}\right][C][V]$$

$$= -[C]\left[\frac{dP}{du}\right][Q]$$

In many instances, as for example when finding the sensitivity with respect to a change in conductor radius, the derivative of the potential coefficient matrix may be a sparse matrix and the calculations required are considerably reduced. The evaluation of the capacitance matrix itself is relatively simple and the multiplication of the three matrices

$$-[C]\left[\frac{dP}{du}\right][C]$$

presents no difficulty.

To illustrate these effects of parameter variation on a practical line configuration, Figure 14 shows a simple three-phase line with a single conductor per phase.

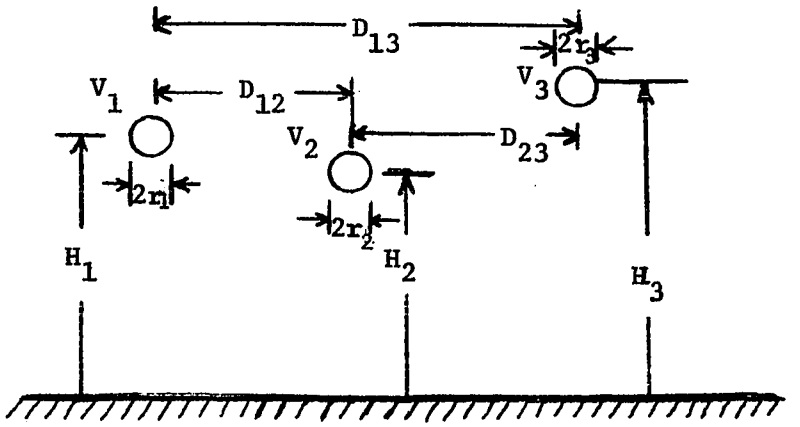

Figure 14. Two-dimensional three-phase line configuration

In most general cases, heights, separations and radii may all be different, and a general potential coefficient matrix can be written as

$$[P] = \frac{1}{2\pi\varepsilon} \begin{vmatrix} \ln \frac{H_{11}-r_1}{r_1} & \ln \frac{H_{12}-r_1}{S_{12}-r_1} & \ln \frac{H_{13}-r_1}{S_{13}-r_1} \\ \ln \frac{H_{12}-r_2}{S_{12}-r_2} & \ln \frac{H_{22}-r_2}{r_2} & \ln \frac{H_{23}-r_2}{S_{23}-r_2} \\ \ln \frac{H_{13}-r_3}{S_{13}-r_3} & \ln \frac{H_{23}-r_3}{S_{23}-r_3} & \ln \frac{H_{33}-r_3}{r_3} \end{vmatrix}$$

where

$$H_{ij} = \sqrt{(H_i+H_j)^2 + D_{ij}^2}$$

$$S_{ij} = \sqrt{(H_i-H_j)^2 + D_{ij}^2}$$

and

$$S_{ii} = 0$$

To understand the effects of parameter changes on the electric fields, the sensitivity of the line charges to changes in conductor size, phase spacing, bundle spacing and conductor heights is developed. From these basic charge sensitivites, and the effects of dimensional changes upon the fields, the sensitivity of the electric field is then determined.

1. Changes in conductor size

If the radius of a single conductor is changed, only the row and column containing that radius will have any elements in the differential

matrix, and these terms will all be essentially zero compared to the diagonal term which will be

$$-\frac{1}{2\pi\epsilon r_i}$$

The derivative of [Q] with respect to the radius r_i will contain only the terms

$$\frac{\partial \rho_i}{\partial r_i} = \frac{C_{ii}\rho_i}{2\pi\epsilon r_i}$$

$$\frac{\partial \rho_j}{\partial r_i} = \frac{C_{ji}\rho_i}{2\pi\epsilon r_i}$$

so that the sensitivity factors become

$$S_{r_i}^{\rho_i} = \frac{C_{ii}}{2\pi\epsilon}$$

$$S_{r_i}^{\rho_j} = \frac{C_{ji}}{2\pi\epsilon}\,\frac{\rho_i}{\rho_j}$$

The off-diagonal terms of the capacitance matrix are all negative. It follows, therefore, from these sensitivity factors, that changing the radius of one phase conductor to effect a change in the fields at its surface may change the fields at the other conductors in an undesirable manner. On the other hand, if the fields are unbalanced, changing parameters of the conductors in one phase may effect a desired balance in the field distribution over the entire system of conductors.

2. Changes in phase spacing

Assuming that the conductor radii are negligible with respect to the heights and horizontal phase separations, the potential coefficients for a simple three-phase transmission line can be defined in terms of a set of quotients X_{ij} where

$$X_{ij}^2 = \frac{(H_i+H_j)^2 + D_{ij}^2}{(H_i-H_j)^2 + D_{ij}^2} \qquad (i \neq j)$$

$$X_{ii}^2 = \frac{4H_i^2}{r_i^2} \qquad P_{ij} = \frac{1}{2\pi\epsilon} \ln X_{ij}$$

$$\frac{\partial P_{ij}}{\partial D_{ij}} = \frac{1}{2\pi\epsilon} \left[\frac{D_{ij}}{(H_i+H_j)^2 + D_{ij}^2} - \frac{D_{ij}}{(H_i-H_j)^2 + D_{ij}^2} \right]$$

$$= \frac{D_{ij}}{2\pi\epsilon} \left[\frac{-4H_i H_j}{(H_i^2 + H_j^2 + D_{ij}^2)^2 - (2H_iH_j)^2} \right]$$

and

$$\left[\frac{\partial P}{\partial D_{ij}} \right]$$

becomes a symmetrical matrix with zeros on the principal diagonal.

For many practical cases, $D_{13} = 2D_{12} = 2D_{23} = 2D$ and $H_1 = H_3 \neq H_2$. In this symmetrical case, the differential matrix reduces to

$$\left[\frac{\partial P}{\partial D}\right] = \frac{1}{2\pi\epsilon} \begin{vmatrix} 0 & \dfrac{-4DH_1H_2}{(H_1^2+H_2^2+D^2)^2-4H_1^2H_2^2} & \dfrac{-DH_1^2}{D^2(H_1^2+D^2)} \\ \dfrac{-4DH_1H_2}{(H_1^2+H_2^2+D^2)^2-4H_1^2H_2^2} & 0 & \dfrac{-4DH_1H_2}{(H_1^2+H_2^2+D^2)^2-4H_1^2H_2^2} \\ \dfrac{-DH_1^2}{D^2(H_1^2+D^2)} & \dfrac{-4DH_1H_2}{(H_1^2+H_2^2+D^2)^2-4H_1^2H_2^2} & 0 \end{vmatrix}$$

Premultiplying this differential matrix by the capacitance matrix will provide a means of determining the sensitivity of the Q matrix to changes in phase separation, as shown in Figure 15.

The sensitivity of the line charge on a particular conductor is, therefore, a function not only of the physical parameters, but of the ratio of the other line charge densities to that of the conductor under investigation.

$$S_D^{\rho_1} = \frac{-DH_1}{2\pi\epsilon} \left\{ \frac{H_1(C_{13}+C_{11}\rho_3/\rho_1)}{D^2(H_1^2+D^2)} + \frac{4H_2[C_{12}(1+\rho_3/\rho_1)+(C_{11}+C_{13})\rho_2/\rho_1]}{(H_1^2+H_2^2+D^2)^2-4H_1^2H_2^2} \right\}$$

$$S_D^{\rho_2} = \frac{-DH_1}{2\pi\epsilon} \left\{ \frac{H_1(C_{23}\rho_1/\rho_2+C_{21}\rho_3/\rho_2)}{D^2(H_1^2+D^2)} + \frac{4H_2\left[C_{21}+C_{23}+C_{22}\left(\frac{\rho_3}{\rho_2}\right)+\left(\frac{\rho_3}{\rho_2}\right)\right]}{(H_1^2+H_2^2+D^2)^2-4H_1^2H_2^2} \right\}$$

$$S_D^{\rho_3} = \frac{-DH_1}{2\pi\varepsilon} \left\{ \frac{H_1(C_{31}+C_{33}\rho_1/\rho_2)}{D^2(H_1^2+D^2)} + \frac{4H_2[V_{32}(1+\rho_1/\rho_3)+(C_{31}+C_{33})\rho_2/\rho_3]}{(H_1^2+H_2^2+D^2)^2-4H_1^2H_2^2} \right\}$$

It should be remembered that the off-diagonal terms of the capacitance matrix are all negative, which will introduce some sign changes in the evaluation of the numerator terms of the expressions given above.

3. Changes in conductor height

By using the general quotient terms X_{ij} of the previous section, it is possible to obtain a general derivative with respect to conductor heights as follows:

$$\frac{\partial p_{ij}}{\partial H_i} = \frac{1}{2\pi\varepsilon} \left[\frac{(H_i+H_j)}{(H_i+H_j)^2+D_{ij}^2} - \frac{(H_i-H_j)}{(H_i-H_j)^2+D_{ij}^2} \right]$$

$$= \frac{-2H_j}{2\pi\varepsilon} \left[\frac{H_i^2-H_j^2-D_{ij}^2}{(H_i^2+H_j^2+D_{ij}^2)^2-4H_i^2H_j^2} \right] \qquad (i\neq j)$$

$$\frac{\partial p_{ii}}{\partial H_i} = \frac{1}{2\pi\varepsilon H_i}$$

Assuming the same simplifying symmetry as in the previous section, the derivatives of the potential coefficient matrix can be written

$$\left[\frac{\partial Q}{\partial D}\right] = \frac{-4DH_1}{2\pi\varepsilon}$$

$$\begin{bmatrix}
-\frac{C_{12}H_2}{(H_1^2+H_2^2+D^2)^2-4H_1^2H_2^2} + \frac{C_{13}H_1}{4D^2(H_1^2+D^2)} & \frac{(C_{11}+C_{13})H_2}{(H_1^2+H_2^2+D^2)^2-4H_1^2H_2^2} & \frac{C_{12}H_2}{(H_1^2+H_2^2+D^2)-4H_1^2H_2^2}+\frac{C_{11}H_1}{4D^2(H_1^2+D^2)} \\
\frac{C_{22}H_2}{(H_1^2+H_2^2+D^2)^2-4H_1^2H_2^2} + \frac{C_{23}H_1}{4D^2(H_1^2+D^2)} & \frac{(C_{21}+C_{23})H_2}{(H_1^2+H_2^2+D^2)-4H_1^2H_2^2} & \frac{C_{22}H_2}{(H_1^2+H_2^2+D^2)^2-4H_1^2H_2^2}+\frac{C_{21}H_1}{4D^2(H_1^2+D^2)} \\
\frac{C_{32}H_2}{(H_1^2+H_2^2+D^2)^2-4H_1^2H_2^2} + \frac{C_{33}H_1}{4D^2(H_1^2+D^2)} & \frac{(C_{31}+C_{33})H_2}{(H_1^2+H_2^2+D^2)^2-4H_1^2H_2^2} & \frac{C_{32}H_2}{(H_1^2+H_2^2+D^2)^2-4H_1^2H_2^2}+\frac{C_{31}H_1}{4D^2(H_1^2+D^2)}
\end{bmatrix} [Q]$$

Figure 15. Partial derivative of charge matrix with respect to phase separation

$$\left[\frac{\partial P}{\partial H_1}\right] = \frac{1}{2\pi\epsilon}\begin{bmatrix} \frac{1}{H_1} & \frac{2H_2(H_2^2-H_1^2+D^2)}{(H_1^2+H_2^2+D^2)^2-4H_1^2H_2^2} & \frac{H_1}{(H_1^2+D^2)} \\ \frac{2H_2(H_2^2-H_1^2+D^2)}{(H_1^2+H_2^2+D^2)^2-4H_1^2H_2^2} & 0 & \frac{+2H_2(H_2^2-H_1^2+D^2)}{(H_1^2+H_2^2+D^2)^2-4H_1^2H_2^2} \\ \frac{H_1}{(H^2+D^2)} & \frac{2H_2(H_2^2-H_1^2+D^2)}{(H_1^2+H_2^2+D^2)^2-4H_1^2H_2^2} & \frac{1}{H_1} \end{bmatrix}$$

$$\left[\frac{\partial P}{\partial H_2}\right] = \frac{1}{2\pi\epsilon}\begin{bmatrix} 0 & \frac{2H_1(H_1^2-H_2^2+D^2)}{(H_1^2+H_2^2+D^2)^2-4H_1^2H_2^2} & 0 \\ \frac{2H_1(H_1^2-H_2^2+D^2)}{(H_1^2+H_2^2+D^2)^2-4H_1^2H_2^2} & \frac{1}{H_2} & \frac{2H_1(H_1^2-H_2^2+D^2)}{(H_1^2+H_2^2+D^2)^2-4H_1^2H_2^2} \\ 0 & \frac{2H_1(H_1^2-H_2^2+D_2)}{(H_1^2+H_2^2+D^2)^2-4H_1^2H_2^2} & 0 \end{bmatrix}$$

Premultiplying these matrices by the capacitance matrix will result in a matrix of charge sensitivity factors with respect to changes in height of the outer and inner phases respectively. Allowing changes in the center phase height only obtains

$$[C]\frac{\partial P}{\partial H_2}=\frac{2H_1(H_1^2-H_2^2+D^2)C_{22}}{2\pi\varepsilon[H_1^2H_2^2+D^2)^2-4H_1^2H_2^2}\begin{bmatrix}\frac{C_{12}}{C_{22}} & \frac{C_{11}+C_{13}}{C_{22}}+\frac{(H_1^2+H_2^2+D^2)^2-4H_1^2H_2^2}{2H_1H_2(H_1^2-H_2^2+D^2)}\frac{C_{12}}{C_{22}} & \frac{C_{12}}{C_{22}}\\ 1 & \frac{C_{21}+C_{23}}{C_{22}}+\frac{(H_1^2+H_2^2+D^2)^2-4H_1^2H_2^2}{2H_1H_2(H_1^2-H_2^2+D^2)} & 1\\ \frac{C_{32}}{C_{22}} & \frac{C_{33}+C_{31}}{C_{22}}+\frac{(H_1^2+H_2^2+D^2)^2-4H^2H^2}{2H_1H_2(H_1^2-H_2^2+D^2)}\frac{C_{32}}{C_{22}} & \frac{C_{32}}{C_{22}}\end{bmatrix}$$

and the sensitivity of the line charges to height of the center phase becomes

$$S_{H_2}^{\rho_1}=\frac{1}{2\pi\varepsilon}\left\{\frac{C_{12}}{H_2}\frac{\rho_2}{\rho_1}+\frac{2H_1(H_1^2-H_2^2+D^2)[C_{12}(1+\rho_3/\rho_1)+(C_{11}+C_{13})\rho_2/\rho_1]}{(H_1^2+H_2^2+D^2)^2-4H_1^2H_2^2}\right\}H_2$$

$$S_{H_2}^{\rho_2}=\frac{1}{2\pi\varepsilon}\left\{\frac{C_{22}}{H_2}+\frac{2H_1(H_1^2-H_2^2+D^2)[C_{22}(\rho_1/\rho_2)+C_{21}+C_{23}]}{(H_1^2+H_2^2+D^2)^2-4H_1^2H_2^2}\right\}H_2$$

$$S_{H_2}^{\rho_3}=\frac{1}{2\pi\varepsilon}\left\{\frac{C_{32}}{H_2}\frac{\rho_2}{\rho_3}+\frac{2H_1(H_1^2-H_2^2+D^2)[C_{32}(1+\rho_1/\rho_3)+(C_{31}+C_{33})\rho_2/\rho_3]}{(H_1^2+H_2^2+D^2)^2-4H_1^2H_2^2}\right\}H_2$$

Starting with a flat horizontal configuration where $H_1 = H_2 = H_3$, and changing only H_2, this reduces to

$$S_{H_2}^{\rho_1} = \frac{1}{2\pi\epsilon} \left\{ C_{12} \frac{\rho_2}{\rho_1} + \frac{2H_1H_2[C_{12}(1+\rho_3/\rho_1)+(C_{11}+C_{13})\rho_2/\rho_1]}{4H_1^2+D^2} \right\}$$

$$S_{H_2}^{\rho_2} = \frac{1}{2\pi\epsilon} \left\{ C_{22} + \frac{2H_1H_2[C_{22}\left(\frac{\rho_1}{\rho_2}+\frac{\rho_3}{\rho_2}\right)+2C_{12}]}{4H_1^2+D^2} \right\}$$

$$S_{H_2}^{\rho_3} = \frac{1}{2\pi\epsilon} \left\{ C_{32} \frac{\rho_2}{\rho_3} + \frac{2H_1H_2[C_{12}(1+\rho_1/\rho_3)+(C_{33}+C_{13})\rho_2/\rho_3]}{4H_1^2+D^2} \right\}$$

Changing only the outer conductor heights equally under the same conditions, the sensitivities are

$$S_{H_1}^{\rho_1} = \frac{1}{2\pi\epsilon} \left\{ C_{11}+C_{13} \frac{\rho_3}{\rho_1} + \frac{H_1^2(C_{13}+C_{11}\rho_3/\rho_1)}{H_1^2+D^2} \right.$$

$$\left. + \frac{2H_1^2[C_{12}(1+\rho_3/\rho_1)+(C_{11}+C_{13})\rho_2/\rho_1]}{4H_1^2+D^2} \right\}$$

$$S_{H_1}^{\rho_2} = \frac{1}{2\pi\epsilon} \left\{ \frac{C_{12}(\rho_1/\rho_2+\rho_3/\rho_2)(2H_1^2+D^2)}{H_1^2+D^2} + \frac{2H_1^2[C_{12}+C_{22}(\rho_1/\rho_2+\rho_3/\rho_2)]}{4H_1^2+D^2} \right\}$$

$$S_{H_1}^{\rho_3} = \frac{1}{2\pi\varepsilon}\left\{C_{11}+C_{13}\frac{q_1}{q_3} + \frac{H_1^2(C_{13}+C_{33}\rho_1/\rho_3)}{H_1^2+D^2}\right.$$

$$\left. + \frac{2H_1^2[C_{12}(1+\rho_1/\rho_3)+(C_{33}+C_{13})\rho_2/\rho_3]}{4H_1^2+D^2}\right\}$$

In both cases, the symmetry is evident by comparing $S_{H_1}^{\rho_3}$ with $S_{H_1}^{\rho_1}$.

4. Changes in bundle radius

The sensitivity of the line charge densities to changes in bundle radii depends upon the number of subconductors and their relative orientation in such a complex manner that a general analytical solution is practically impossible. For a system of n subconductors per bundle, the p matrix will be a 3n x 3n matrix in which (n-1)/n of the elements will involve logarithmic terms in which the bundle diameter and the angles between these n subconductors, as well as the distances from each subconductor of one bundle to each subconductor of the other bundles must be included. The general [P] matrix element might be written

$$P_{i+m,j+q} = \frac{1}{4\pi\varepsilon}\ln\frac{[H_i+H_j-R(\sin\frac{2m\pi}{n}+\sin\frac{2q\pi}{n})]^2+[D_{ij}+R(\cos\frac{2m\pi}{n}-\cos\frac{2q\pi}{n})]^2}{[H_i-H_j-R(\sin\frac{2m\pi}{n}-\sin\frac{2q\pi}{n})]^2+[D_{ij}+R(\cos\frac{2m\pi}{n}-\cos\frac{2q\pi}{n})]^2}$$

Differentiating this with respect to the bundle radius R provides a formidable equation of the form

$$\frac{dp_{i+m,j+q}}{dR} = \frac{-1}{2\pi\varepsilon}\left\{\frac{(\sin\frac{2m\pi}{n}+\sin\frac{2q\pi}{n})B-(\cos\frac{2m\pi}{n}-\cos\frac{2q\pi}{n})A}{B^2+A^2}\right.$$

$$\left.-\frac{(\sin\frac{2m\pi}{n}-\sin\frac{2q\pi}{n})C-(\cos\frac{2m\pi}{n}-\cos\frac{2q\pi}{n})A}{C^2+A^2}\right\}$$

where

$$A = D_{ij}+R(\cos\frac{2m\pi}{n}-\cos\frac{2q\pi}{n})$$

$$B = H_i+H_j-R(\sin\frac{2m\pi}{n}+\sin\frac{2q\pi}{n})$$

$$C = H_i-H_j-R(\sin\frac{2m\pi}{n}-\sin\frac{2q\pi}{n})$$

A computer routine to obtain numerical solutions for this derivative could be programmed without too much difficulty, but it appears much more practical to use the programs already available for computing the fields and to obtain finite differences by incrementing the parameters in these routines. The sensitivities can then be obtained from these difference calculations.

C. Capacitance Sensitivity

As shown in the development of line charge sensitivity above, the capacitance derivative is obtained by the triple matrix product

$$\frac{d[C]}{du} = -[C]\left[\frac{dP}{du}\right][C]$$

$$\frac{dC_{ij}}{du} = - \Sigma C_{ik} \frac{dP_{k\ell}}{du} C_{\ell j}$$

and is easily evaluated from the derivative of the potential coefficient matrix. The normalized sensitivity of any capacitance element to a line parameter change can then be obtained by multiplying the appropriate element of the derivative matrix by the ratio of the initial parameter value to the initial capacitance value.

D. Inductance Sensitivity

By definition, the inductance is the ratio of flux linkages due to a particular current divided by that current (8).

$$L_{ij} = \frac{\lambda_{ij}}{I_j}$$

To define the various flux linkages between phases of a three-phase transmission line circuit, a flux linkage matrix can be generated in terms of these partial inductances.

$$[\lambda_i] = [L_{ij}][I_j]$$

where λ_i is the total flux linkages to the ith conductor from all currents in the system.

By integrating the magnetic flux density around a cylindrical conductor over a unit length, the linkages per unit length between any two radii can be obtained as

$$\lambda_n = \frac{\mu_o I}{2\pi} \ln \frac{R_2}{R_1}$$

If we assume a three-phase system with no neutral, the sum of the currents in the three-phases must add to zero. For the simple three-

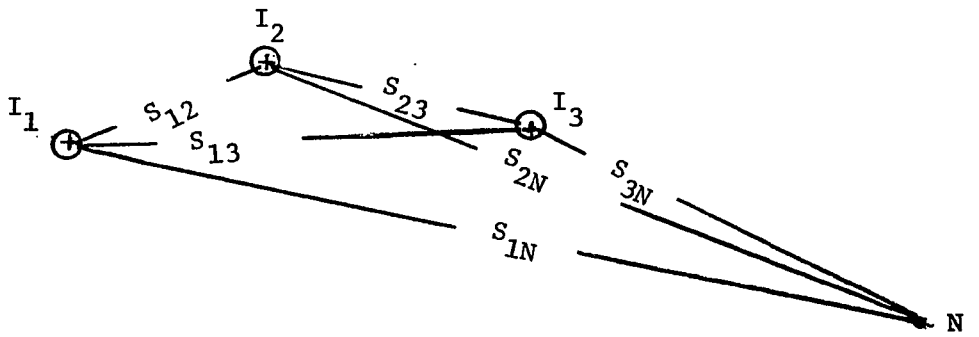

Figure 16. Three-conductor system for flux linkage calculations

phase system shown in Figure 16, the total flux linkages between the point N and the current in conductor 1 can be written as

$$\lambda_1 = \frac{\mu_o}{2\pi} \left[\frac{I_1}{4} + I_1 \ln \frac{S_{1N}}{r_1} + I_2 \ln \frac{S_{2N}}{S_{12}} + I_3 \ln \frac{S_{3N}}{S_{13}} \right]$$

Similarly,

$$\lambda_2 = \frac{\mu_o}{2\pi} \left[I_1 \ln \frac{S_{1N}}{S_{12}} + \frac{I_2}{4} + I_2 \ln \frac{S_{2N}}{r_2} + I_3 \ln \frac{S_{3N}}{S_{23}} \right]$$

$$\lambda_3 = \frac{\mu o}{2\pi} \left[I_1 \ln \frac{S_{1N}}{S_{13}} + I_2 \ln \frac{S_{2N}}{S_{23}} + \frac{I_3}{4} I_3 \ln \frac{S_{3N}}{r_3} \right]$$

Rewriting the first equation as

$$\lambda_1 = \frac{\mu_o}{2\pi}\left[I_1 \ln \frac{e^{\frac{1}{4}}}{r_1} + I_2 \ln \frac{1}{S_{12}} + I_3 \ln \frac{1}{S_{13}} + I_1 \ln S_{1N} + I_2 \ln S_{2N} + I_3 \ln S_{3N}\right]$$

and letting the distance to N approach infinity, $S_{1N} = S_{2N} = S_{3N} = S_N$, so that the last three terms disappear because of the zero net current.

The exponential, $e^{\frac{1}{4}}$, is generally combined with r_1 to give an effective radius, $r_1' = e^{-\frac{1}{4}} r_1$, which allows for the internal inductance of the conductor. This constant will disappear in the differentiation of the logarithmic terms. The general inductance terms then become

$$L_{ij} = \frac{\mu_o}{2\pi} \ln \frac{1}{S_{ij}} = M_{ij}$$

$$L_{ii} = \frac{\mu_o}{2\pi}\left[\frac{1}{4} + \ln \frac{1}{r_i}\right] = \frac{\mu_o}{2\pi} \ln \frac{1}{r_i'}$$

where

$$S_{ij} = \sqrt{(H_i - H_j)^2 + D_{ij}^2}$$

1. Single conductor case

The sensitivity of the diagonal terms is only a function of radius and will involve only the self-inductance terms so that

$$S_{r_i}^{L_{ii}} = \frac{1}{\ln r_i'}$$

$$S_{r_i}^{M_{ij}} = 0$$

The mutual terms are not functions of the radii and show sensitivities with respect to height and phase separation only.

$$S^{L_{ii}}_{H_i} = 0 \qquad S^{M_{ij}}_{H_i} = \frac{+(H_i - H_j)(H_i)}{(S_{ij})^2 \ln S_{ij}}$$

$$S^{L_{ii}}_{D_{ij}} = 0 \qquad S^{M_{ij}}_{D_{ij}} = \frac{(D_{ij})^2}{(S_{ij})^2 \ln S_{ij}}$$

2. Bundled conductor case

In the case of bundled conductors, the sensitivity evaluation becomes quite complicated since S_{ij} must be replaced by a Geometric Mean Distance (GMD) term involving the products of all possible distances between subconductors of the i-th and j-th phases. The radii must also be replaced by a self-GMD or GMR relating the effective radii of the subconductors and their separations within the bundle. The GMD and GMR are generally defined as

$$GMD = \sqrt[mn]{S_{aa'} S_{ab'} \cdots S_{an'} S_{ba'} \cdots S_{mn'}}$$

$$GMR = \sqrt[n^2]{r'_a S_{ab} S_{ac} \cdots S_{an} r'_b S_{bc} \cdots r'_n}$$

The derivatives of these terms are more easily obtained by numerical methods, as was indicated in the previous section on capacitance sensitivity.

E. Electric Field Sensitivity

From the basic equations for the electric field produced by a filament of charge

$$\overline{E} = \frac{\rho \overline{R}}{2\pi\epsilon|\overline{R}|^2}$$

where

$$\overline{R} = (x-x_o)\hat{a}_x + (y-h)\hat{a}_y$$

It becomes evident that the sensitivity of $|\overline{E}|$ depends not only upon the sensitivity of the line charge ρ, but upon the sensitivity of $|\overline{R}|$ to changes in physical parameters of the line. At some distance from the conductors, the sensitivity of $|\overline{R}|$ to the radius of the conductor would be expected to be negligible, while a change in height, spacing or even bundle radius, could have significant effect on this radial position. At the conductor surface, however, it would appear that a change in radius would significantly effect both ρ and the field position $|R|$, while changes in height, phase separation and bundle dimensions would only effect the charge densities.

At the conductor surface, then

$$\frac{d|\overline{E}|}{dr} = \frac{\frac{\partial \rho}{\partial r}}{2\pi\epsilon R} - \frac{\rho \frac{\partial R}{\partial r}}{2\pi\epsilon R^2} = \frac{r\frac{d\rho}{dr} - \rho}{2\pi\epsilon r^2}$$

so that the sensitivity of $|E|$ would be

$$S_r^{|E|} = \frac{\frac{d|E|}{dr}(r)}{|E|} = \frac{r\frac{\partial \rho}{\partial r} - \rho}{\rho} = S_r^{\rho} - 1$$

In general, then

$$\frac{d|E|}{du} = \frac{R\frac{\partial \rho}{\partial u} - \rho\frac{\partial R}{\partial u}}{2\pi\epsilon R^2}$$

$$S_u^{|E|} = \frac{\frac{\partial \rho}{\partial u}u}{\rho} - \frac{\frac{\partial R}{\partial u}u}{R} = S_u^{\rho} - S_u^{R}$$

The effect on the unit vectors associated with $|E|$ can be found in similar fashion and will depend a great deal upon how far the point of interest is from the changing element.

It can be seen that although analytical solutions for the sensitivities may be found for relatively simple transmission line configurations, numerical solutions using computer techniques are much more practical for EHV and UHV systems where multiconductor bundles are generally used.

VI. ANALYSIS OF SENSITIVITY FROM ELECTRIC FIELD DATA

A. Introduction

An investigation of the sensitivity of the electric fields in the vicinity of HV and EHV transmission lines is undertaken using a point matching method similar to that used by Parekh (29) to determine the high voltage d.c. field distribution at the surface of stranded conductors. The actual program is a modification of the FORTRAN program, PTMAT, originally developed by A. A. Read (30) for plotting d.c. electric fields around cylindrical conductors. The program is significantly modified to obtain the a.c. fields around overhead transmission lines and to allow for phasor representation of the transmission line charge densities. With these modifications, it is possible to compute the amplitude and relative phase of both the horizontal and vertical components of the electric field and the resultant total electric field magnitude at any point in the space. The modifications resulted in a new program, HIVAC2, which is used to provide data for this study of the sensitivity of the a.c. electric fields near HV lines. The results of these analyses indicate that, at heights corresponding to that of large mobile equipment used in construction of farming operations, the magnitude of the horizontal electric field component is significant and can exceed that of the vertical electric field component.

A study of the relationships between the maximum electric field within five meters of the ground and the associated conductor surface

field for a number of transmission line configurations has shown that effective control of both quantities requires knowledge of the sensitivity of each to various key parameter variations.

B. Electric Field Calculations

1. Basic transmission line configuration

The data utilized for this study are largely based upon a standard three-phase transmission line configuration which is referred to as the "base case." This base case is used in making comparisons with data obtained from other configurations which represent modifications of the various dimensions from the standard case shown in Figure 17.

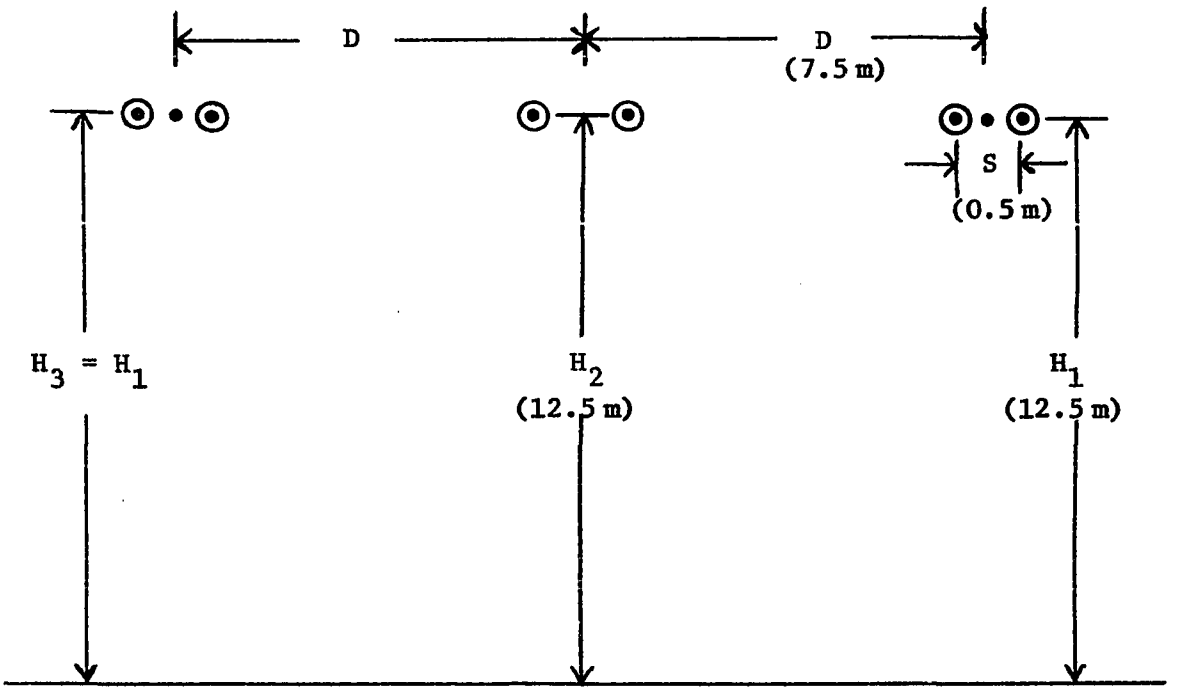

Figure 17. Dimensions for base case configuration

The base case transmission line is a flat horizontal configuration at a nominal height ($H_1 = H_3$) of 12.5 meters above a zero potential ground plane. The nominal horizontal phase separation, D, between the centers of the conductor bundles is chosen as 7.5 meters. For the base case, the bundles consist of two subconductors with a diameter of three centimeters and with a horizontal separation, S, between the subconductor centers of fifty centimeters. Bundles of three and four such conductors equally spaced around a circle of diameter equal to S are also considered.

For the purpose of this investigation, a balanced three-phase system with nominal 345 kV, 60 Hz transmission is assumed. Using these data as inputs to the line, a maximum rms electric field intensity on the center phase conductor surface of 1640 kV/m is obtained. The corona onset value of field intensity obtained from Peek's Law[a], under normal temperature and pressure conditions, is found to be 1890 kV/m, assuming a surface roughness factor of 0.72 (22; 23). This roughness factor is typical of a 7-strand subconductor. Using the base case dimensions, the maximum electric

---

[a]Peek's Law may be written as

$$E_{max} = 2110\ \delta\ m_o\ 1 + \left[\frac{0.426}{\sqrt{\delta d}}\right] \text{kV/m (rms)}$$

where

δ = (0.392 b)/T = air density factor
b = barometric pressure in mm Hg
T = absolute temperature in °K
d = conductor diameter in cm
m_o = surface roughness factor (≤ 1.0)

field strengths for the outer phase conductors are found to be 1490 kV/m and 1540 kV/m for the outermost and nearer subconductors respectively.

At the ground level, the maximum rms value of the electric field is found to be 3.5 kV/m at a distance of approximately 10 meters, measured horizontally, from the centerline of the system. At a horizontal distance of 22.86 meters, which represents the edge of a typical 150 feet right-of-way, the ground level electric field was found to be 1.45 kV/m. Along the centerline of the right-of-way, the ground level electric field is found to be approximately 1.56 kV/m, as shown in Figure 18a. This figure illustrates a typical electric field distribution along the ground beneath a flat horizontal transmission line.

2. Effect of shield wires

The addition of a pair of shield wires above the basic configuration transmission line has little effect upon either the ground level field or the conductor surface field. The two shield wires are assumed to be at a height of 22.2 meters above the ground and placed symmetrically about the central plane of the system with a horizontal separation of 9.4 meters. The conductors are assumed to be 0.95 cm in diameter. The fields calculated with the addition of the two shield wires indicate that their presence reduces the maximum electric fields at both the ground level and at the conductor surfaces by approximately 1%.

3. Electric fields at levels above ground

The electric field values obtained at ground level are generally used for determining the electrostatic effects on conducting fences and animals which might be located beneath the high voltage transmission lines. For equipment which reaches four or five meters above the ground, however, the tops of the equipment may encounter fields which are significantly higher than those at ground level. This can be seen by examining Figure 18b, which shows an increase in the maximum vertical component to 4.2 kV/m and a significant horizontal component of 2.5 kV/m. By comparing this figure with Figure 18a, it can be seen that the electric field magnitude at the edge of the right-of-way is not changed appreciably with height, although an increase of 50% in the electric field can be seen along the centerline. A closer comparison of these figures also shows that the distance between the electric field maxima is decreased to approximately 18 meters at the 4 meter height.

4. Experimental field measurements

A set of electrical field strength measurements was taken for several positions beneath an existing 345 kV transmission line. This line is used by the Iowa Test and Evaluation Facility of Iowa State University to provide a realistic environment for EHV research projects. Three sections of this line are accessible for a distance of approximately 1 km, with a large variation in height. The line runs north and south adjacent to a county road with minimum ground clearances in the three sections of 12

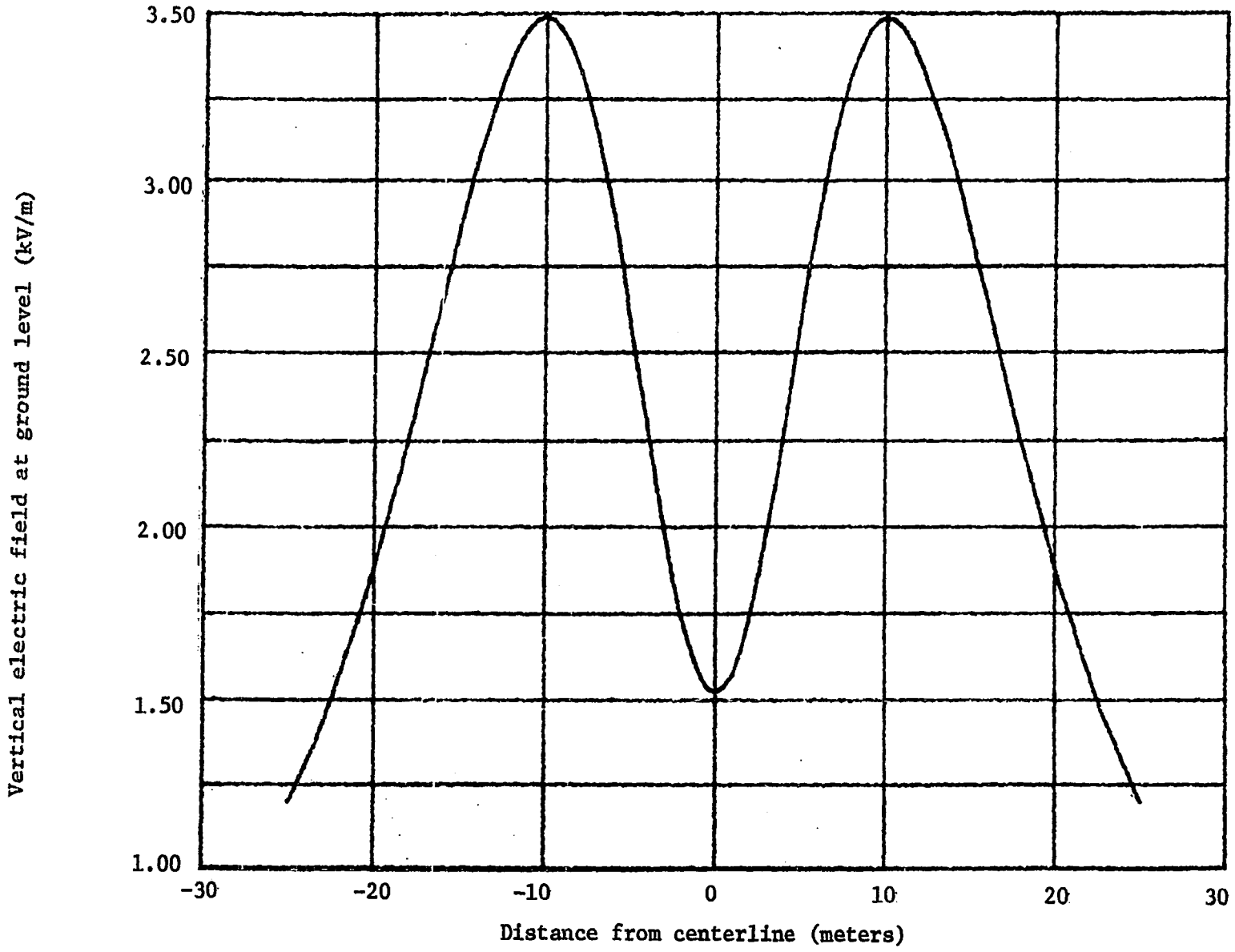

Figure 18a. Electric field magnitude at ground level for base case

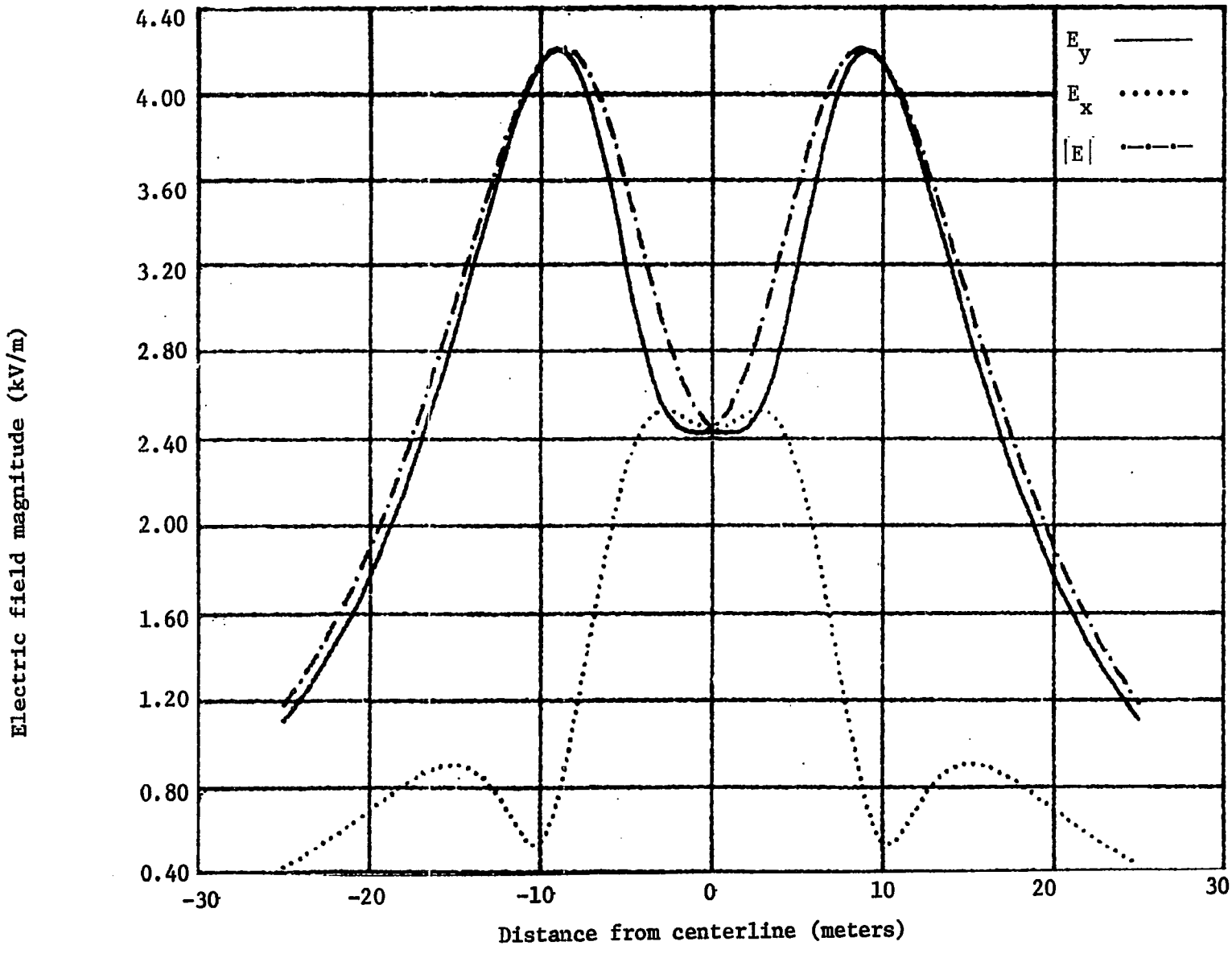

Figure 18b. Electric field contour at 4-meter height for base case transmission line

meters, 15.5 meters, and 22 meters from the south to the north. From these minimum clearances and the tower heights, catenarian curves are calculated to obtain the contours shown in Figure 19.

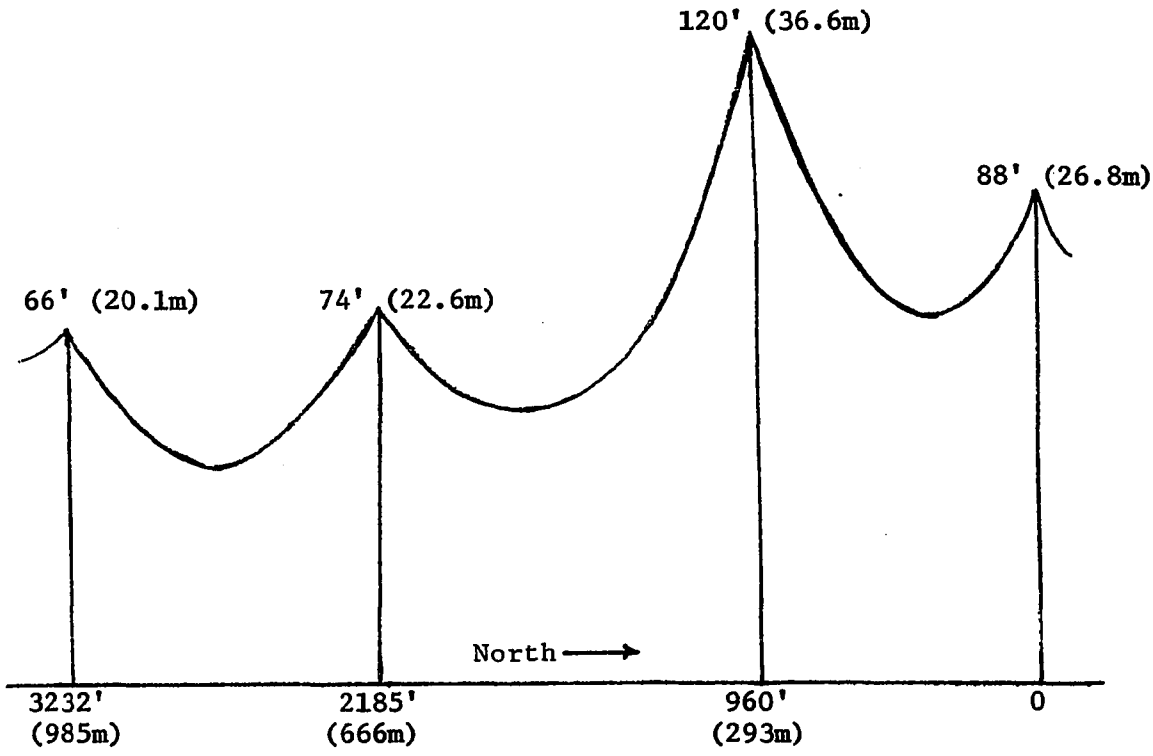

Figure 19. Profile of 345 kV transmission line at ITEF

A transverse set of electrical field measurements were taken with a Monroe model 238A-1 a.c. field strength meter. These measurements were made at intervals of approximately 10 feet (3.05 m) from the centerline of the system out to 100 feet. Measurements were made at distances of 170, 435, 485, and 825 meters from the northern tower. The measurements at 170 meters, however, were suspect due to the proximity of a 161 kV line which crosses below the 345 kV line.

The electric field measurements for the 425, 485 and 825 meters sets are plotted in Figure 20. As reference, the height of the transmission line for each position is demonstrated and a calculation of the field to be expected from a perfectly horizontal line at those heights is shown.

The measured values in each set appear to be consistently lower than the calculated values. The general shape of the contours agrees fairly well and the shift of the maximum field position with height is easily seen. The error between the actual measured values and the calculated values may be attributed to several factors. Not the least of these factors is a lack of exact height dimensions which change with system load and environmental conditions. The catenarian shape of the transmission line conductor spans may also contribute to the errors obtained by an assumption of a perfectly horizontal configuration.

C. Sensitivity Analysis

1. Method of calculation

The sensitivity of electric fields to changes in dimensional parameters of the system can be calculated by following the matrix method shown in the previous chapter using a partial capacitance matrix and the derivative of the potential coefficient matrix. For multiple conductor systems with bundled conductors, this involves the multiplication of large order matrices. For the purpose of this study, the field strength data

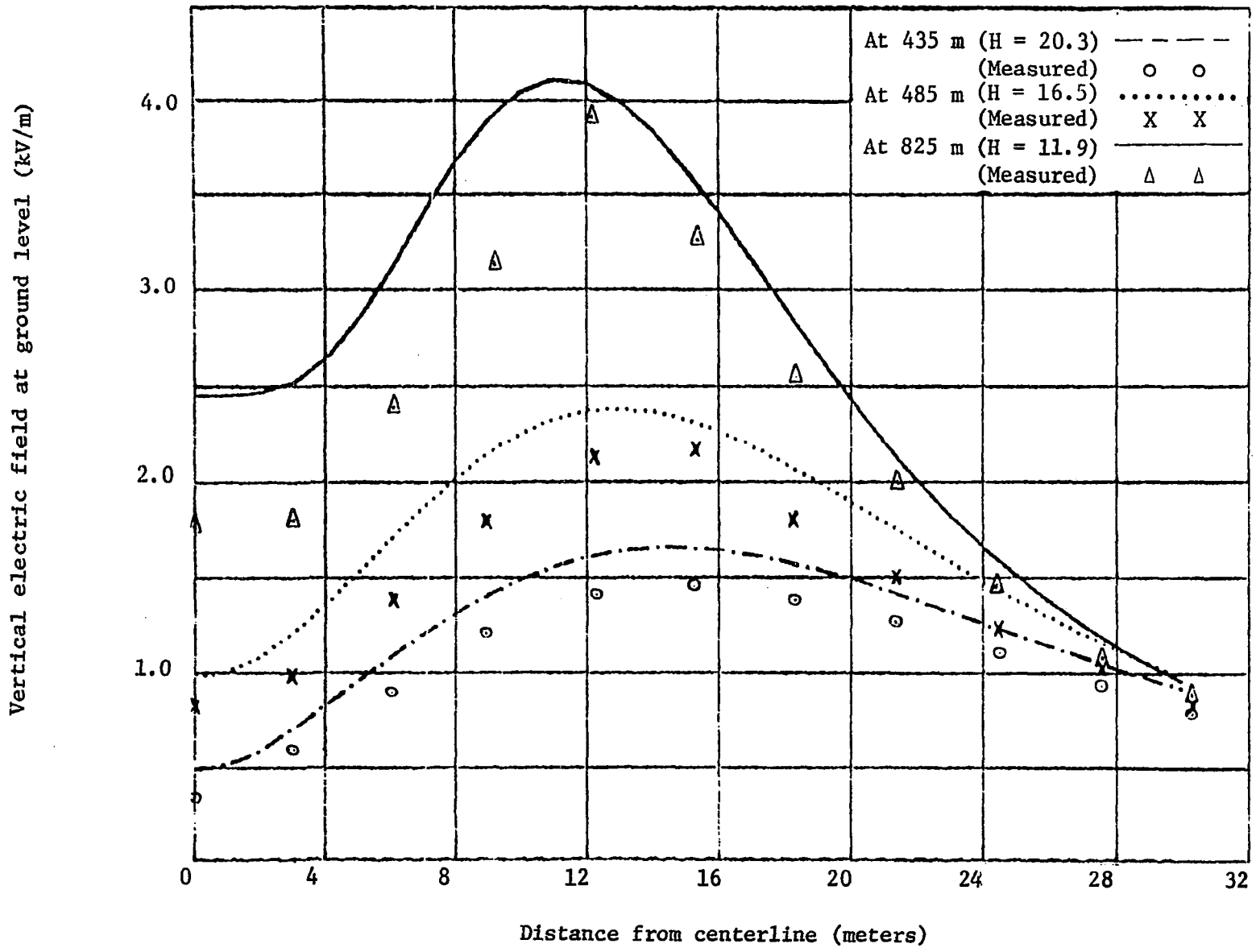

Figure 20. Variation of maximum ground level field with height under 345 kV line at ITEF

generated utilizing HIVAC2 are analyzed using numerical methods, since the exact values are not as important as the relative magnitudes.

Recalling that the normalized sensitivity factor by definition is given as

$$S_u^E = \frac{dE}{du} \cdot \frac{u}{E}$$

S_u^E can be approximated for small parameter changes by

$$\frac{E(u_2) - E(u_1)}{E(u_2) + E(u_1)} \cdot \frac{u_2 + u_1}{u_2 - u_1}$$

where u is the parameter to be considered as an independent variable. S_u^E is generally a phasor quantity and may not indicate directly the expected changes in the magnitude of the electric field.

2. The deviation factor

Since this investigation is focused on problems which are functions of the electric field magnitudes only, a "deviation factor" is defined here and used in place of the sensitivity factor when only amplitude changes are being considered. This deviation factor is defined as

$$F_u^E = \left|\frac{\Delta E}{\Delta u}\right| \cdot \left|\frac{u}{E}\right|$$

Since both of these factors are normalized to a ratio between two dimensionless fractions, the deviation factor may be defined in terms of the complex sensitivity factor and an incremental fraction i of the independent variable (u).

$$F_u^E = \frac{|1 + i(S_u^E)| - 1}{i}$$

For example, a 50 centimeter change at the standard height of 12.5 meters would be represented by a normalized height increment of

$$i = \frac{0.5}{12.5} = 0.04$$

In the analysis which follows, the sensitivities of the electric field are considered with respect to four parameters: H, D, S and d. These will represent the independent variables height, phase spacing, bundle diameter and conductor diameter, respectively. These symbols are used as subscripts on the sensitivity and deviation factors to indicate the independent variable. Since in each case the dependent variable is an electric field maximum, the superscripts, used with the sensitivity factor or deviation factor, are simplified to let c represent the maximum electric field at the conductor surfaces, $E_{c(max)}$, and to let g represent the maximum electric field at the surface of the ground, $E_{g(max)}$.

D. Parameter Variations for Flat Horizontal Line

1. Height variations

From the discussion of transmission line parameters, it is recalled that changing the height of a transmission line changes the capacitance of the line to ground, and therefore changes the net charge density

required to maintain its potential. Since this capacitance decreases as the height is increased, one expects to see a reduction in both the maximum conductor surface field and the maximum electric field strength at the ground level as the height of the transmission line is increased. To obtain some quantitative information about these relationships, the electric fields at the conductor surfaces and at the ground level are computed for a series of transmission line heights from 10 meters to 15 meters in increments of 50 centimeters. All other parameters are held constant so that any changes can be attributed solely to the height changes.

The electric field strengths obtained at the points of interest by using the HIVAC2 program are summarized in Table 1. These results show the electric field variations as a function of conductor height for two-, three- and four-subconductor bundles.

In all cases shown, the maximum field at the surface of the subconductors appears to be located on a center phase subconductor and is directed radially outward from the center of the bundle. The conductor surface electric field variation with height is found to be small. The magnitude of this field appears to pass through a minimum near the basic configuration height of 12.5 meters with the other dimensions as assumed for the base case.

a. Sensitivity of ground level maxima The maximum ground level electric field shows a wide variation as the transmission line height is varied. The magnitude of this field decreases by approximately 50% as

the height increases from 10 meters to 15 meters. These data are plotted in Figure 21, where the similarity of the curves for different bundle sizes can be clearly seen.

The data summarized in Table 1 were used to determine the values of the deviation factor for the maximum ground level field, E_g, as a

Table 1. Variation of maximum electric fields at the conductor surfaces and at the ground level due to changes in conductor height

	Two Subconductors		Three Subconductors		Four Subconductors	
Height	E_c	E_g	E_c	E_g	E_c	E_g
m	kV/m	kV/m	kV/m	kV/m	kV/m	kV/m
10.0	1638.6	5.0822	1303.4	5.6627	1096.9	5.9587
10.5	1638.0	4.6900	1302.8	5.2231	1096.9	5.4948
11.0	1637.5	4.3406	1302.3	4.9320	1095.8	5.0824
11.5	1637.3	4.0279	1302.0	4.4822	1095.5	4.7136
12.0	1637.2	3.7468	1301.9	4.1681	1095.5	4.3827
12.5	1637.3	3.4931	1301.8	3.8849	1095.6	4.0844
13.0	1637.5	3.2633	1301.9	3.6285	1095.8	3.8245
13.5	1637.8	3.0545	1302.1	3.3957	1096.1	3.5695
14.0	1638.2	2.8641	1302.4	3.1836	1096.5	3.3463
14.5	1638.6	2.6899	1302.8	2.9740	1096.9	3.1425
15.0	1639.2	2.5303	1303.2	2.8122	1097.4	2.9957

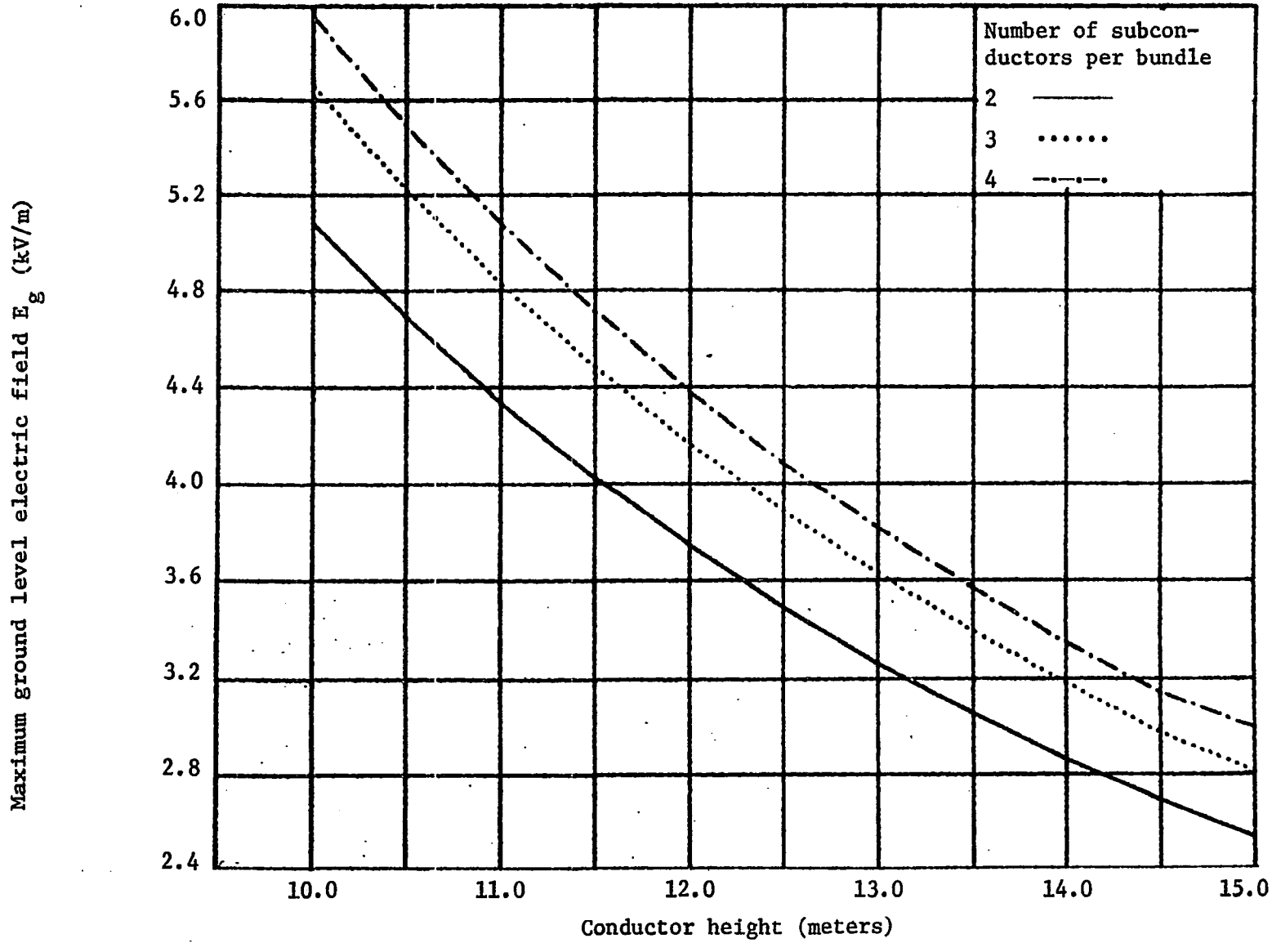

Figure 21. Variation of maximum ground level field, E_g, with line height

function of height for the three bundle types used. These values of F_H^g are shown in Figure 22. It is observed that the magnitude of the deviation factor increases with height in each case, ranging from 1.636 to 1.815. The difference due to the number of subconductors is found to be small within the height range from 10 meters to 15 meters. Over the same height variation, the range of the sensitivity factor magnitude $|S_H^g|$ is slightly less (1.627 to 1.815) due to a phase angle of approximately 186° at the lower height. This phasor displacement reduces the effectiveness of the sensitivity in producing changes in magnitude. The angles have not been included in Table 1, since they have no particular significance except to make the sign of the deviation factor negative.

b. Sensitivity of conductor surface maximum The data in Table 1 also indicate that the sensitivity of the maximum electric field at the surface of the conductors, E_c, to changes in height is almost negligible in the range of heights studied. The perceivable changes appear to show that for the flat transmission line configuration with a 7.5 meter phase separation, the maximum conductor surface field is least near the nominal base case height of 12.5 meters.

2. Phase spacing variations

Similar to height, phase spacing is a very important parameter since it determines allowable compaction of transmission lines. Reduction of the overall width of a transmission line system by compaction is found to reduce the magnitude of the maximum electric field at ground level, E_g. The distance from the centerline of the right-of-way to the maximum

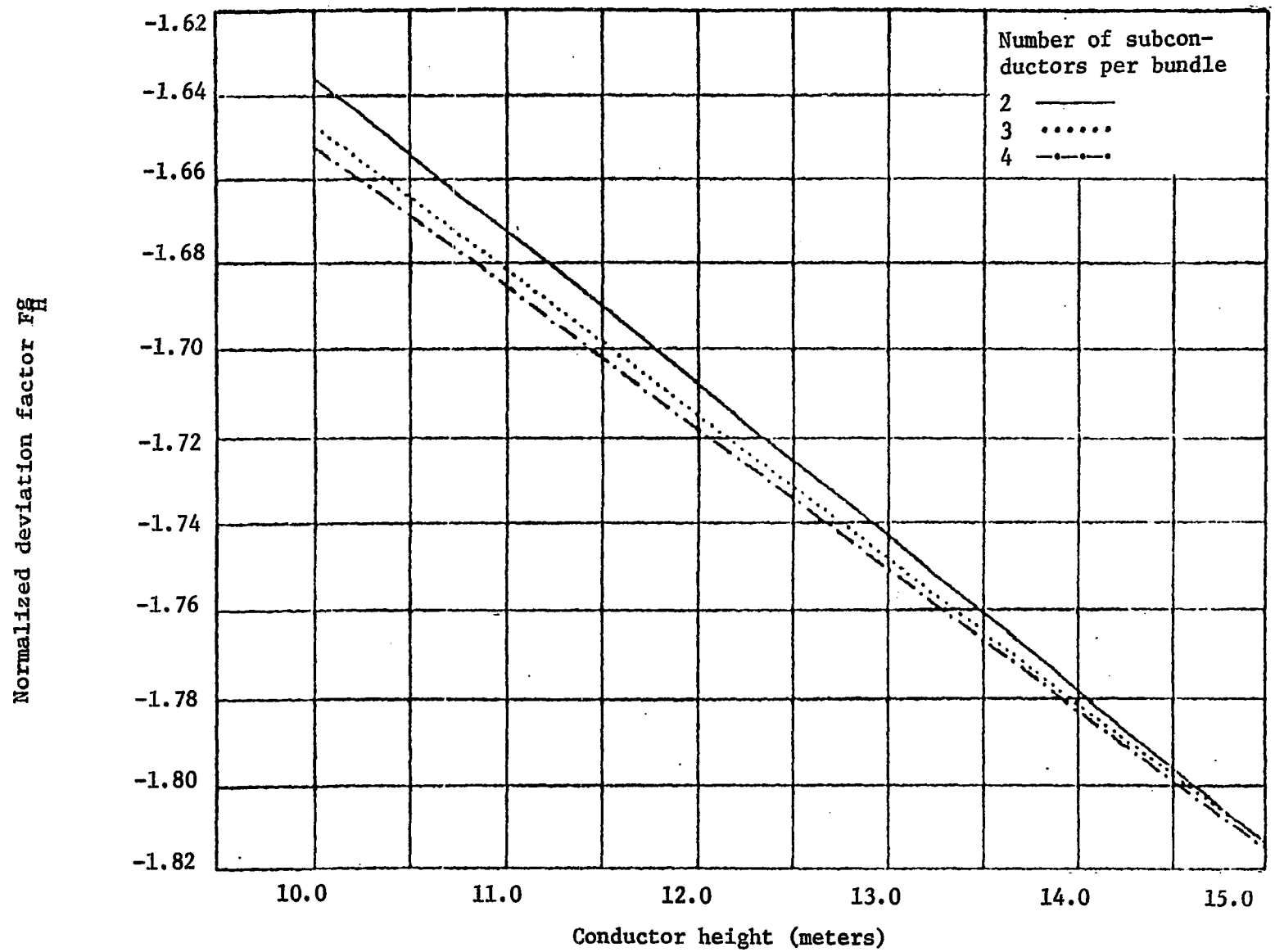

Figure 22. Deviation factor F^g_H for two-, three- and four-subconductors

field location is also reduced. Such reductions of the overall width of the system are usually accompanied by a reduction in the phase spacing.

From the base case configuration shown in Figure 1, the phase spacing D is changed to vary from 5 meters to 10 meters in increments of 50 cm. The maximum electric field at the conductor surfaces, E_c, and at the ground level, E_g, is obtained using the HIVAC2 routine. A summary of these data is given in Table 2.

Table 2. Maximum electric fields at the conductor surface and at ground level as a function of the horizontal phase spacing for H = 12.5 m

Phase Spacing	Two Subconductors		Three Subconductors		Four Subconductors	
	E_c	E_g	E_c	E_g	E_c	E_g
m	kV/m	kV/m	kV/m	kV/m	kV/m	kV/m
5.0	1808.9	2.7793	1458.6	3.1169	1236.3	3.2908
5.5	1764.4	2.9435	1417.6	3.2936	1199.3	3.4734
6.0	1726.1	3.0963	1382.5	3.4580	1167.8	3.6433
6.5	1692.7	3.2384	1352.0	3.6208	1140.5	3.8013
7.0	1663.3	3.3704	1325.4	3.7527	1116.6	3.9481
7.5	1637.7	3.4930	1301.9	3.8846	1095.6	4.0844
8.0	1614.1	3.6070	1282.0	4.0071	1076.9	4.2110
8.5	1593.3	3.7131	1262.3	4.1211	1060.3	4.3288
9.0	1573.5	3.8119	1245.5	4.2272	1045.3	4.4385
9.5	1557.5	3.9041	1230.3	4.3262	1031.7	4.5409
10.0	1542.0	3.9902	1216.5	4.4188	1019.5	4.6365

a. Sensitivity of ground level maxima The maximum electric field magnitude at ground level, E_g, is shown as a function of the phase spacing for a height of 12.5 meters in Figure 23. For all three bundles, the maximum electric field strength increases as the distance between the separate phase bundles is increased over the range from 5 to 10 meters. The total field strength variation is approximately ±15% for a phase separation variation of approximately ±33%. The deviation factors for the three bundle configurations are computed from the data in Table 2 and shown in Figure 24.

The phase angle of the sensitivity factor relating E_g to the phase spacing, D, varies from a negative value of approximately -5° at a 5 meter separation to approximately +25° at a separation of 10 meters. The effect of this increasing phase angle is to increase the difference between the magnitudes of the sensitivity factor and the deviation factor. The deviation factor is approximately equal to the sensitivity factor magnitude times the cosine of the phase angle associated with the sensitivity factor. The magnitude of the sensitivity factor is shown in Figure 26 for comparison with the deviation factor of Figure 25. It can be seen that their magnitudes are approximately 10% different at the higher end of the separation range. At the nominal separation of 7.5 meters, the deviation factor is approximately 0.52 and since it is positive in sign, this indicates that a 10% increase in the phase separation would produce approximately a 5.2% increase in the magnitude of E_g for the two subconductor system. A somewhat smaller change in the ground level field would be expected for a system with the four subcon-

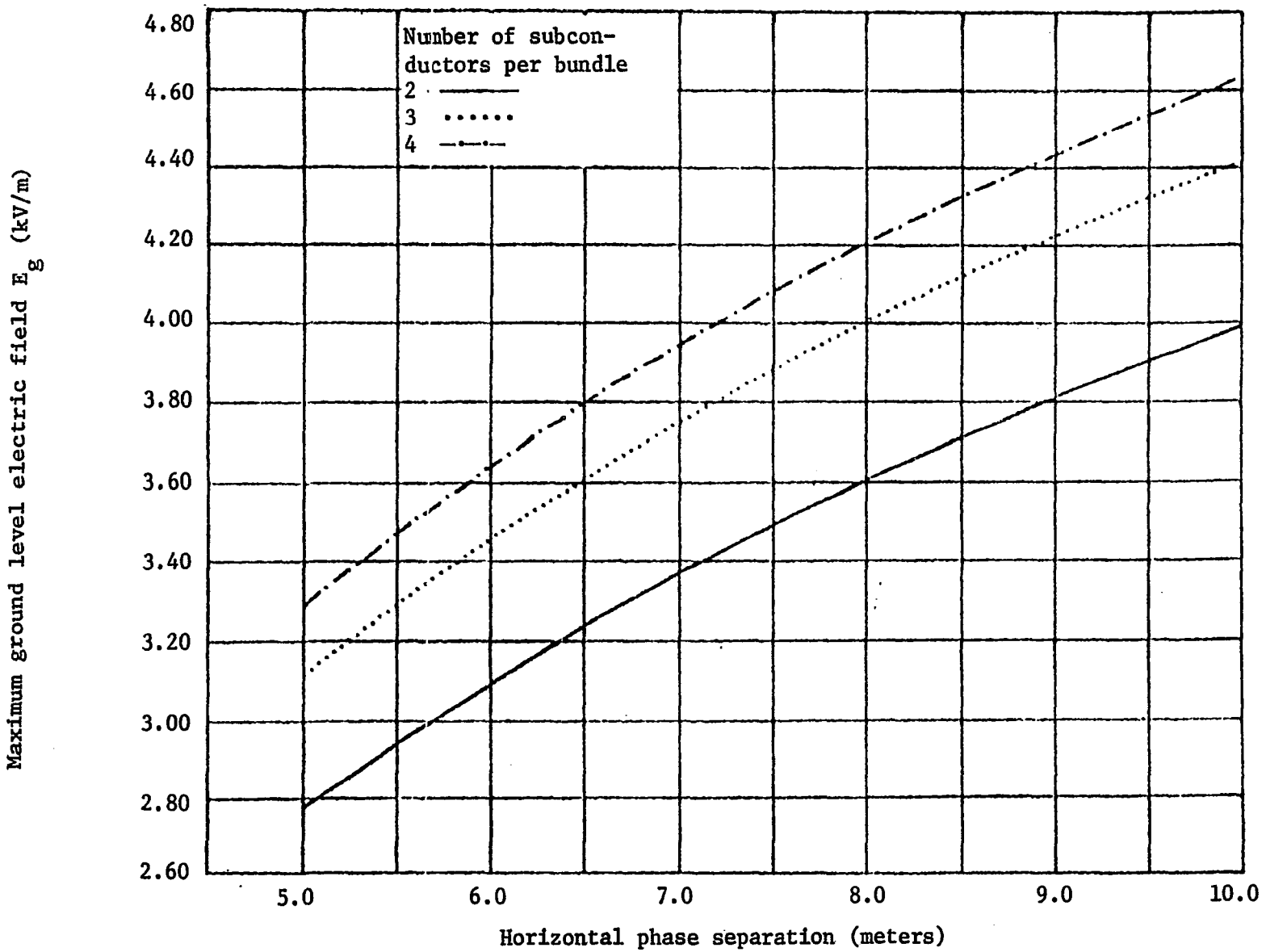

Figure 23. Variation of maximum ground level fields with phase separation

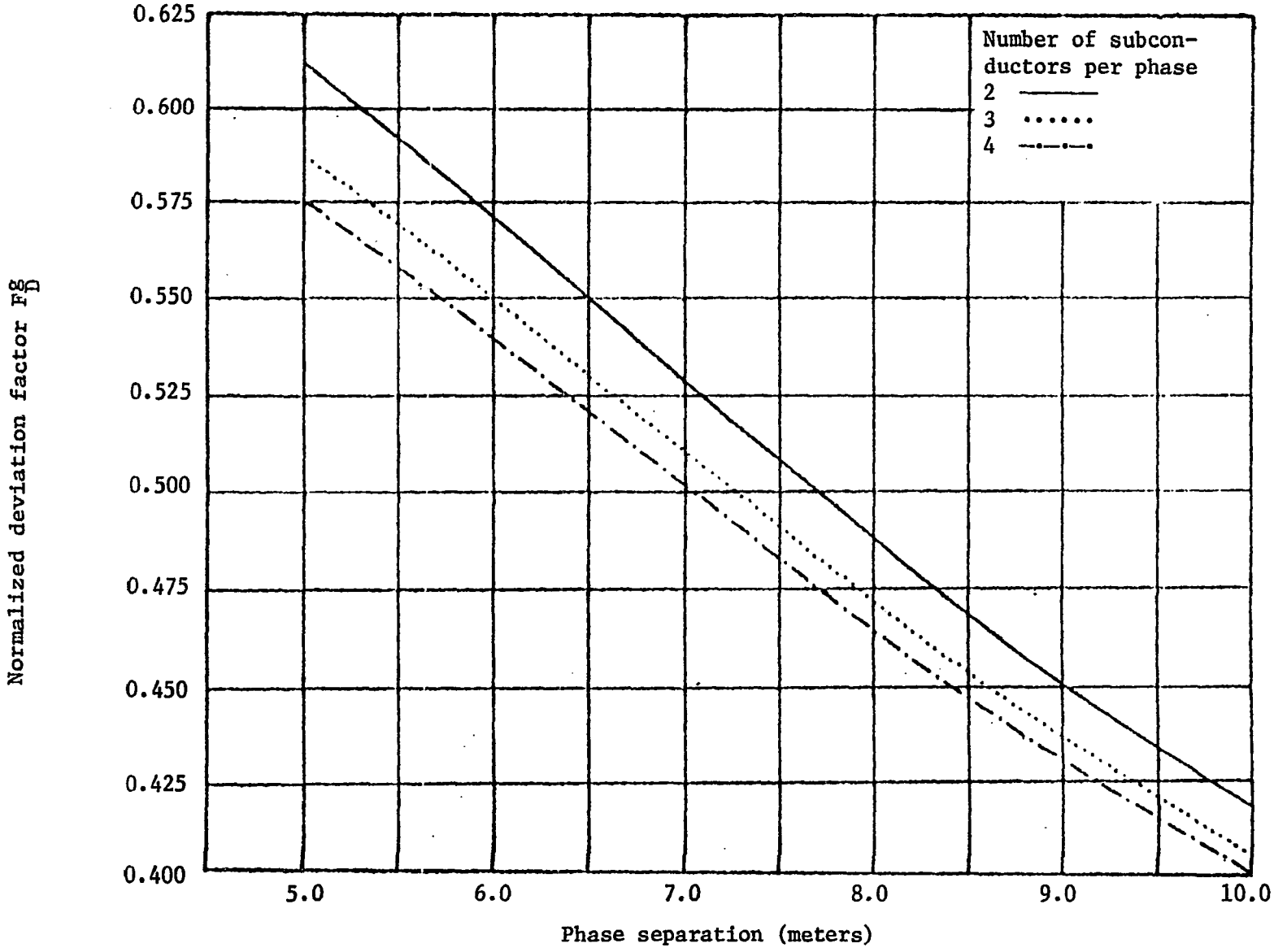

Figure 24. Deviation factor F_D^g for two-, three-, and four-subconductors

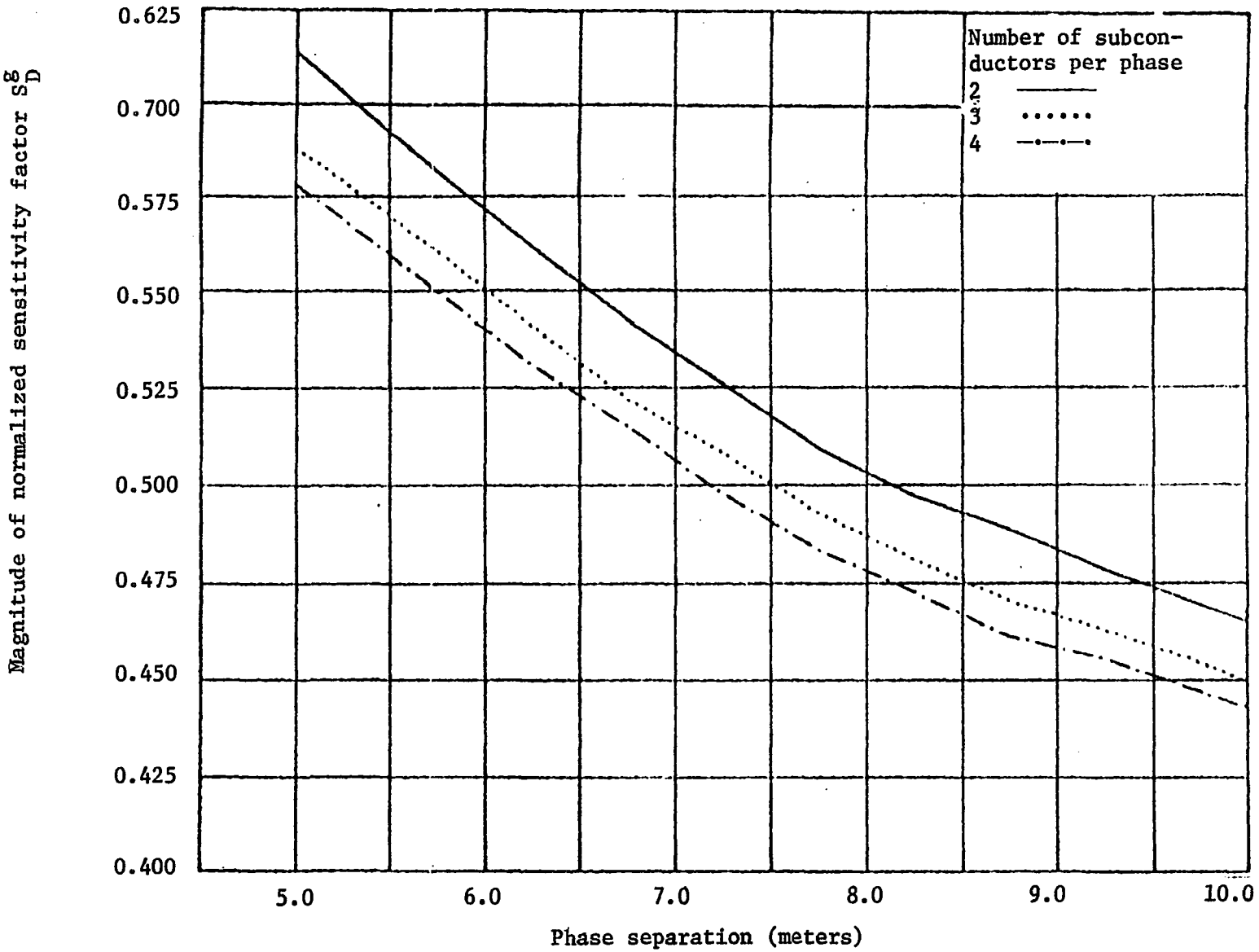

Figure 25. Magnitude of sensitivity factor S_D^g for 2, 3, and 4 subconductors

ductor bundle. A similar reduction in the phase spacing should produce a similar reduction of the electric field E_g in the same ratio.

b. Sensitivity of conductor field From the data given in Table 2, the electric fields at the conductor surfaces appear to be much more sensitive to changes in the phase spacing than to the changes in conductor height. The sensitivity factor magnitudes and the deviation factors with respect to changes in the phase spacing for the maximum conductor field, E_c, are given in Figures 26 and 27.

This deviation factor, F_D^c, is computed from the data in Table 2 and plotted as a negative number in Figure 26. It is shown that the magnitude of the deviation factor for the four-subconductor bundles is considerably higher than for the two-subconductor bundles. The center of the range for these deviation factors is approximately -0.25. The ratio of the deviation factor to the sensitivity factor magnitude is almost constant since the phase angle associated with the sensitivity factor is approximately 170° throughout the entire range of separations used. This relationship can be seen in Figure 27 where the magnitudes are both shown on the same scale.

It is interesting to note that for this particular configuration, the deviation factor F_D^g is approximately twice the magnitude of the deviation factor F_D^c and of opposite sign. This emphasizes one of the problems of trying simplistic solutions to solve one field maximum difficulty by varying only one dimensional parameter. Varying only the phase

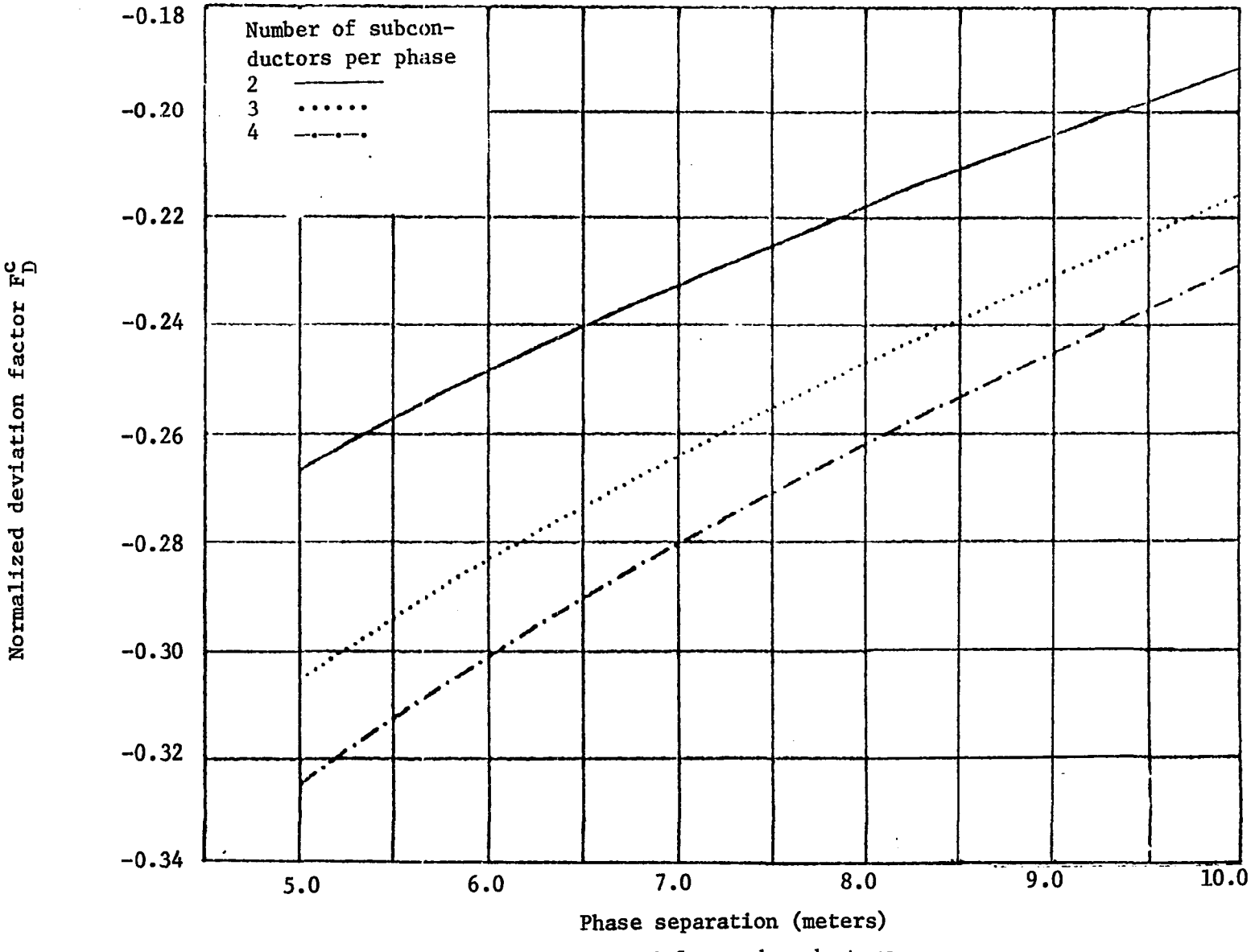

Figure 26. Deviation factor F_D^c for two-, three-, and four-subconductors

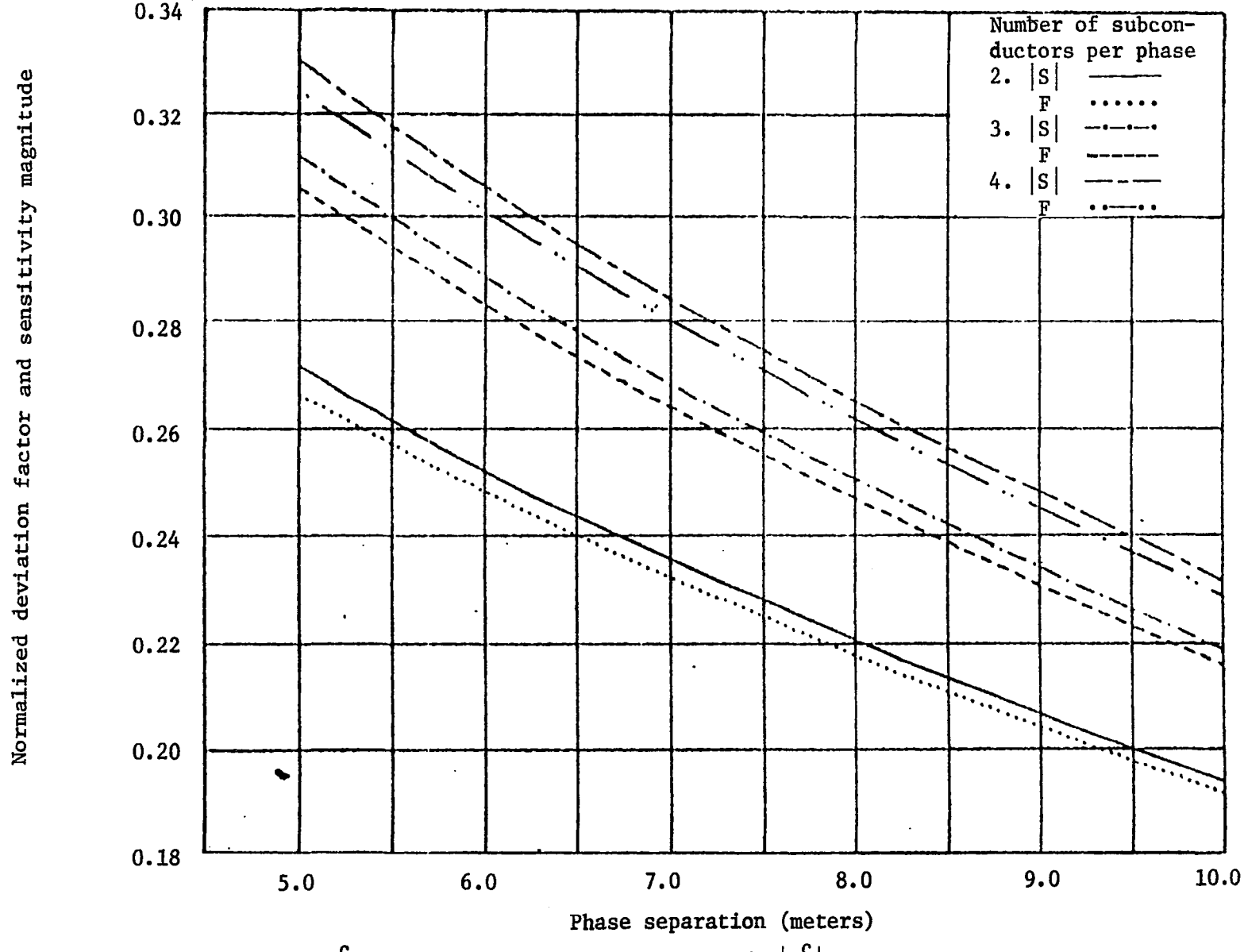

Figure 27. Comparison of F_D^c with sensitivity factor magnitude $|S_D^c|$

spacing, for example, to obtain a 10% reduction in the maximum conductor field would cause a corresponding increase in the ground level maximum of 20%.

3. Bundle spacing variations

The effects of bundle spacing on the electric field maxima at the ground level and on the conductor surfaces are obtained from the data given in Table 3 and plotted in Figures 28 and 29. With all other parameters (H, D, d) remaining constant, the bundle diameter is varied from 10 cm to 100 cm in increments of 10 cm. The electric fields of interest are computed for these variations using the HIVAC2 computer routine. Since the spacings in the bundle are related to this diameter by a constant, this is equivalent to changing the spacing between conductors by the same relative increment. The data are again given for two-, three- and four-subconductor bundles for further comparison.

a. Sensitivity of ground level maxima As might be expected from earlier calculations of the deviation factors for the ground level electric field maxima, the relatively small dimensional changes in the bundle spacing with respect to the overall system dimensions produce less disturbance in the ground field values than other dimensional changes already considered.

The sensitivity factors and deviation factors appear to increase as the number of subconductors increases. At the nominal base case diameter of 50 cm, F_S^g is approximately 0.100 for the two-subconductor bundle and

Table 3. Variation of maximum electric field at the conductors surface and at the ground level as a function of bundle diameter

Bundle Diameter	Two Subconductors		Three Subconductors		Four Subconductors	
	E_c	E_g	E_c	E_g	E_c	E_g
cm	kV/m	kV/m	kV/m	kV/m	kV/m	kV/m
10	1636.9	3.0088	1381.9	3.2402	1244.6	3.1973
20	1590.8	3.1985	1285.8	3.4164	1114.8	3.5169
30	1597.9	3.3227	1273.9	3.6080	1085.3	3.7456
40	1616.3	3.4167	1284.1	3.7586	1084.9	3.9288
50	1637.3	3.4903	1301.9	3.8846	1095.6	4.0844
60	1548.7	3.5575	1322.5	3.9940	1111.4	4.2211
70	1679.6	3.6135	1344.2	4.0925	1129.5	4.3442
80	1699.7	3.6630	1366.1	4.1797	1148.8	4.4566
90	1719.2	3.7072	1387.9	4.2606	1168.8	4.5607
100	1737.8	3.7473	1409.5	4.3355	1188.9	4.6579

has increased to 0.178 for the four-subconductor bundle with the same diameter. It can also be seen in Figure 30 that the range of variation is increased for the larger number of subconductors. The phase angle of the sensitivity factor is limited to approximately 5% for the entire range of diameters so that the deviation factor and the sensitivity factor magnitude are essentially the same. The sign of the deviation factor is positive throughout the range.

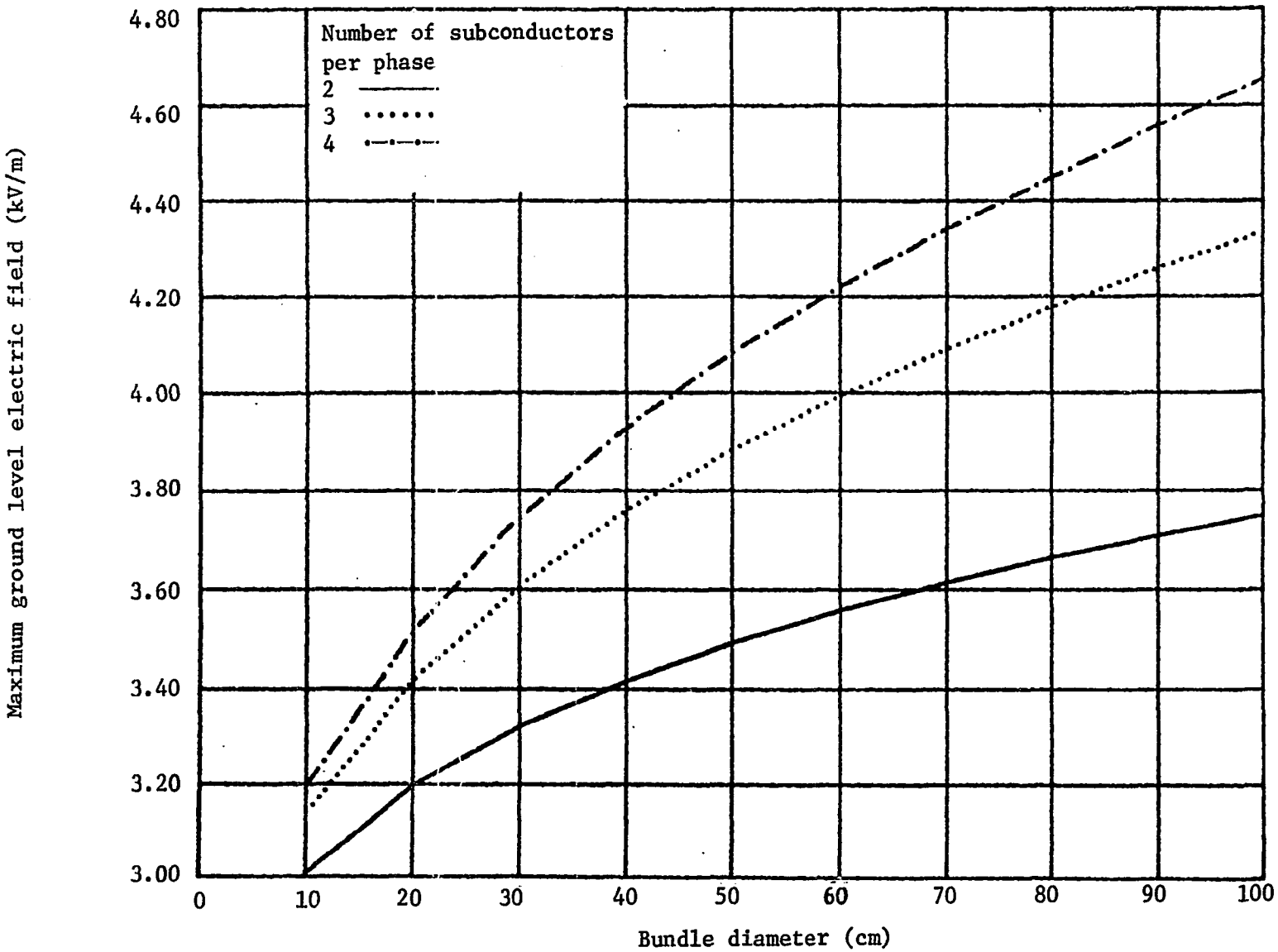

Figure 28. Variation of maximum ground level field with bundle diameter

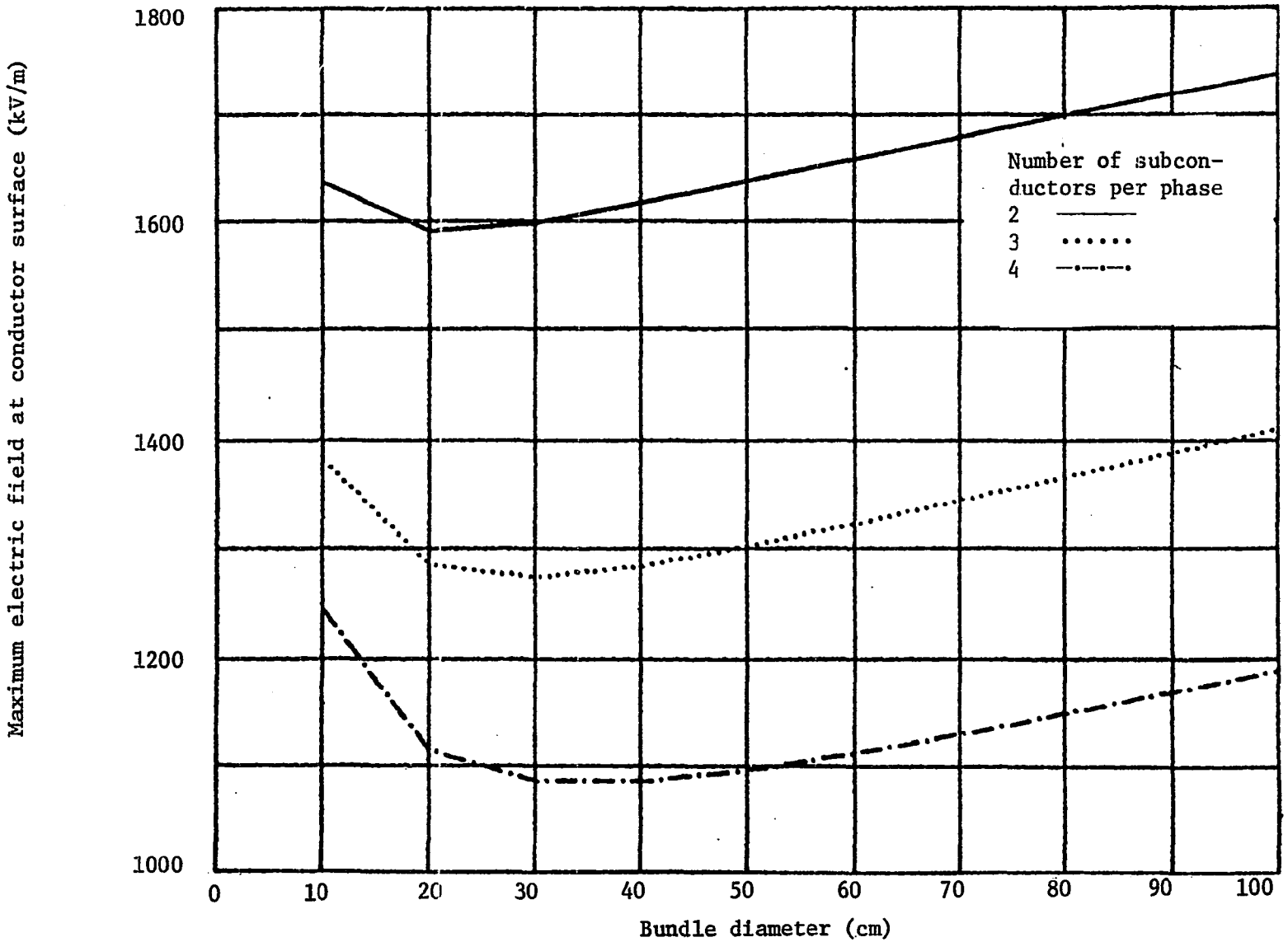

Figure 29. Variation of maximum conductor field with bundle diameter

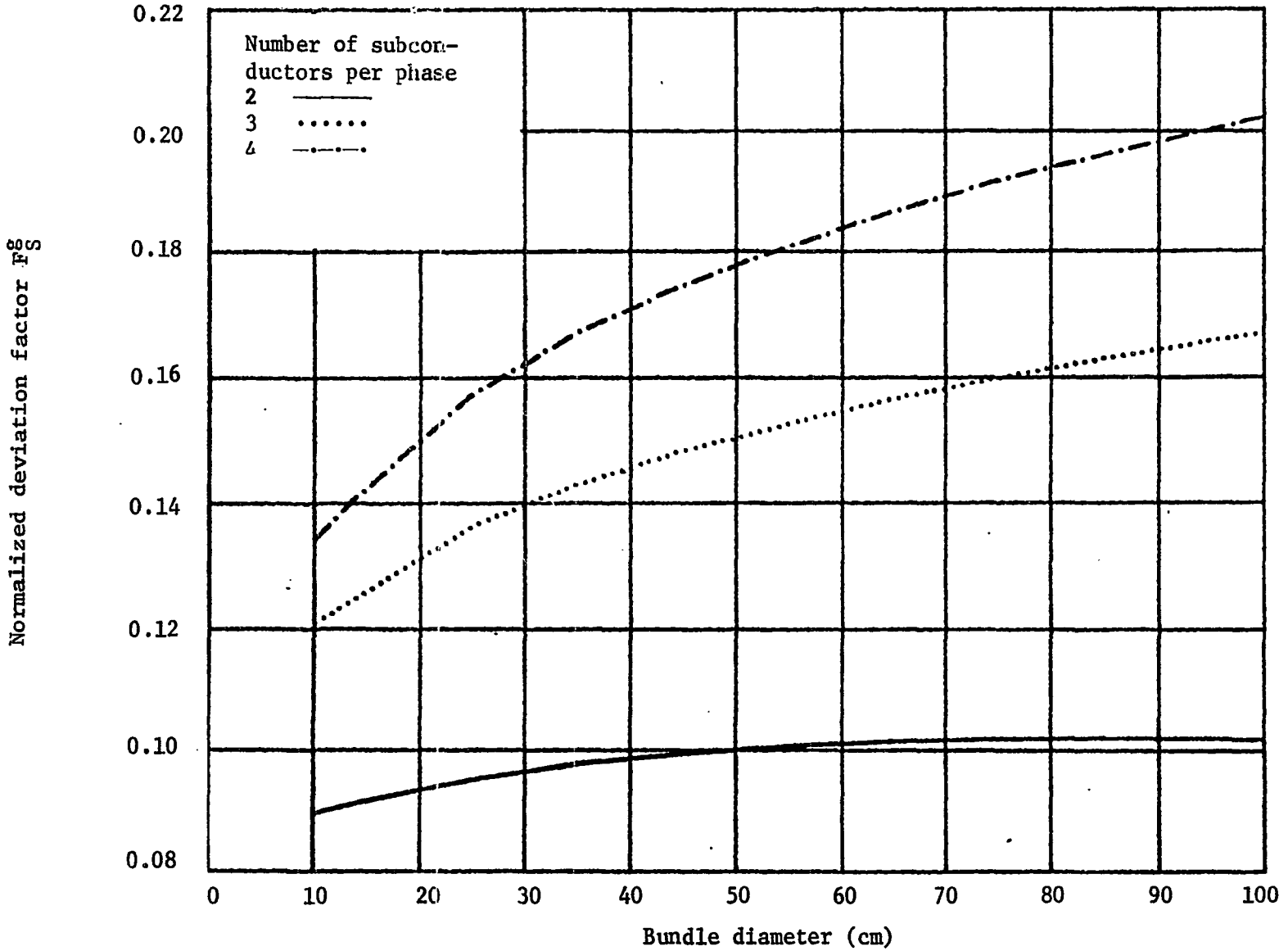

Figure 30. Deviation factor, F_S^g, for two-, three-, and four-subconductors

b. Sensitivity of conductor surface field The change in maximum electric field at the conductor surface as a result of changing the bundle spacing shows an interesting characteristic which is more evident in the three- and four-subconductor cases. In general, the deviation factor increases as the bundle diameter increases and is positive in sign. Below a certain critical spacing, however, the deviation factor changes sign indicating a drastic change in the phase of the sensitivity factor. Below this critical bundle spacing, the magnitude of the sensitivity factor increases with decreasing spacing. This critical diameter varies with the number of subconductors from about 23 cm for the two-subconductor bundle to 35 cm for the four-subconductor bundle. These critical values in the deviation function F_S^c can be seen clearly in Figure 31, which is plotted from data given in Table 3. The sign change is the result of a change in the phase of the sensitivity factor from approximately -175° at 10 cm to -15° at a diameter of 100 cm.

4. Conductor diameter variations

The effects of changing conductor diameters upon the maximum electric fields E_g and E_c are of considerable importance. It should also be pointed out that these changes may also have considerable effect upon the mechanical design of the system. The static mechanical loading on various mechanical elements of the transmission line system is proportional to the square of the conductor diameter. Other loading factors such as ice and wind loading are also related to the conductor diameters.

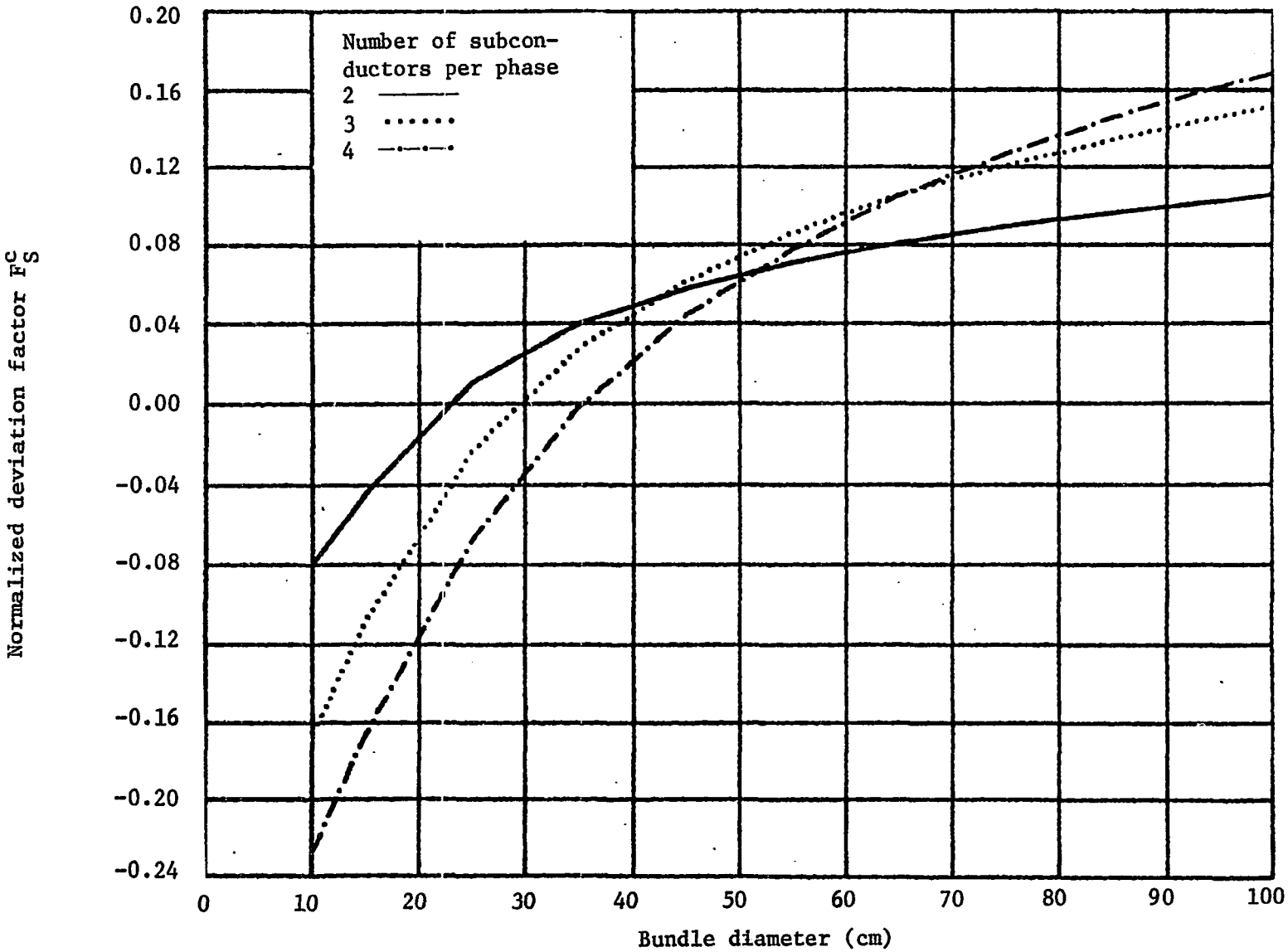

Figure 31. Deviation factor F_S^c for two-, three-, and four-subconductors

The maximum electric fields, E_g and E_c, are calculated for a series of conductor diameters ranging from 1 cm to 10 cm. All other dimensions remain the same as those of the base case. These data are given for two-, three-, and four-subconductors with a constant bundle diameter of 50 cm in Table 4. The trends in these field strength values are quite noticeable in the tabulation and even more readily apparent in Figures 32 and 33.

Table 4. Variation of maximum electric field at the conductor surfaces and at the ground level as a function of conductor diameter

	Two Subconductors		Three Subconductors		Four Subconductors	
Diameter cm	E_c kV/m	E_g kV/m	E_c kV/m	E_g kV/m	E_c kV/m	E_g kV/m
1	4192.1	3.1406	3310.3	3.5856	2472.9	3.8325
2	2301.7	3.3540	1829.5	3.7684	1517.7	3.9869
3	1637.3	3.4930	1301.9	3.8846	1095.6	4.0844
4	1293.5	3.5990	1036.3	3.9719	880.3	4.1573
5	1082.1	3.6858	873.8	4.0428	749.0	4.2164
6	938.1	3.7601	763.7	4.1031	660.3	4.2668
7	833.4	3.8254	683.9	4.1560	595.9	4.3112
8	753.7	3.8840	623.3	4.2034	547.1	4.3513
9	690.8	3.9384	575.5	4.2466	508.5	4.3880
10	639.8	3.9865	536.8	4.2865	477.2	4.4223

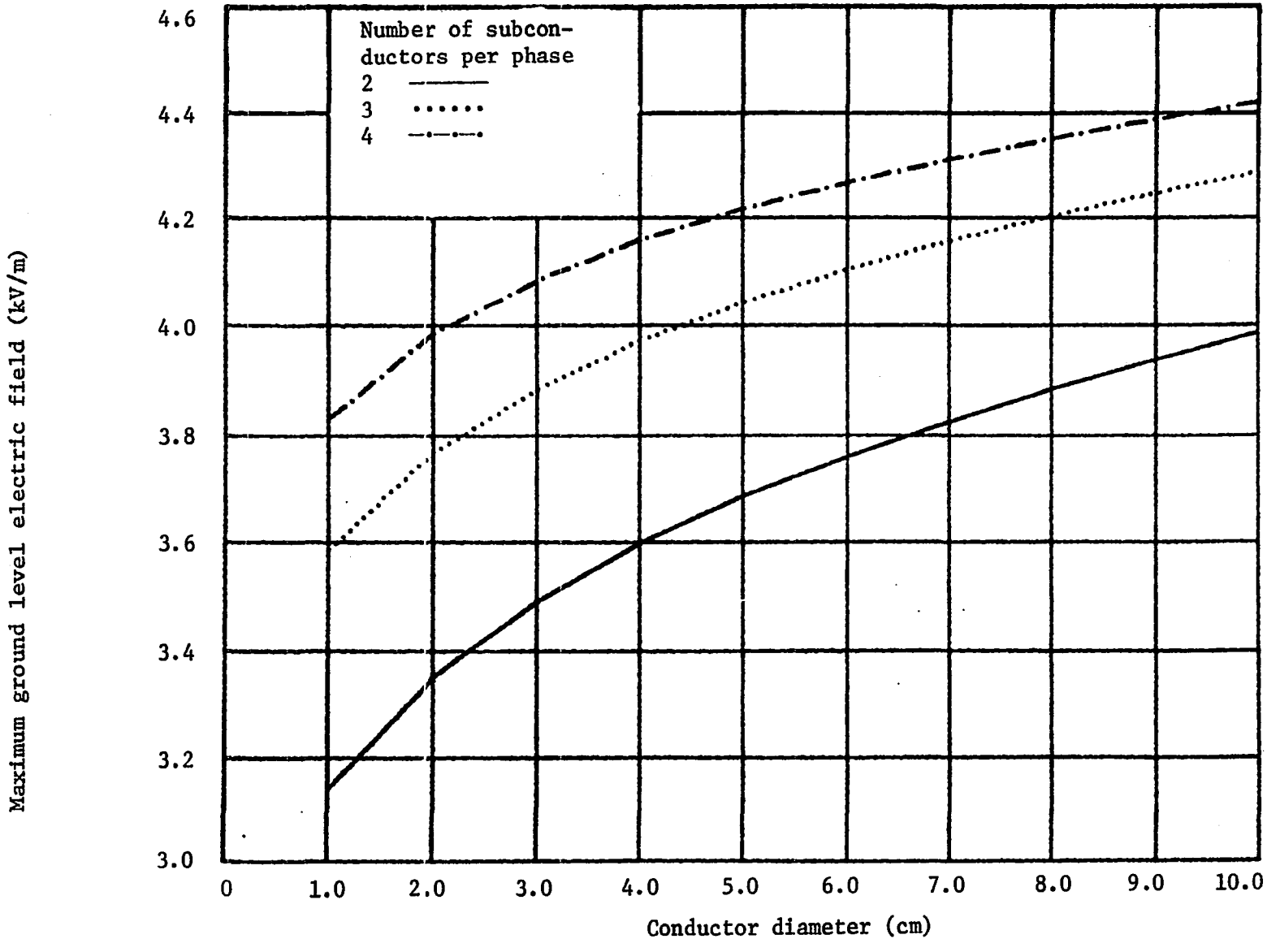

Figure 32. Variation of E_g with conductor diameter

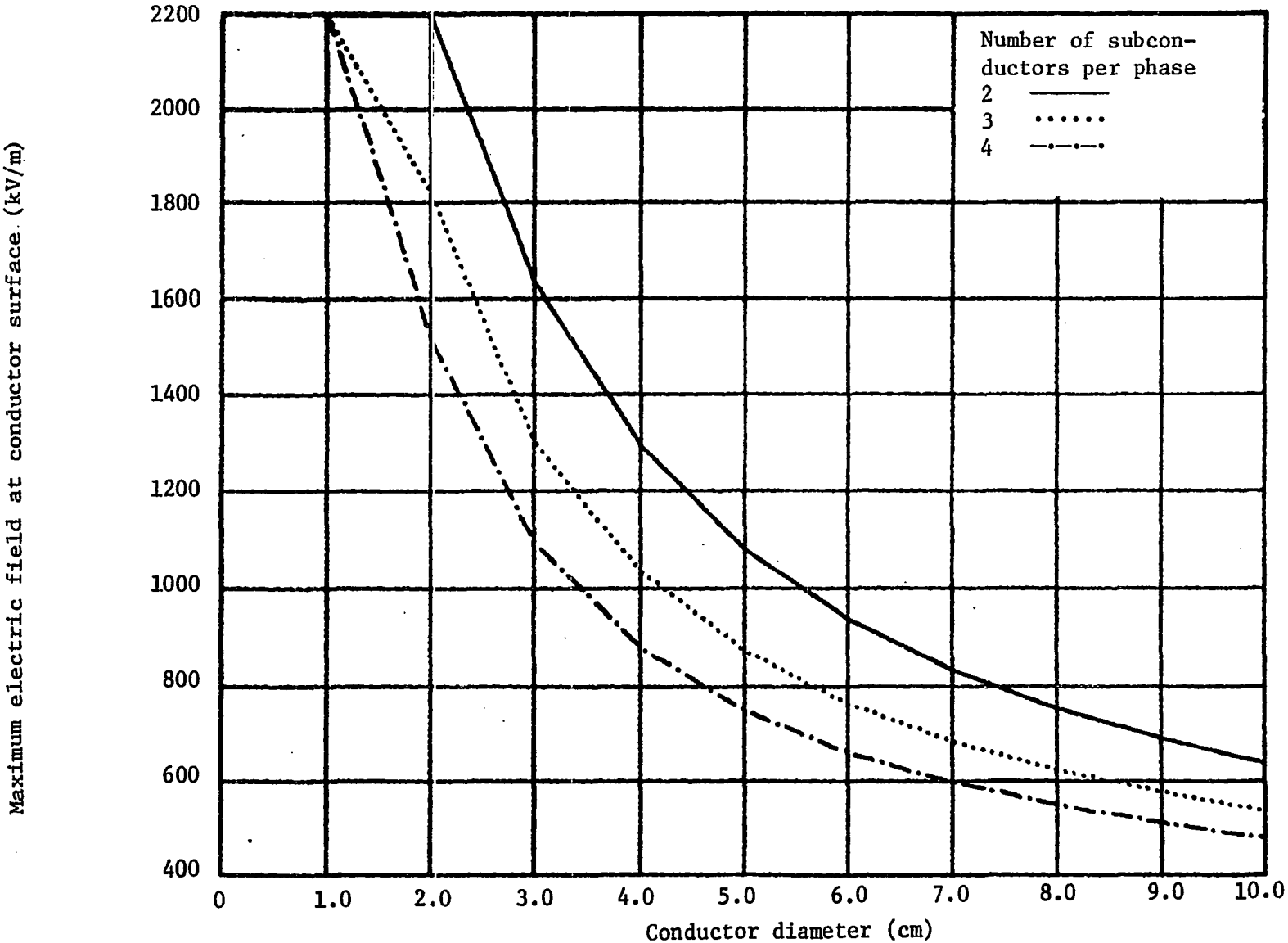

Figure 33. Veriation of E_c with conductor diameter

a. Sensitivity of ground level maxima The ground level electric fields will be effected by changes in the conductor diameter primarily because of the resulting change in capacitance. As was mentioned earlier in this paper, the increase in capacitance requires a larger equivalent line charge to maintain the potential at the surface of the conductor. The change in equivalent line charge will change the ground level field accordingly.

For the range of conductor diameters utilized, the value of the maximum ground level field can be seen to vary approximately 10% above and below the base case values. The variation for the two-subconductor case is the larger (12%), while the four-subconductor case shows a somewhat smaller range of variaton (8%). In either case, the deviation factor itself is quite small, being on the order of 0.1 or less, as shown in Figure 34. The magnitude of the sensitivity factor is very close to that of the deviation factor since the angle associated with the sensitivity factor is only about 6° and has little variation over the range of diameters considered.

b. Sensitivity of conductor surface field The data given in Table 4 show a very sharp increase in the maximum electric field, E_c, as the conductor diameter is reduced from the nominal three centimeter diameter to two centimeters. Since the percent change in the conductor diameter at this point is also large, the sensitivity factor and deviation factor are not as large as might at first be expected. These factors are, however, greatest for the smaller diameters.

Figure 35 shows the deviation factors for the three different cases of two-, three-, and four-subconductor bundles, and relate the changes in the maximum conductor surface field to the changes in conductor diameter. The phase angle of the sensitivity factors is approximately 181° over the entire range of diameters so that the deviation factors are negative and are essentially the same magnitude as the sensitivity factors. As shown in Figure 35, the range of these magnitudes increases as the number of subconductors increases. It should follow that changes in conductor diameters for a bundle of two subconductors will be more effective in changing the conductor surface field than the same change in diameter for a four-subconductor bundle. Overall, it appears that changes in conductor diameter are about 75% efficient in changing the maximum field strength at the conductor surface. A 10% change in diameter produces approximately a 7.5% change in the surface electric field intensity.

It should be noted in Figure 33 that the vertical scale has been truncated at 2200 kV/m, since the rms value of the dielectric strength of air is 2121 kV/m. Any values above this are not valid for open-wire lines. It would appear that for a 345 kV transmission line that the three centimeter diameter assumed is very close to the minimum allowable for this configuration with a two-subconductor bundle.

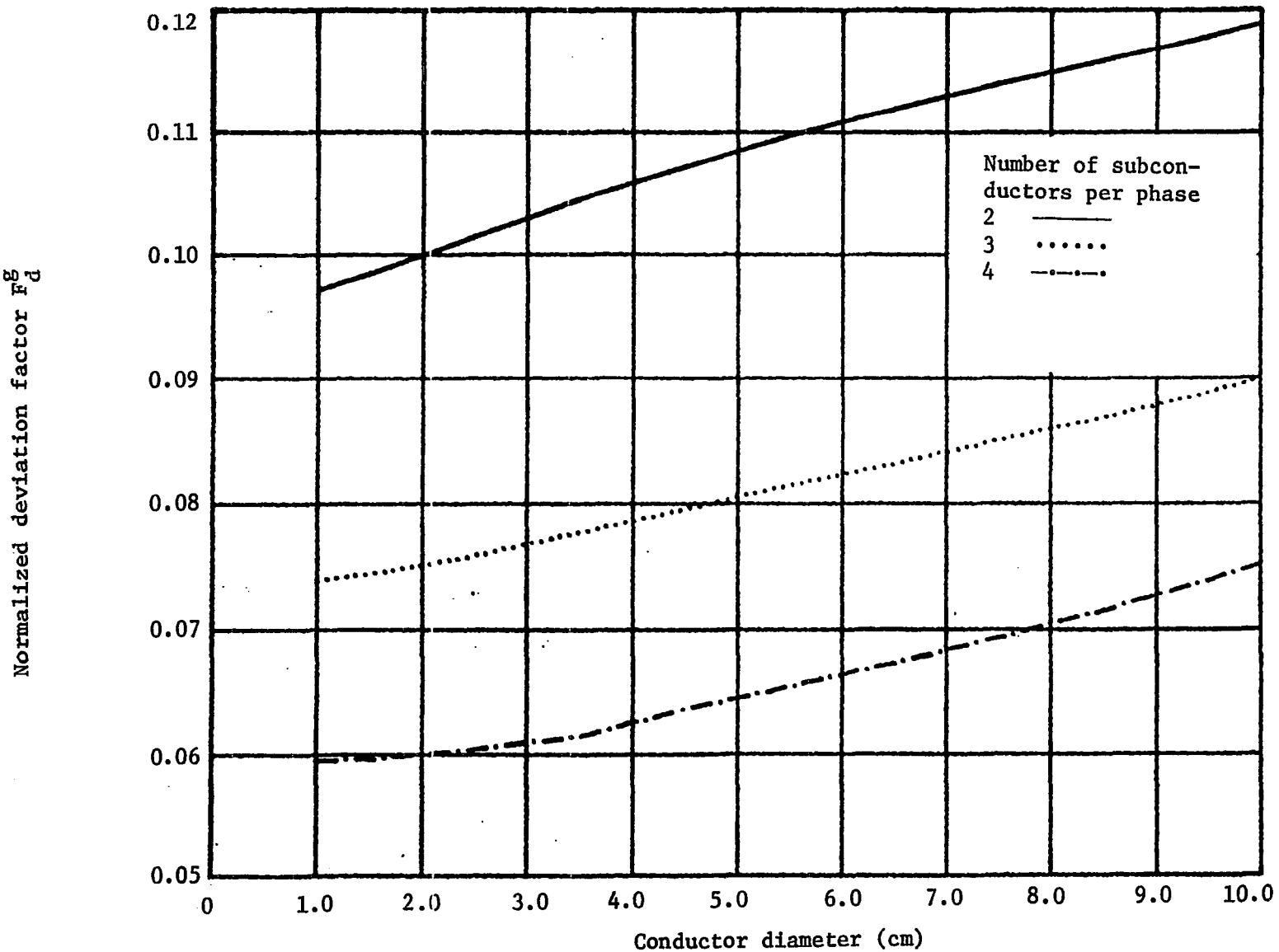

Figure 34. Deviation factor F_d^g for two-, three-, and four-subconductors

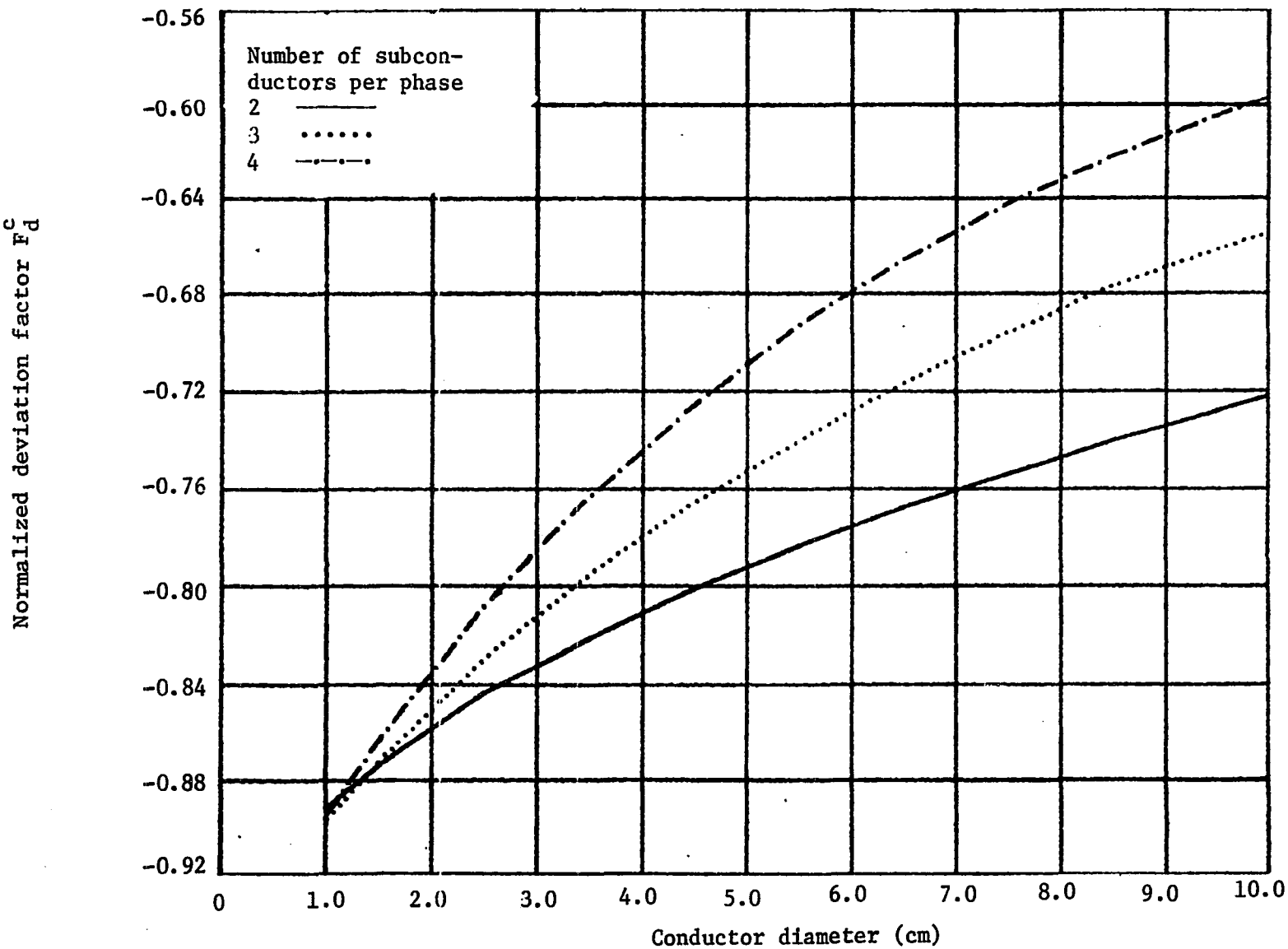

Figure 35. Deviation factor F_d^c for two-, three-, and four-subconductors

E. Parameter Variations for Staggered Horizontal Line

1. Height variations

Since all HV and UHV transmission lines are not mounted in the flat configuration, it is necessary to consider the effect of mounting the center phase bundle out of the plane of the other two-phase bundles.

Table 5. Variation of maximum electric fields at the conductor surfaces and at ground level due to selected changes in conductor heights

	$H_1 = H_3$ variable		H_2 variable		$H_1 = H_2 = H_3$	
Height	E_c	E_g	E_c	E_g	E_c	E_g
m	kV/m	kV/m	kV/m	kV/m	kV/m	kV/m
10.0	1604.0	5.2067	1632.0	3.4353	2638.5	5.0803
10.5	1614.8	4.7834	1634.6	3.4419	1637.9	4.6879
11.0	1623.1	4.4057	1636.7	3.4507	1637.5	4.3390
11.5	1629.8	4.0677	1638.0	3.4620	1637.2	4.0265
12.0	1634.5	3.7645	1638.2	3.4758	1637.2	3.7455
12.5	1637.2	3.4919	1637.2	3.4919	1637.2	3.4919
13.0	1637.9	3.2467	1335.0	3.5102	1637.4	3.2622
13.5	1636.6	3.0258	1631.6	3.5305	1637.7	3.0534
14.0	1633.4	2.8267	1627.0	3.5524	1638.1	2.8631
14.5	1628.5	2.6474	1621.4	3.5756	1638.6	2.6889
15.0	1622.0	2.4863	1615.0	3.5998	1639.1	2.5292

Two sets of data were obtained for these non-planar conditions using the HIVAC2 computer program. In one case, the height of the center bundle (H_2) is held constant at 12.5 meters, while the outer phase bundle heights ($H_1 = H_3$) are varied from 10 meters to 15 meters in 0.5 meter increments. In the second case, the outer phase bundles are held constant at 12.5 meters, while the center phase bundle height is varied over the same range. These data are tabulated in Table 5 with the two subconductor, flat configuration data added for reference.

a. Sensitivity of ground level maxima From the data in Table 5 and given in graphic form in Figure 36, it is obvious that the height of the center phase bundle has much less effect upon the maximum ground level electric field maxima than the heights of the outer phase bundles. Height variations of ±20% in H_2 produce less than 5% overall variation in E_g. On the other hand, changes in the heights H_1 and H_3 of ±20% produce an overall variation of nearly 80% in the maximum ground level field strength. The plot of these data in Figure 36 shows clearly the close correspondence of the fields of the flat configuration to those obtained by changing only H_1 and H_3. Since the slope of the latter curve is always greater than the slope of the flat configuration curve, changing only the outer bundle heights is slightly more effective in controlling the ground level maxima than changing all three heights in the flat configuration.

The deviation factors $F^g_{H_1}$, relating the ground level maxima to changes in the outer phase bundles only, and F^g_H, relating these fields to changes in the height of the flat configuration, are plotted in

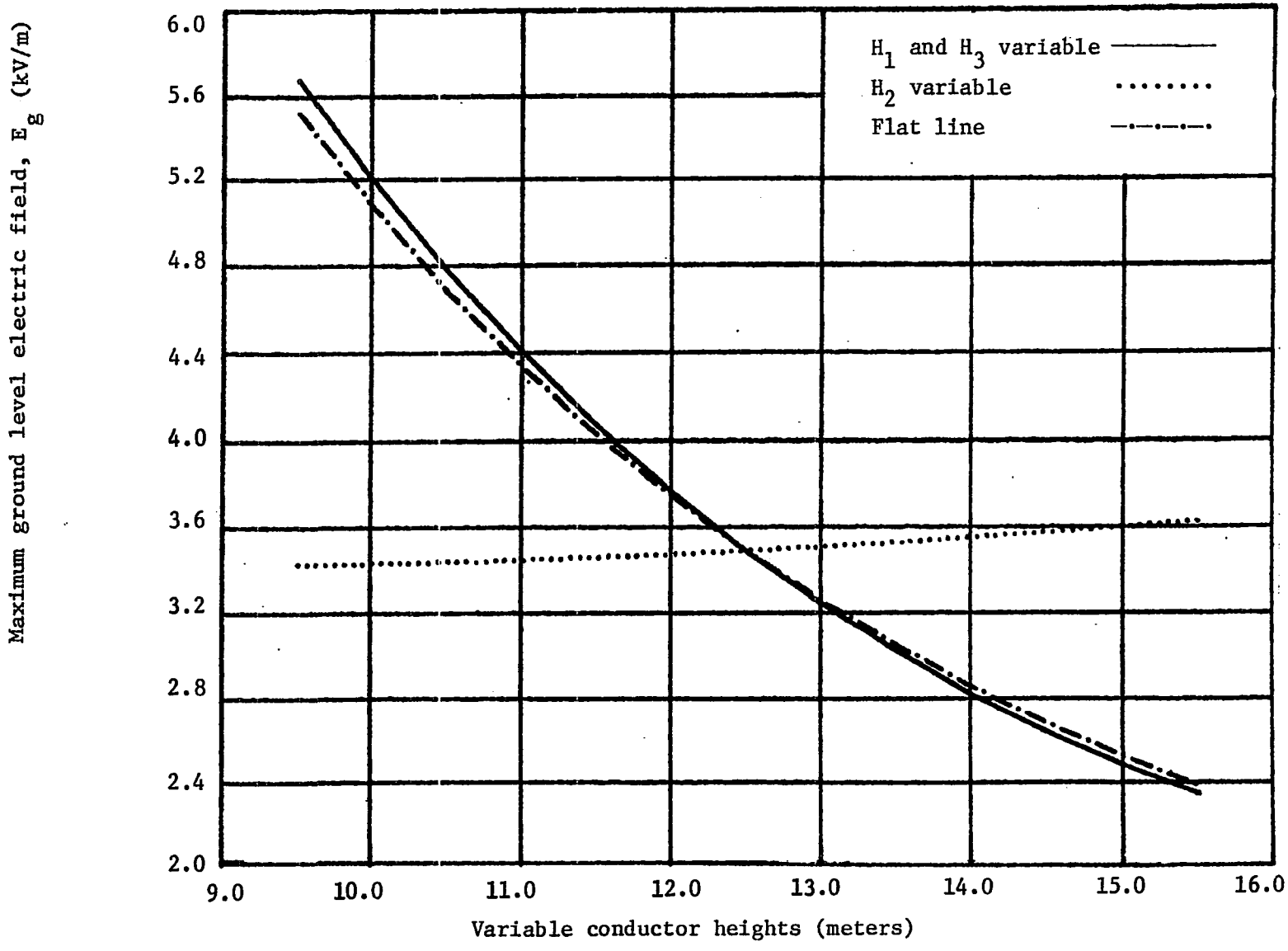

Figure 36. Variation of maximum ground level electric field, E_g, for staggered line heights

Figure 37. At the 12.5 meter height, $F^g_{H_1}$ is found to be -1.832 and F^g_H is -1.725. These deviation factors are closer than they might appear in Figure 37 because of the suppressed origin of the graph. Above the 15 meter height, it appears that the magnitude of F^g_H continues to increase while the magnitude of $F^g_{H_1}$ decreases.

b. Sensitivity of conductor surface field The data for conductor surface field maxima given in Table 5 have been plotted in Figure 38. It is evident that these fields are relatively insensitive to changes in height. The variation shown appears to be more a function of the bundle separation than of the proximity of the ground.

2. Other variations in physical parameters

Since phase separation, bundle diameter and subconductor dimensions are primarily effective in changing local fields, the uneven conductor heights should have only a secondary effect upon deviation factors which involve changes in these parameters. The deviation factors obtained for the flat transmission line should therefore be accurate enough for most purposes.

F. Application of Sensitivity Analysis to Compaction

Analysis of the deviation factors developed in this study indicates that a "V" shaped transmission line configuration will provide a better distribution of the electric fields than the flat or inverted "V" con-

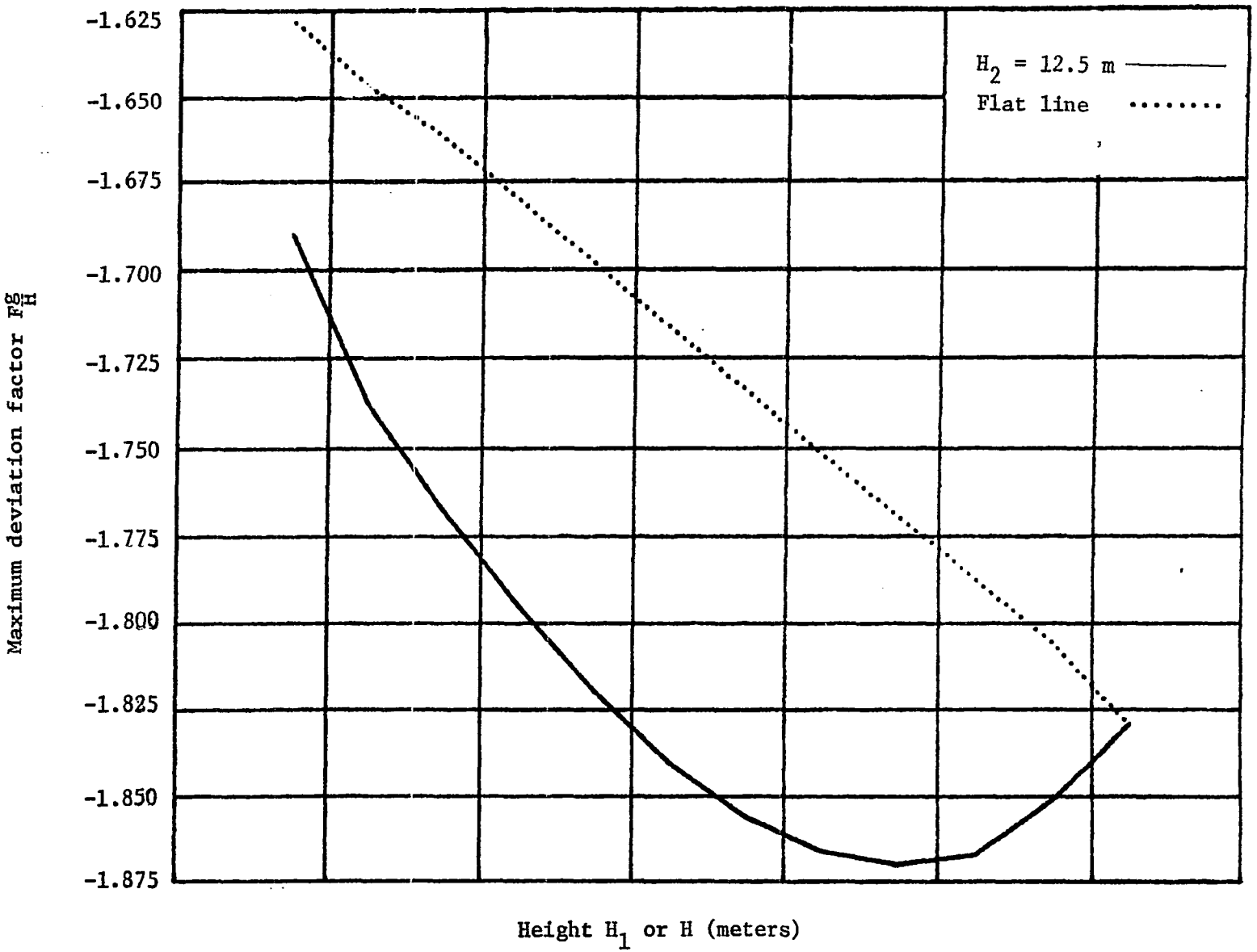

Figure 37. Comparison of deviation factor F_H^g for flat and staggered lines

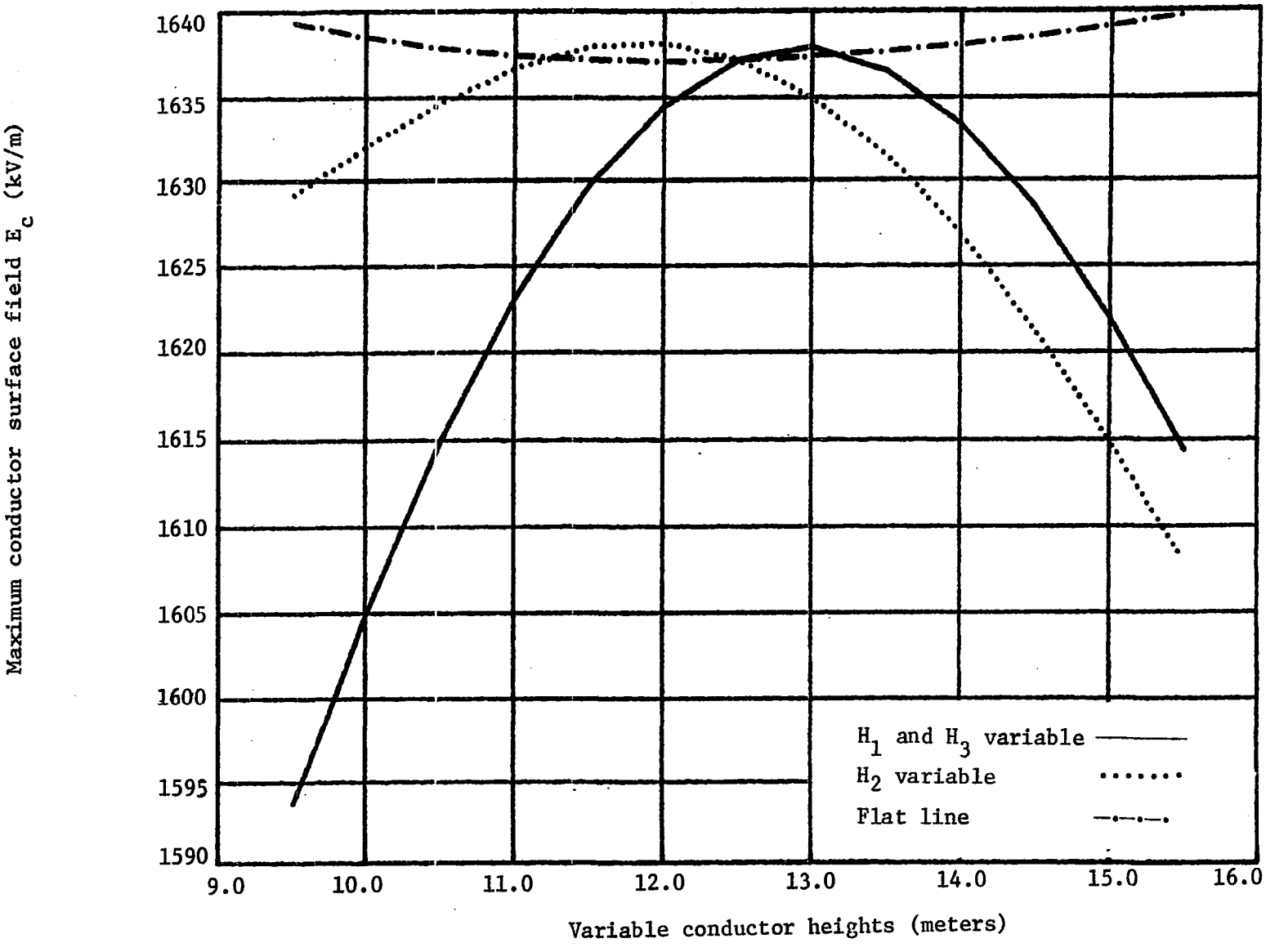

Figure 38. Comparative E_c fields for variation in H_1, H_2 and H

figurations which are presently in common use. This is particularly true if the maximum ground level fields are of primary importance. A compacted model of a 345 kV three-phase transmission line has been developed and studied with these factors in mind. The effects of any parameter changes upon mechanical characteristics of the system have not been considered in this study. For reduction of electric fields, the compacted "V" shows considerable promise. One simple structural change to obtain such a configuration can be seen in Figure 39.

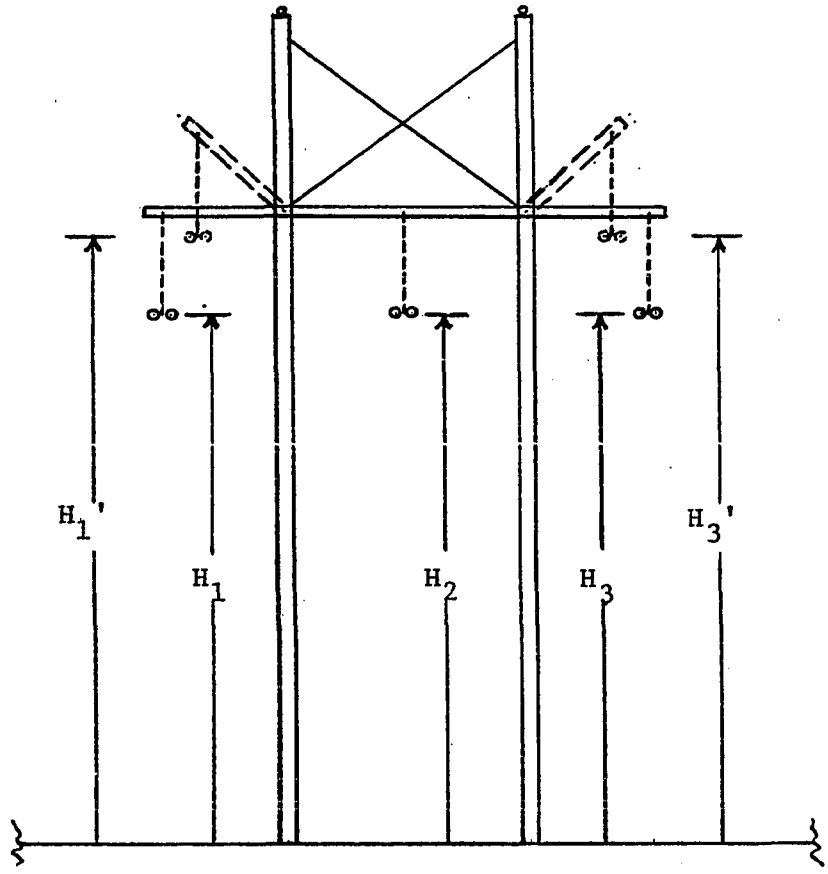

Figure 39. Possible structural change to obtain staggered configuration

For comparison with the base case field distribution shown in Figures 17 and 18, each phase bundle consists of two subconductors with a diameter of 3 cm. The minimum clearance above ground (H_2) is assumed to be 12.5 meters and the outer phase bundles have been raised 20% in height to 15.0 meters. The horizontal phase separation is reduced by 20% to 6.0 meters. According to the calculated deviation factors, these parameter changes should reduce the maximum ground level field strength by approximately 40% and move the peak value locations closer to the centerline of the system. These same changes will increase the maximum field at the conductor surface by approximately 3.5%. The sensitivity factors suggest that a reduction of the bundle spacing should help compensate for this increase in conductor surface field strength. The bundle spacing is therefore reduced 40% from 50 cm to 30 cm for the compacted model. The maximum electric field at the conductor surface under these conditions is found to be only 1.5% over the base case value.

Figure 40 shows the ground level electric field distribution for this compacted transmission line model. The field strengths at 4 meters from the ground are shown in Figure 41. According to the field data obtained using HIVAC2, the ground level maxima are reduced by approximately 35% from 3.5 kV/m to 2.1 kV/m by this compaction. It also appears that the 1.5 kV/m width beneath the transmission line is reduced from 150 feet (45.7 m) for the base case to 120 feet (36.6 m) for the compacted line.

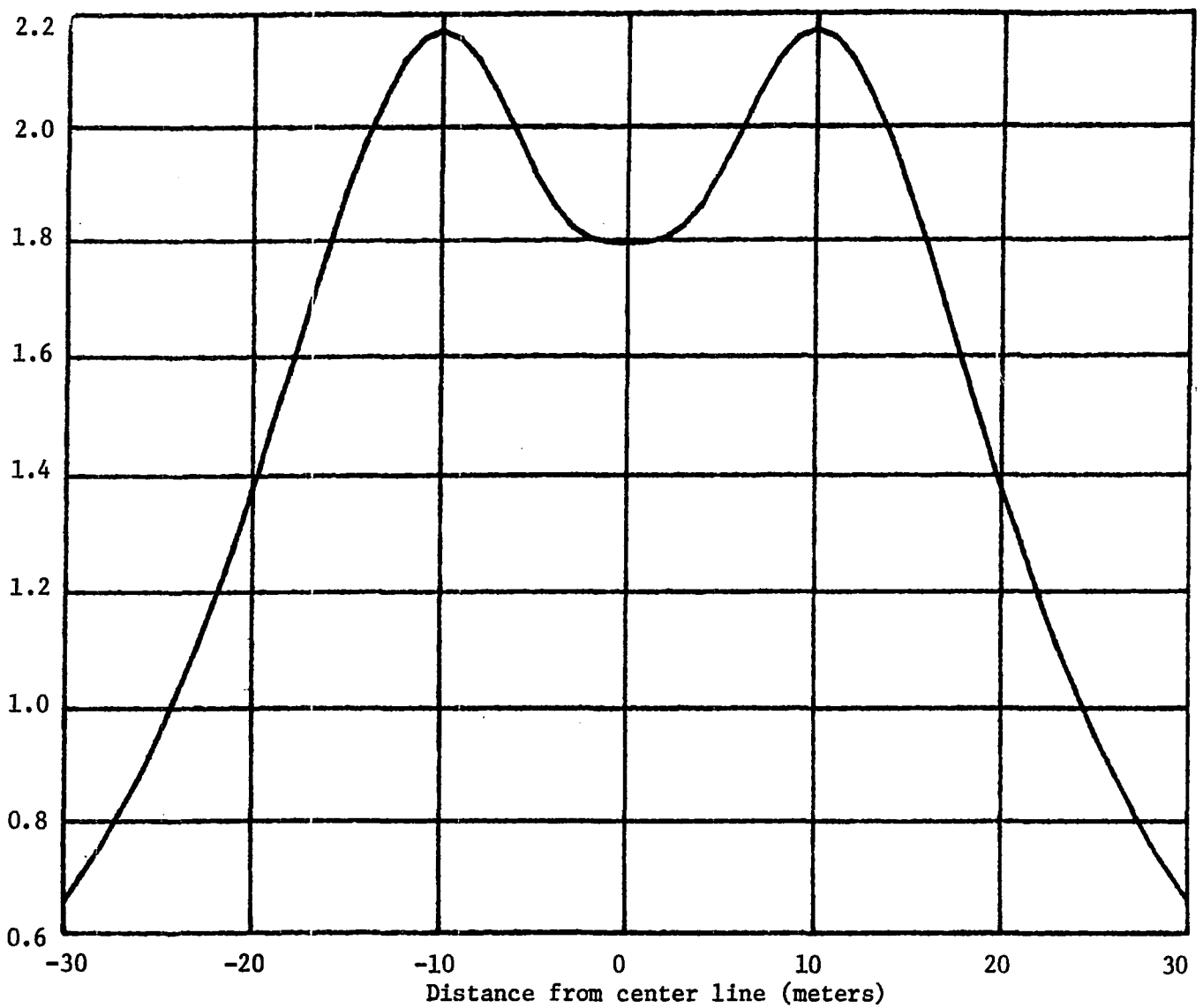

Figure 40. Ground level electric field for compact transmission line

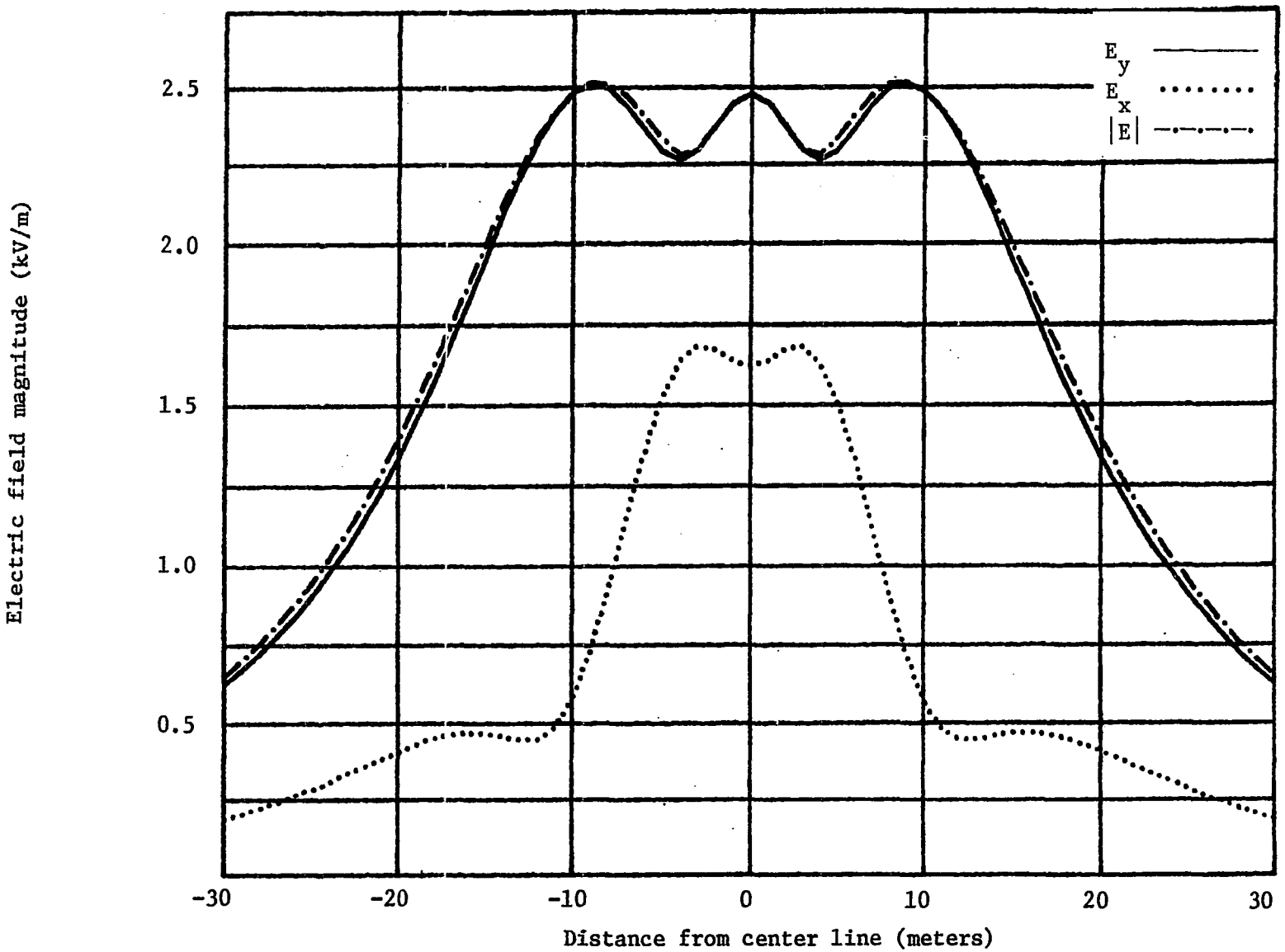

Figure 41. Electric fields at 4 m for compacted line

For the compacted "V" configuration, the reduction of maximum field strength at a height of 4 meters above ground is found to be approximately 40% from the base case value. The 2.5 kV/m value is considerably less than the ground level maximum under the flat configuration of the base case. The improvement can be easily seen by comparing Figure 40 with Figure 18.

VII. CONCLUSIONS

The sensitivities of electric fields from high voltage transmission lines to changes in certain physical parameters have been investigated and analyzed. The electrical characteristics of transmission lines have been developed in terms of the physical dimensions and applied specifically to a balanced three-phase system with bundled conductors. The relative importance of changes in various physical parameters of the transmission line has been discussed and analyzed. A method for analyzing these changes has been developed and is described in terms of modified sensitivity factors. These modified sensitivity factors are normalized and defined as deviation factors for a function f(u) as

$$F_u^f = \left|\frac{\partial f}{\partial u}\right| \left|\frac{u}{f}\right|$$

The electric fields for various transmission line configurations are computed using a point-matching routine called HIVAC2. This computer program was developed for application to multiphase a.c. systems from an earlier d.c. program. By using finite difference methods, the deviation factors are computed from the electric field data obtained by using HIVAC2.

The computed electric fields for a horizontal transmission line configuration are shown to agree with actual field measurements. It has been observed that the actual lines used for measurements are not straight, but have an approximately parabolic contour due to the mechani-

cal loading on the uniform conductors. The field measurements indicate that the mathematical model used predicts results that are reasonably close to the measured values. It is therefore reasonable to expect the calculated deviation factors to be applicable to the actual transmission line fields.

It is found that the deviation factors of major significance are those relating the maximum electric field at ground level to changes in height and phase spacing (F_H^g and F_D^g), as well as those relating the maximum electric field at the conductor surface to phase spacing and conductor size (F_D^c and F_d^c). The other deviation factors appear to be of minor importance in the control of the electric fields investigated.

This study indicates that the percentage change in phase spacing would need to be more than three times the percentage of change in conductor height to make compensation and maintain the maximum electric field at a constant value at ground level. It is also found that the only deviation factor of those considered which has a magnitude greater than unity is F_H^g. This indicates that the percentage change in the maximum ground level electric field is greater than the percentage of change in height. The mean value of this deviation factor is found to be approximately -1.72 over the range of heights from 10 meters to 15 meters. The deviation factor F_D^g which relates the maximum ground level field to the phase spacing is positive and has a magnitude approximately one-third that of F_H^g. For the range of phase spacings from 5 meters to 10 meters, F_D^g changes from about 0.624 to 0.41 with

less than 0.025 variation due to changes in the number of subconductors used per phase.

The most effective parameter for controlling the maximum electric field at the conductor surface is found to be the conductor diameter. The calculated data indicate that the deviation factor F_d^c which relates this conductor field maximum to the conductor diameter is negative and various from -0.72 to -0.90 for the two subconductors per phase. It appears that this factor tends to be somewhat less in magnitude than 0.72 as the number of subconductors per phase is increased. It is observed that the deviation factor F_D^c which relates the maximum conductor surface field to the phase spacing has a magnitude of approximately half that of F_D^g and is negative. It appears, therefore, that an attempt to reduce the maximum ground level field by decreasing the phase spacing increases the maximum conductor surface field, but only at half the rate.

It is also observed that the deviation factor F_S^c which relates the maximum conductor field strength to the bundle spacing or diameter changes sign within the range investigated (10 - 100 cm). Therefore, it is concluded that there exists a critical bundle spacing at which small changes in the diameter have no effect upon the maximum electric field at the conductor surfaces. This deviation factor changes from approximately -0.24 for the smaller diameters to +0.17 for the larger. Changes in bundle diameter in either direction from the critical dimension will increase the maximum field at the conductor surfaces. This strongly

suggests that there exist optimum bundle diameters for the reduction of corona and associated physical phenomena RFI, TVI, and audible noise.

This investigation also shows that the other deviation factors F_S^g and F_d^g are of minor importance for bundles of four or less subconductors per phase. It appears, however, that these factors may assume more importance as the number of subconductors per phase is increased. The deviation factor F_H^c appears to be negligible within the limits of this study.

As a test of the applicability of deviation factors in modifying current transmission line designs, a compacted 345 kV transmission line has been considered for electrical performance only. The effects of any parameter changes upon mechanical characteristics of the system have not been determined in this study.

From an analysis of the deviation factors considered in this investigation, a "V" shaped configuration with a minimum height above ground of 12.5 meters was assumed for comparison with the base case. The outer phase conductors were raised by 20% to a height of 15 meters, and the horizontal phase separation was reduced by 20% to 6 meters. According to the calculated deviation factors, these changes should reduce the maximum ground level electric field by approximately 40% and move the peak value positions closer to the centerline. These same changes should increase the maximum field at the conductor surface by approximately 3.5%. To compensate for this increase in the maximum conductor field, the sensitivity factors suggest a reduction of bundle

spacing. By reducing the bundle spacing from 50 cm to 30 cm in each phase, the net change in maximum conductor field strength is only 1.5% over that of the base case. The ground level electric field maxima are reduced by approximately 35% from 3.5 kV/m to 2.1 kV/m, according to the data obtained using HIVAC2. It also appears that the 1.5 kV/m width beneath the transmission line is reduced from 150 feet (45.7 m) to 120 feet (36.6 m) due to these changes. This reduction indicates the possibility of a 20% reduction in the necessary right-of-way where maximum field strength is the limiting factor.

VIII. REFERENCES

1. Federal Power Commission. The 1970 National Power Survey, Pt. I. Washington, D.C.: Government Printing Office, 1970.

2. Federal Power Commission. "Task Force Report: Energy Distribution Research." The National Power Survey. Washington, D.C.: Government Printing Office, 1973.

3. Mahmoud, Aly A. "High Voltage Engineering." Unpublished classroom notes, Department of Electrical Engineering, Iowa State University, 1979.

4. Neuenswander, John R. Modern Power Systems. Scranton: International Textbook Co., 1971.

5. Stephenson, William D., Jr. Elements of Power System Analysis. New York: McGraw-Hill, Inc., 1975.

6. Ramo, Simon, et al. Fields and Waves in Communication Electronics. New York: John Wiley & Sons, Inc., 1965.

7. Smyth, William R. Static and Dynamic Electricity. New York: McGraw-Hill, Inc., 1950.

8. Boast, Warren B. Vector Fields. New York: Harper and Row, Publishers, 1964.

9. Chipman, Robert A. Theory and Problems of Transmission Lines. New York: McGraw-Hill, Inc., 1968.

10. Bowman, Frank. Introduction to Bessel Functions. New York: Dover Publications, Inc., 1958.

11. Dwight, Herbert B. Tables of Integrals and Other Mathematical Data. New York: Macmillan Publishing Co., Inc., 1961.

12. Jahnke, Eugene, and Fritz Emde. Tables of Functions. New York: Dover Publications, Inc., 1945.

13. Royal Society of London. Mathematical Tables, Vol. 10. Bessel Functions, Part IV: "Kelvin Functions." Young, Andrew, and Alan Kirk, eds. Cambridge: University Press, 1964.

14. National Bureau of Standards. Handbook of Mathematical Functions with Formulas, Graphs and Mathematical Tables. Washington, D.C.: Government Printing Office, 1964.

15. Rexford, M. Morey. "Continuous Subsurface Profiling by Impulse RADAR." Proceedings of a Specialty Conference on Subsurface Exploration for Underground Excavation and Heavy Construction. New York: American Society of Civil Engineers, August 1974.

16. Kuffel, E., and M. Abdullah. High Voltage Engineering. Oxford: Pergamon Press, 1970.

17. Nasser, Essam. Fundamentals of Gaseous Ionization and Plasma Electronics. New York: Wiley-Interscience, 1971.

18. Loeb, Leonard B. Electrical Coronas: Their Basic Physical Mechanisms. Berkeley: University of California Press, 1965.

19. Perkins, J. R. "Some General Remarks on Corona Discharges." Corona Measurement and Interpretation, Vol. I, Engineering Dielectrics STP 669. Philadelphia: American Society of Testing and Measurements, 1979.

20. Azaroff, Leonid V., and James J. Brophy. Electronic Processes in Materials. New York: McGraw-Hill, Inc., 1963.

21. Tralli, Numzio, and Frank A. Momilla. Atomic Theory: An Introduction to Wave Mechanics. New York: McGraw-Hill, Inc., 1969.

22. Peek, F. W., Jr. "Law of Corona and the Dielectric Strength of Air." AIEE Transactions Vol. 30, Pt. III (1911).

23. Peek, F. W., Jr. Dielectric Phenomena in High Voltage Engineering. New York: McGraw-Hill, Inc., 1929.

24. Peterson, W. S. "Discussion." AIEE Transactions PAS-52 (1933): 62.

25. Comber, M. G., and L. E. Zaffanella. "Corona Loss." Transmission Line Reference Book: 345 kV and Above. Palo Alto: Electric

26. Johnson, David E. Introduction to Filter Theory. Englewood Cliffs, New Jersey: Prentice-Hall, Inc., 1976.

27. Pipes, Louis A. Matrix Methods for Engineering. Englewood Cliffs, New Jersey: Prentice-Hall, Inc., 1963.

28. Fishbeiner, D. T. Introduction to Matrices and Linear Transformations. San Francisco: W. H. Freeman and Company, 1960.

29. Parekh, Harshad J. "Computation of Electric Fields for EHV and UHV Transmission Lines." Ph.D. dissertation, Iowa State University, Ames, Iowa, 1975.

30. Read, Alvin A. Private communications on PTMAT computer program developed for introductory fields courses, Department of Electrical Engineering, Iowa State University, 1979.

31. Hallèn, Eric. Electromagnetic Theory. Gasstrom, Runar, tr. New York: John Wiley & Sons, Inc., 1962.

IX. ACKNOWLEDGMENTS

The author is deeply indebted to Dr. Aly A. Mahmoud and Dr. Robert E. Post for their special encouragement and guidance during the preparation of this dissertation and the research which it involved. My thanks also are extended to Dr. Alvin A. Read for his valuable assistance in the development of many of the computer programs used, and to Ms. Gretchen Triplett for typing the manuscript. Acknowledgment must also be made to the Iowa Test and Evaluation Facility of Iowa State University for their provision of financial assistance and necessary facilities for measurements on an active EHV circuit.

To my wife, Barbara, whose patience and unflagging faith have sustained me through many difficult days and nights, I offer my heartfelt gratitude.

X. APPENDIX A: SURGE IMPEDANCE OF A UNIFORM TRANSMISSION LINE

An incremental analysis of the distributed parameter transmission line results in the first order differential equations:

$$\frac{dv}{dx} = - Ri(x,t) - L \frac{di}{dt}$$

$$\frac{di}{dx} = - Gv(x,t) - C \frac{dv}{dt}$$

where R, G, L and C are respectively the resistance, conductance, inductance and capacitance per unit length. These two equations may be combined to obtain the second order differential equations commonly referred to as the "Telegraphers' Equations" (31).

$$\frac{\partial^2 y}{\partial x^2} = RGv(x,t) + (RC + GL) \frac{\partial v}{\partial t} + LC \frac{\partial^2 v}{\partial t^2}$$

$$\frac{\partial^2 i}{\partial x^2} = RGi(x,t) + (RC + GL) \frac{\partial i}{\partial t} + LC \frac{\partial^2 i}{\partial t^2}$$

The solution of these equations for harmonic time variations are wave equations of the form

$$v(x,t) = V_1 e^{j\omega t - \gamma x} + V_2 e^{j\omega t + \gamma x}$$

$$i(x,t) = I_1 e^{j\omega t - \gamma x} + I_2 e^{j\omega t + \gamma x}$$

where the exponential term $e^{j\omega t - \gamma x}$ represents a wave traveling in the forward or positive x direction, and the term $e^{j\omega t + \gamma x}$ represents a wave traveling in the negative x direction, and $\gamma = \sqrt{(R+j\omega L)(G+j\omega C)}$.

If only the forward wave is present,

$$\frac{dv}{dx} = - v(x,t) = - (R + j\omega L)\ i\ (x,t)$$

and suppressing the harmonic time function

$$\gamma V_1 = (R + j\omega L)\ I_1$$

The characteristic impedance or surge impedance is defined as the ratio of the forward voltage to the forward current

$$Z_o = \frac{V_1}{I_1} = \frac{R + j\omega L}{\gamma} = \sqrt{\frac{R + j\omega L}{G + j\omega C}}$$

If the transmission line is lossless or satisfies Heaviside's criteria for a distortionless line (RC = GL), this will reduce to

$$Z_o = \sqrt{\frac{L}{C}}$$

If only a negative wave is present on the transmission line,

$$\frac{V_2}{I_2} = - Z_o$$

XI. APPENDIX B: π EQUIVALENT CIRCUIT FOR DISTRIBUTED PARAMETER TRANSMISSION LINES

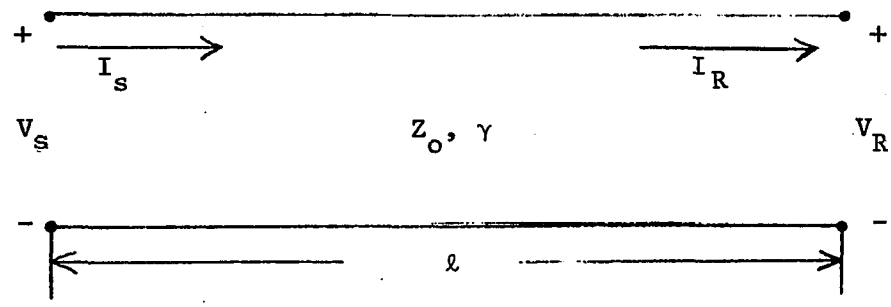

Figure B.1. Typical transmission line model

A uniform transmission line can be described in terms of its length, ℓ, characteristic impedance, Z_o, and propagation constant, $\gamma = \alpha + \beta$, rather than the parameters, R, S, L and C.

If the sending end voltage, V_s, and the sending end current, I_s, at $x = 0$, is given by

$$V_s = V_1 + V_2$$

$$I_s = I_1 + I_2$$

the voltage and current at the receiving end, $x = \ell$, can be written

$$V_R = V_1 e^{-\gamma\ell} + V_2 e^{+\gamma\ell}$$

$$= (V_1 + V_2) \cosh\gamma\ell - (V_1 - V_2) \sinh\gamma\ell$$

$$I_R = I_1 e^{-\gamma\ell} + I_2 e^{+\gamma\ell}$$

$$= (I_1 + I_2) \cosh\gamma\ell - (I_1 - I_2) \sinh\gamma\ell$$

Substituting $V_1 = Z_o I_1$ and $V_2 = -Z_o I_2$, these can be written

$$V_R = (V_1 + V_2) \cosh\gamma\ell - Z_o (I_1 + I_2) \sinh\gamma\ell$$

$$I_R = (I_1 + I_2) \cosh\gamma\ell - \frac{(V_1 + V_2)}{Z_o} \sinh^1\ell$$

or

$$\begin{bmatrix} V_R \\ I_R \end{bmatrix} = \begin{bmatrix} \cosh\gamma\ell & -Z_o \sinh\gamma\ell \\ -Y_o \sinh\gamma\ell & \cosh\gamma\ell \end{bmatrix} = \begin{bmatrix} V_s \\ I_s \end{bmatrix}$$

Solving this latter equation for the sending end voltage and current

$$\begin{bmatrix} V_s \\ I_s \end{bmatrix} = \begin{bmatrix} \cosh\gamma l & Z_o \sinh\gamma l \\ Y_o \sinh\gamma l & \cosh\gamma l \end{bmatrix} = \begin{bmatrix} V_R \\ I_R \end{bmatrix}$$

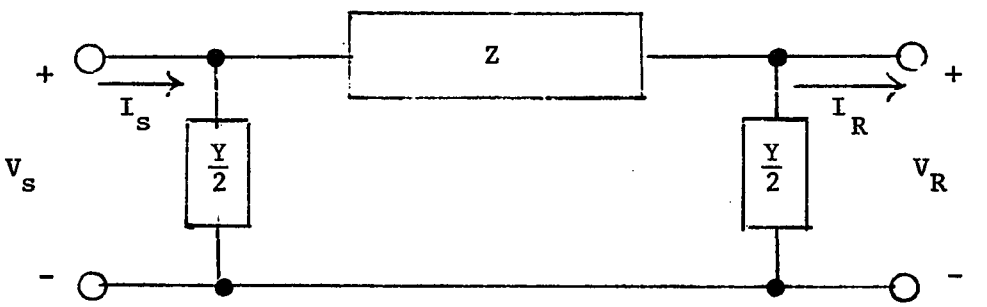

Figure B.2. Symmetrical π equivalent with lumped elements

The ABCD matrix for the circuit of B.2 can be obtained by matrix multiplication

$$\begin{bmatrix} V_s \\ I_s \end{bmatrix} = \begin{bmatrix} 1 & 0 \\ \frac{Y}{2} & 1 \end{bmatrix} \begin{bmatrix} 1 & Z \\ 0 & 1 \end{bmatrix} \begin{bmatrix} 1 & 0 \\ \frac{Y}{2} & 1 \end{bmatrix} \begin{bmatrix} Y_R \\ I_R \end{bmatrix}$$

$$= \begin{bmatrix} 1 + \frac{ZY}{2} & Z \\ Y(1 + \frac{ZY}{2}) & 1 + \frac{ZY}{2} \end{bmatrix} \begin{bmatrix} V_R \\ I_R \end{bmatrix}$$

Equating terms with those for the transmission line

$$Z = Z_o \sinh\gamma\ell$$

$$1 + \frac{ZY}{2} = \cosh\gamma\ell$$

By substitution and a little mathematical manipulation,

$$\frac{Y}{2} = \frac{\tanh \frac{\gamma\ell}{2}}{Z_o}$$

Substituting these values into the lumped element circuit obtains

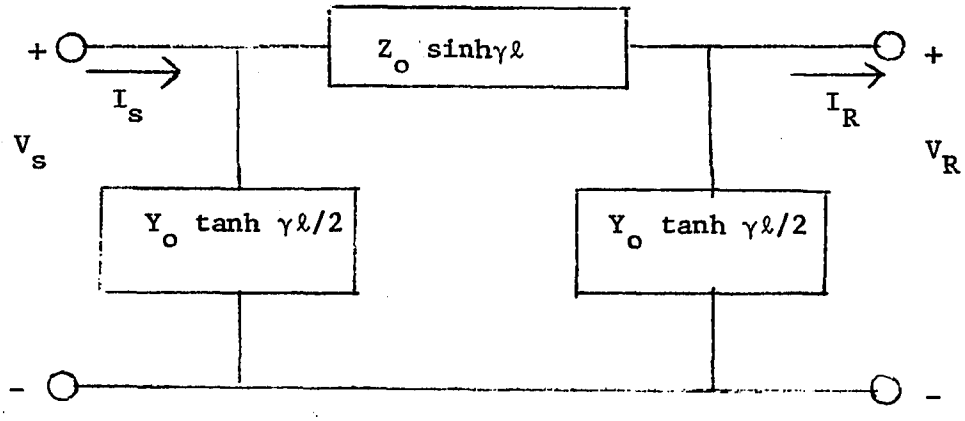

Figure B.3. π equivalent circuit for distributed transmission line

If $\gamma\ell$ is small, the small argument approximations for the hyperbolic functions can be used to give

$$Z = Z_o \gamma\ell = (R + j\omega L)\ 1$$

$$\frac{Y}{2} = Y_o \frac{\gamma\ell}{2} = \frac{(G + j\omega C)\ 1}{2}$$

For lossless lines, the real parts will disappear, and

$$Z \simeq j\omega L\ell$$

$$Y \simeq j\omega C\ell$$

From these approximations, it can be seen that the ratio of Z to Y will be very large so that only the series element is significant unless the system approaches a resonant length or is very lightly loaded. The circuit equations then become simply

$$V_s = V_R + j\omega L\ell I_R$$

$$I_s = I_R$$

XII. APPENDIX C: HIVAC2 COMPUTER PROGRAM

The computer program HIVAC2 was developed from a point matching program, PTMAT. The original program was designed for use in illustrating d.c. fields in the vicinity of a parallel conducting cylinders parallel to a conducting ground plane. The conductors can be of arbitrary sizes and at arbitrary distances from one another and the ground plane. HIVAC2 is designed to incorporate phasor representations for time varying electrical quantities and to determine the instantaneous orientation of the electric fields at any point. This allows the calculation of electric fields which vary in both magnitude and orientation with time.

The sources of these phasor fields are considered to be a set of time varying line charges equally spaced around a cylindrical surface with a diameter equal to half that of the associated conductor. The number of charges on each conductor is established as one of the initial parameters describing a conductor. To find the field near a particular conductor, the field can be calculated more precisely by increasing the number of charges on that conductor without necessarily increasing the charges on more distant conductors.

From the specified parameters for a set of cylindrical conductors, the computer program calculates the location of each charge filament and a potential matching location on the conductor surface radially outward from each filament of charge. The program then computes the potential coefficient matrix necessary to force these surface locations to the

potentials specified in the conductor description. In the original program, the maximum number of charges allowed in the system was 102, which generated a matrix with 10404 elements. It is possible to increase this limit when additional storage space is available and the increase in processing time is not considered excessive.

The m unknown filaments of charge are obtained by solution of the m simultaneous equations with a subroutine called SIMEQS. This routine solves the m equations by substitution and destroys the original matrix in the process. The line charge values and locations are stored and a printout of their locations and values is available.

The vertical and horizontal components of the electric field and the potential at any point are computed by a summation of the partial fields from each filament of charge and its image in the ground plane. These summations are made for both the real and imaginary parts of the phasor representations of the field. The results are converted to magnitude and phase for tabulation and plotting.

Plotting routines are available for either contour or linear plotting with the fields represented in either linear of logarithmic form, depending upon the details desired. A listing of the HIVAC2 program is given in Table C.1. The program language is FORTRAN IV.

Table C.1. HIVAC2 computer program

```
c        This is a main program HIVAC2
c      A program for point matching 3-phase lines
       Dimension xc(102),yc(102),rc(102),vc(102),pc(102),nqc(102),
      1 vr(102),vi(102),qr(102),qi(102),xq(102),yq(102),xv(102),
      2 yv(102),qc(102),qq(102),vv(102),ss(59),cc(59),vm(102),
      3 aa(10404),bb(10404),xme(102),yme(102),vpm(102),xpe(102),
      4 ype(102),tme(102),xx(102)
       equivalence (vv(1),qq(1))
c
       logical*1 yes
4      continue
       print 100
100    format(2x,'This is a program for approximating AC fields ',
      1'around circular',/,2x,'conductors in a set of parallel ',
      2'conductors above a flat conducting ground',/,2x,'plane.',
      3'  No explicit solution exists for this problem for two or',
      4 /,2x,'more conductors.  Hence an approximate solution is ',
      5'necessary.  The',/,2x,' potential and phase of each conduc',
      6'tor relative to the ground plane',/,2x,'is assumed to be ',
      7'known and specified.  Each conductor charge ',/,2x,
      8'distribution is approximated by several line charges.',/)
c
12     continue
       print 101
101    Format(/,5x,'Assign your conductors continuous numbers star',
      1'ting from 1.',/,7x,'Now input your conductors giving!',/,
      2 7x,'Number,x-position,y-position,radius,potential,phase,',
      3/,7x,'and the number of approximating charges.',/,12x,'Terminate',
      4' with a line number => 999.',/)
15     continue
       newv=0
       nc=0
       print 102
102    format(5x,'Input your first conductor number.     :     ',$)
       go to 104
5      continue
       print 103
103    format(5x,'Input your next conductor number.      :     ',$)
104    continue
       read *,k
       If(k.ge.999) go to 6
       Print 106
106    Format(5x,'Input x-pos,y-pos,radius,voltage,phase,No.charges',
      1 /,8x,$)
       Read *,xc(k),yc(k),rc(k),vc(k),pc(k),nqc(k)
```

Table C.1. (Continued)

```
      If(k.gt.nc) nc=k
      Print 107,k,xc(k),yc(k),rc(k),vc(k),pc(k),nqc(k)
107   Format(6x,I8,1p5E13.5,I7)
      go to 5
6     continue
        rad=180./3.141592
      vlow =1.0E+30
      vhigh=-vlow
      I=0
      nqs=0
      do 25 j=1,nc
      mqs=nqc(j)
      if(mqs.eq.0) go to 25
      if(vc(j).gt.vhigh) ivh=j
      if(ivh.eq.j) vhigh=vc(j)
      if(vc(j).lt.vlow) ivl=j
      if(ivl.eq.j) vlow=vc(j)
      nqs=nqs+mqs
      div=6.283185/float(mqs)
      do 7 II=1,mqs
      an=div*float(II-1)
      cc(II)=cos(an)
7     ss(II)=sin(an)
      x=xc(j)
      y=yc(j)
      rr=rc(j)
      r=rr/2.
      if(mqs.eq.1) r=0.0
      p=pc(j)/rad
      vcr=vc(j)*cos(p)
      vci=vc(j)*sin(p)
      do 25 kk=1,MQS
      i=i+1
      xq(I)=x+r*ss(kk)
      yq(I)=y-r*cc(kk)
      xv(I)=x+rr*ss(kk)
      yv(I)=y-rr*cc(kk)
      vr(I)=vcr
      vi(I)=vci
25    continue
        pk=1.0
        print 300
300     format(/,2x,'Is ground plane a dielectric? Yes or No:   ',$)
        accept 112,yes
        if(yes.ne.'y'.and.yes.ne.'Y') go to 30
```

Table C.1. (Continued)

```
      print 310
310   format(/,2x,'Input relative dielectric constant:     ',$)
      accept *,dc
      pk=(dc-1.0)/(dc+1.0)
      print 315,pk
315   format(/,5x,'Image scale factor pk=   ',f8.5,/)
      go to 30
41    print 110
110   Format(5x,'For some reason no solution exists for the data ',
     1'supplied.  Reexamine',/,5x,'your input data and insert ',
     2'corrected data.',/,/)
      go to 12
30    continue
      print 109,nqs
109   Format(5x,'You have now input data on all your conductors.',/,
     1 5x,'We will now procede to determine the',I5,' unknown line ',
     2'charges.')
      Q=1.0
      Do 40 I=1,nqs
      x=xv(I)
      y=yv(I)
      kk=I-nqs
      Do 40 J=1,nqs
      k=kk+j*nqs
      qx=xq(j)
      qy=yq(j)
      aa(k)=Field(x,y,qx,qy,q,ex,ey,et,1,1,1,pk)
      bb(k)=aa(k)
40    continue
      call Simeqs(aa,vr,nqs,nqsol)
      if(nqsol.ne.0) go to 41
      call simeqs(bb,vi,nqs,nqsol)
      if(nqsol.ne.0) go to 41
      Print 111
111   Format(/,5x,'Do you want a table of line charge positions and',
     1 ' values?',/,7x,'Answer Yes or No.   :   '$)
      accept 112,yes
112   format(a1)
      if(yes.ne.'y'.and.yes.ne.'Y') go to 60
      Type 113
113   Format(//,5x,'A table of line charge positions and values:',
     1 //,6x,'Q-No.',8x,'XQ',14x,'YQ',10x,'QR/(2 Pi e)',5x,
     2 'QI/(2 Pi e)',/)
      do 47 I=1,NQS
      Type 114,I,XQ(I),yq(I),VR(I),VI(I)
```

Table C.1. (Continued)

```
114   Format(4x,I6,1P6e16.6)
47    continue
60    continue
      Print 120
120   Format(//,5x,'Do you wish to evaluate and output the potential',
     1',and fields at specific',//,7x,' locations?',' Answer ',
     2' Yes or No.   :    ',$)
      accept 112,yes
      if(yes.ne.'y'.and.yes.ne.'Y') go to 75
62      continue
        Print *,'  Input x and y.  Exit x=>1.0E+30'
        accept *,x,y
      If(x.ge.1.0E+30) go to 75
      ReV=field(x,y,xq,yq,vr,exr,eyr,etr,1,nqs,0,pk)
      QuV=field(x,y,xq,yq,v,exi,eyi,eti,1,nqs,0,pk)
      V=sqrt(reV*reV+quV*quV)
      EX=sqrt(exr*exr+exi*exi)
      EY=sqrt(eyr*eyr+eyi*eyi)
      if(quv.eq.0.0.and.rev.eq.0.0) vph=0.0
      if(vph.eq.0.0.and.rev.eq.0.0) go to 63
      vph=atan2(quv,rev)*rad
63    if(exi.eq.0.0.and.exr.eq.0.0) exp=0.0
      if(exp.eq.0.0.and.exr.eq.0.0) go to 64
      exp=atan2(exi,exr)*rad
64    if(eyi.eq.0.0.and.eyr.eq.0.0) eyp=0.0
      if(eyp.eq.0.0.and.eyr.eq.0.0) go to 65
      eyp=atan2(eyi,eyr)*rad
65    continue
c
c       This is a  routine for calculating the maximum
c       amplitude of an elliptically polarized electric field
c       when the X and Y magnitudes and phases are given.
c       EX  is the x-magnitude and EXP is the x-phase.
c       EY  is the y-magnitude and EYP is the y-phase.
c       The output is given as EMAG.
        If(ex.eq.0.0) emag=ey
        If(ex.eq.0.0.and.ey.eq.0.0) go to 150
        If(ey.eq.0.0) emag=ex
        If(ex.eq.0.0.or.ey.eq.0.0) go to 150
        ALPH=exp*2./rad
        BETA=eyp*2./rad
        Com=(ey*ey)/(ex*ex)
        ARG=-(sin(alph)+com*sin(beta))/(cos(alph)+com*cos(beta))
        Angl=atan(arg)
        TEST=cos(angl+alph)+com*cos(angl+beta)
```

Table C.1. (Continued)

```
        If(test.lt.0.0) angl=angl+3.141592
        EMAG=sqrt((1.+com+cos(angl+alph)+com*cos(angl+beta))/2.)*ex
150     continue
      Type 125,x,y,v,vph,ex,exp,ey,eyp,emag
125   Format(5x,'For x and y = ',1p2e15.5,/,5x,'V = ',1p2e15.5,
     1 /,5x,'EX = ',1p2e15.5,/,5x,'EY = ',1p2e15.5,/,5x,'EMAG = ',
     2  1p2e15.5)
      go to 62
75      continue
        scale =1.25000
        print 320
320     format(/,2x,'Are you using decwriterII? Yes or No:    ',$)
        accept 112,yes
        if(yes.eq.'y'.or.yes.eq.'Y') scale=1.66667
70    continue
      print 130
130   format(/,5x,'Do you want a contour map of the electric ',
     1 'potential around the conductors?',/,7x,'Answer Yes or ',
     2 'No.     :    ',$)
      accept 112,yes
      if(yes.ne.'y'.and.yes.ne.'Y') go to 80
      print 134
134   format(5x,'Do you want the contour map to be of the log '
     1 'of the potential?',/,7x,'Answer Yes or No.    :    ',$)
      accept 112,yes
      log=0
      if(yes.eq.'y'.or.yes.eq.'Y') log=10
      print 131
131   format(5x,'Over what x and y range do you want your ',
     1 'potential contour map?',/,7x,'Input xmin,xmax,ymin,ymax',
     2 ',    :  ',$)
      accept *,xmin,xmax,ymin,ymax
c
      call plimits(xmin,xmax,ymin,ymax,dx,dy,ix0,iy,scale)
132   format(//,5x,'A map of the electric potential contours ',
     1 'between',/,8x,'x=',1pe13.5,' to x=',1pe13.5,
     2 ' in increments of dx=',1pe13.5,/,5x,'and from',/,8x,
     3 'y=',1pe13.5,' to y=',1pe13.5,' in increments of dy=',
     4 1pe13.5,/,7x,'Plot symbol 0 =',1pe13.5,
     5 '     Plot symbol 5 =',1pe13.5,//)
      ntry=0
      high=abs(vhigh)
      if(high.lt.abs(vlow)) high=abs(vlow)
      if(log.ne.0) high=alog(1.0+high)
      base=0.0
```

Table C.1. (Continued)

```
      nylong=ifix((ymax-ymin)/dy+1.5)
      type 132,xmin,xmax,dx,ymin,ymax,dy,base,high
      do 79 i=1,nylong
      iy=iy-1
      y=ymax-dy*float(i-1)
      jy=inside(y,yc,rc,1,nc)
      do 77 j=1,101
      x=xmin+dx*float(j-1)
      if(jy.eq.0) go to 73
      jx=jump(x,y,xc,yc,rc,jy,nc)
      if(jx.eq.0) go to 73
      aa(j)=1.0E+18
      go to 77
73    continue
        RVI=field(x,y,xq,yq,vr,exr,eyr,etr,1,nqs,1,pk)
        RVJ=field(x,y,xq,yq,vi,exi,eyi,eti,1,nqs,1,pk)
        volt=sqrt(RVI*RVI+RVJ*RVJ)
      if(log.eq.0) then
        aa(j)=abs(volt)
        else
        aa(j)=alog(1.0+abs(volt))
      end if
77    continue
C
      call cplot(aa,1,101,iy,base,high,ntry,ix0)
79    continue
      type 139
139   format(////)
      go to 70
80      continue
      print 140
140   format(5x,'Do you want a contour map of the electric',
     1 ' field magnitude around the',/,7x,'conductors?  Answer ',
     2 'Yes or No.    :   ',$)
      accept 112,yes
      if(yes.ne.'y'.and.yes.ne.'Y') go to 490
      print 144
144   format(5x,'Do you want the contour map to be of the log '
     1 'of the field?',/,7x,'Answer Yes or No.    :    ',$)
      accept 112,yes
      log=0
      if(yes.eq.'y'.or.yes.eq.'Y') log=10
      print 141
```

Table C.1. (Continued)

```
141   format(5x,'Over what x and y range do you want your ',
     1 'field contour map?',//,7x,'Input xmin,xmax,ymin,ymax',
     2 '.    :    ',$)
      accept *, xmin,xmax,ymin,ymax
c
      call plimits(xmin,xmax,ymin,ymax,dx,dy,ix0,iy,scale)
c
c       Determine the highest Electric Field Magnitude.
        Elow=1.0E+18
        Ehigh=-Elow
        Do 430 I=1,NQS
        X=XV(I)
        Y=YV(I)
        RV=Field(x,y,xq,yq,vr,exr,eyr,etr,1,nqs,0,pk)
        QV=Field(x,y,xq,yq,vi,exi,eyi,eti,1,nqs,0,pk)
        EX=sqrt(exr*exr+exi*exi)
        EY=sqrt(eyr*eyr+eyi*eyi)
        IF(exi.eq.0.0.and.exr.eq.0.0) exp=0.0
        IF(exp.eq.0.0.and.exr.eq.0.0) go to 483
        EXP=atan2(exi,exr)*rad
483     IF(eyi.eq.0.0.and.eyr.eq.0.0) eyp=0.0
        IF(eyp.eq.0.0.and.eyr.eq.0.0) go to 485
        EYP=atan2(eyi,eyr)*rad
485     Continue
        IF(ex.eq.0.0) emag=ey
        IF(ex.eq.0.0.and.ey.eq.0.0) go to 90
        IF(ey.eq.0.0) emag=ex
        IF(ex.eq.0.0.or.ey.eq.0.0) go to 90
        ALPH=exp*2./rad
        BETA=eyp*2./rad
        COM=(ey*ey)/(ex*ex)
        ARG=-(sin(alph)+com*sin(beta))/(cos(alph)+com*cos(beta))
        ANGL=atan(arg)
        TEST=cos(angl+alph)+com*cos(angl+beta)
        IF(test.lt.0.0) angl=angl+3.141592
        EMAG=sqrt((1.0+com*cos(angl+alph)+com*cos(angl+beta))/2)*ex
90      Continue
        IF(EMAG.gt.EHIGH) EHIGH=EMAG
        IF(EMAG.lt.ELOW) ELOW=EMAG
430     Continue
        Base=0.0
        IF(log.ne.0) EHIGH=alog(1.+EHIGH)
       type 142,xmin,xmax,dx,ymin,ymax,dy,base,ehigh
```

Table C.1. (Continued)

```
      type 142,xmin,xmax,dx,ymin,ymax,dy,base,ehigh
142   format(///,5x,'A contour map of the electric field inten',
     1 'sity magnitude from',/,8x,'x=',1pe13.5,' to x=',1pe13.5,
     2 ' in increments of dx=',1pe13.5,/,5x,'and from',/,8x,
     3 'y=',1pe13.5,' to y=',1pe13.5,' in increments of dy=',
     4 1pe13.5,//,7x,'Plot symbol 0 =',1pe13.5,
     5 '      Plot symbol 5 =',1pe13.5,/)
      nylons=ifix((ymax-ymin)/dy+1.5)
      ntry=0
      do 89 i=1,nylons
      iy=iy-1
      y=ymax-dy*float(i-1)
      Jy=inside(y,yc,rc,1,nc)
        do 87 j=1,101
        x=xmin+dx*float(j-1)
        if(jy.eq.0) go to 84
        Jx=Jump(x,y,xc,yc,rc,Jy,nc)
        if(Jx.eq.0) go to 84
        aa(j)=1.0E+18
       go to 87
84     continue
       RV=Field(x,y,xq,yq,vr,exr,eyr,etr,1,nqs,0,pk)
       QV=Field(x,y,xq,yq,vi,exi,eyi,eti,1,nqs,0,pk)
       EX=sqrt(exr*exr+exi*exi)
       EY=sqrt(eyr*eyr+eyi*eyi)
       IF(exi.eq.0.0.and.exr.eq.0.0) exp=0.0
       IF(exp.eq.0.0.and.exr.eq.0.0) go to 463
       EXP=atan2(exi,exr)*rad
463    IF(eyi.eq.0.0.and.eyr.eq.0.0) eyp=0.0
       IF(eyp.eq.0.0.and.eyr.eq.0.0) go to 465
       EYP=atan2(eyi,eyr)*rad
465    Continue
       IF(ex.eq.0.0) emag=ey
       IF(ex.eq.0.0.and.ey.eq.0.0) go to 650
       IF(ey.eq.0.0) emag=ex
       IF(ex.eq.0.0.or.ey.eq.0.0) go to 650
       ALPH=exp*2./rad
       BETA=eyp*2./rad
       COM=(ey*ey)/(ex*ex)
       ARG=-(sin(alph)+com*sin(beta))/(cos(alph)+com*cos(beta))
       ANGL=atan(arg)
       TEST=cos(angl+alph)+com*cos(angl+beta)
       IF(test.lt.0.0) angl=angl+3.141592
       EMAG=sqrt((1.0+com*cos(angl+alph)+com*cos(angl+beta))/2)*ex
650    continue
```

Table C.1. (Continued)

```
        IF(los.eq.0) aa(j)=emas
        IF(los.ne.0) aa(j)=alos(1.+emas)
87      continue
c
        call cplot(aa,1,101,iy,base,ehish,ntry,ixo)
89      continue
        type 139
        so to 80
490     continue
200     continue
c
c  This is an addition to the program HIVAC2 to allow plottins
c       if the fields and potentials usins the sub-program
c       plotter.
        Print 210
210     Format(//,5x,'Do you wish to plot outputs for a series',
     1 'of points at a fixed heisht? ',' Answer Yes or No.   :',
     2 '      ',$)
        accept 112,yes
        If(yes.ne.'y'.and.yes.ne.'Y') so to 220
212     continue
        Print*,'Input: Heisht,Xmin,Xmax,LX0,and No.of points.'
        accept *,y,xmin,xmax,LX0,npt
        delX=(xmax-xmin)/float(npt-1)
        X=Xmin
        Do 230 I=1,npt
        xx(I)=x
        Rev=field(x,y,xq,yq,vr,exr,eyr,etr,1,nqs,0,pk)
        Quv=field(x,y,xq,yq,vi,exi,eyi,eti,1,nqs,0,pk)
        V=sqrt(rev*rev+quv*quv)
        EX=sqrt(exr*exr+exi*exi)
        EY=sqrt(eyr*eyr+eyi*eyi)
        If(quv.eq.0.0.and.rev.eq.0.0) vph=0.0
        If(vph.eq.0.0.and.rev.eq.0.0) so to 263
        VPH=atan2(quv,rev)*rad
263     If(exi.eq.0.0.and.exr.eq.0.0) exp=0.0
        If(exp.eq.0.0.and.exr.eq.0.0) so to 264
        EXP=atan2(exi,exr)*rad
264     If(eyi.eq.0.0.and.eyr.eq.0.0) eyp=0.0
        If(eyp.eq.0.0.and.eyr.eq.0.0) so to 265
        EYP=atan2(eyi,eyr)*rad
265     continue
        VM(I)=V
        VPM(I)=vph
        XME(I)=EX
```

Table C.1. (Continued)

```
          XPE(I)=exp
          YME(I)=EY
          YPE(I)=eyp
          X=X+delX
c
c         This is a routine for calculating the maximum
c         amplitude of an elliptically polarized electric field
c         when the X and Y magnitudes and phases are given.
c         EX  is the x-magnitude and EXP is the x-phase.
c         EY  is the y-magnitude and EYP is the y-phase.
c         The output is given as EMAG.
          If(ex.eq.0.0) emag=ey
          If(ex.eq.0.0.and.ey.eq.0.0) go to 340
          If(ey.eq.0.0) emag=ex
          If(ex.eq.0.0.or.ey.eq.0.0) go to 340
          ALPH=exp*2./rad
          BETA=eyp*2./rad
          Com=(ey*ey)/(ex*ex)
          ARG=-(sin(alph)+com*sin(beta))/(cos(alph)+com*cos(beta))
          Angl=atan(arg)
          TEST=cos(angl+alph)+com*cos(angl+beta)
          If(test.lt.0.0) angl=angl+3.141592
          EMAG=sqrt((1.+com+cos(angl+alph)+com*cos(angl+beta))/2.)*ex
340       tme(I)=emag
230       continue
          Print 232
232       Format(//,5x,'Do you wish a plot of potential with phase',
     1 ' and magnitude? ',' Answer Yes or No.    :     ',$)
          accept 112,yes
          If(yes.ne.'y'.and.yes.ne.'Y') go to 235
          Print 248,y,xmin,xmax
248       Format(//,5x,'Y = ',1pe15.5,'  Xmin/Xmax= ',1p2e15.5)
          Print 920
920       Format(//,5x,' Do you wish to use electronic plotting? ',
     1    //,' Answer: Yes or No.    :    ',$)
          Accept 112,yes
          If(yes.eq.'y'.or.yes.eq.'Y') then
          Type *,npt,-2
          Type 950,(XX(I),vm(I),vpm(I),i=1,npt)
950       Format(3E15.7)
          Else
          Type 249,y,xmin,xmax
249       Format(//,5x,' A plot of Electric Potential for ',//,
     1 5x,'Y = ',1pe15.5,'  X = ',1pe15.5,' to X = ',1pe15.5,//)
c
```

Table C.1. (Continued)

```
      Call plotter(vm,vpm,xme,xpe,yme,ype,-2,lxo,1,npt)
      End If
235   continue
      Print 237
237   Format(//,5x,'Do you wish a plot of EY with magnitude and ',
     1 'phase? ',' Answer Yes or No.    :    ',$)
      accept 112,yes
      If(yes.ne.'y'.and.yes.ne.'Y') go to 240
      print 248,y,xmin,xmax
      print 920
      accept 112,yes
      If(yes.eq.'y'.or.yes.eq.'Y') then
      Type *,npt,-2
      np2=(npt+1)/2
      Type 950,(xx(i),Yme(i),ype(i),i=1,npt)
      Else
      Type  241,y,xmin,xmax
241   Format(//,5x,'A Plot of Electric Field Ey for',//,
     1 5x,'Y =',1pe15.5,' X = ',1pe15.5,' to X = ',1pe15.5,//)
c
      Call plotter(yme,ype,vm,vpm,xme,xpe,-2,lxo,1,npt)
      End If
240   Continue
      Print 242
242   Format(//,5x,'Do you wish a plot of EY, EX and ET with magni',
     1 'tudes only? ',' Answer Yes or No.    :    ',$)
      accept 112,yes
      If(yes.ne.'y'.and.yes.ne.'Y') go to 245
      Print 248,y,xmin,xmax
      print 920
      accept 112,yes
      If(yes.eq.'y'.or.yes.eq.'Y') then
      Type *,npt,3
      np2=(npt+1)/2
      Type 960,(xx(i),yme(i),xme(i),tme(i),i=1,npt)
960   Format(4e15.7)
      Else
      Type 246,y,xmin,xmax
246   Format(//,5x,'A Plot of Ey, Ex, and Et magnitudes for',//,
     1 5x,'Y =',1pe15.5,' X = ',1pe15.5,' to X = ',1pe15.5,//)
c
      Call plotter(YME,XME,tme,xpe,vm,vpm,3,lxo,1,npt)
      End If
245   continue
      Print 247
```

Table C.1. (Continued)

```
247      Format(//,5x,'Do you wish a plot of EX with magnitude ',
         accept 112,yes
         If(yes.ne.'y'.and.yes.ne.'Y') go to 250
         Print 248,y,xmin,xmax
         Print 920
         Accept 112,yes
         If(yes.eq.'y'.or.yes.eq.'Y') then
         Type *,Npt,-2
         np2=(npt+1)/2
         Type 950,(xx(i),xme(i),xpe(i),i=1,npt)
         Else
         Type 243,y,xmin,xmax
243      Format(//,5x,'A Plot of electric field Ex for ',//,
     1 5x,'Y =',1pe15.5,' X = ',1pe15.5,' to X = ',1pe15.5,//)
         Call plotter(XME,XPE,yme,ype,vm,vpm,-2,ixo,1,npt)
         End If
250      Continue
         Print 270
270      Format(//,5x,'Do you want another plot at a different ',
     1 'height?',/,7x,'  Answer Yes or No.    :    ',$)
         accept 112,yes
         If(yes.ne.'y'.and.yes.ne.'Y') go to 220
         go to 212
220      continue
         Print 221
221      Format(//,5x,'Do you wish to insert new line data?',
     1   /,7x,'  Answer Yes or No.    :    ',$)
         accept 112,yes
         If(yes.ne.'y'.and.yes.ne.'Y') go to 225
         go to 5
225      continue
       stop
       END
```

Table C.1. (Continued)

```
      Function Field(x,y,xq,yq,qq,ex,ey,et,kb,ke,kf,pk)
C
C   Purpose: To compute the electric potential and the electric
C    fields around a set of parallel fine lines of electric charge
C    above a conducting ground plane.  The y-axis is normal to the
C    ground plane while the x- and z-axes are parallel to the ground
C    plane with the fine lines of charge parllel to the z-axis.
C
C    x,y      - the position where the potential and fields are to be
C               computed.
C
C    xq,yq    - the vector arrays giving the x- and y-positions of the
C               fine lines of charge.
C
C    qq       - the vector array giving the linear charge density of
C               the fine lines already divided by 2 pi epsilon
C
C    ex,ey    - the components of the electric field returned to the
C               calling program.
C
C    et       - the magnitude of the electric field=sqrt(ex*ex+ey*ey)
C
C    kb,ke    - the beginning and end locations in the xq,yq,qq arrays
C               to be used in computing the potential and the fields.
C
C    kf       - a key permitting different kinds of calculations:
C      kf > 0 compute potential only and return as function value.
C      kf = 0 compute both potential and field components and return
C               potential as function value and fields as ex,ey,et
C               in the function argument list.
C      kf < 0 compute the fields but return magnitude of the net
C               electric field et as the function value and ex,ey,
C               as well as et in the function argument list.
C
C      pk     - the scale factor for qq(k) image due to dielectric
       DIMENSION XQ(1),YQ(1),QQ(1)
C
       v=0.0
       EX=0.0
       EY=0.0
       DO 10 k=kb,ke
       a=x-xq(K)
       b=y-yq(k)
       c=y+yq(k)
       d=a*a+b*b
```

Table C.1. (Continued)

```
      if(d.lt.1.0E-18) go to 20
      e=a*a+c*c
      if(e.le.1.0E-18) go to 20
        sx=xq(k)
        sy=yq(k)
        s=sy*sy+sx*sx
        if(s.le.1.0E-18) go to 20
      if(kf.gt.-1) v=v+qq(k)*(alog(s/d)+pk*alog(e/s))/2.0
      if(kf.gt.0) go to 10
      EX=EX+QQ(k)*(a/d-pk*a/e)
      EY=EY+QQ(k)*(b/d-pk*c/e)
10    continue
c
      if(kf.gt.-1) field=v
      if(kf.lt.1) et=sqrt(ex*ex+ey*ey)
      if(kf.lt.0) field=et
      return
20    continue
      EX=1.0E+18
      EY=EX
      ET=EX
      V=1.0E+30
      return
      end
c
      subroutine PLIMITS(xl,xh,yl,yh,dx,dy,ix0,iy0,scale)
c  Make sure upper and lower limits were entered correctly.
      if(xl.gt.xh) then
       a=xl
       xl=xh
       xh=a
      end if
      if(yl.gt.yh) then
       a=yl
       yl=yh
       yh=a
      end if
c  Determine x- and y-increments of map.  Adjust y-increment to fact
c   one space between lines is equal to 1.6666 letters.
      dx=(xh-xl)/100.0
      dy=scale*dx
      ix0=-ifix(xl/dx-1.5)
      iy0= ifix(yh/dy+1.5)
      return
      end
c
```

Table C.1. (Continued)

```
c
      function inside(z,zc,rc,jj,kk)
c
c  Purpose:  To test if z is at a level (vertical or horizonal) of
c    any conductor, j.  If so set function to j, otherwise to 0.
c
      dimension zc(1),rc(1)
      do 20 j=jj,kk
      if(abs(zc(j)-z).lt.rc(j)) go to 30
20    continue
      inside=0
      return
30    continue
      inside=j
      return
      end
c
      function jump(x,y,xc,yc,rc,jy,nc)
c
c  Purpose:  To provide a signal to jump the plottins of any point
c   inside a conductor.
      dimension xc(1),yc(1),rc(1)
20      continue
        ix=jy
30      continue
      jx=inside(x,xc,rc,ix,nc)
      if(jx.eq.0) go to 60
          if(jx.eq.jy) go to 40
          ky=inside(y,yc,rc,jx,jx)
          if(ky.eq.0) then
            ix=jx
            go to 50
          end if
40      a=x-xc(jx)
        b=y-yc(jx)
        rr=a*a+b*b-rc(jx)*rc(jx)
        if(rr.lt.0.0) go to 60
50      continue
        ix=ix+1
        if(ix.le.nc) go to 30
          jump=0
        return
60        jump=jx
      return
      end
```